UNIVERSITÀ DEGLI STUDI DI PADOVA

DIPARTIMENTO DI SCIENZE CHIMICHE

SCUOLA DI DOTTORATO DI RICERCA IN SCIENZE MOLECOLARI

INDIRIZZO: SCIENZE CHIMICHE

CICLO XXV

Structural studies of protein kinase CK2:

Inhibition mechanisms and structure-activity relationships

Direttore della Scuola: Ch.mo Prof. Antonino Polimeno

Coordinatore d'indirizzo: Ch.mo Prof. Antonino Polimeno

Supervisore: Ch.mo Prof. Roberto Battistutta

Dottorando: Alessandro Ranchio

Tutte le partite sono facili, una volta vinte.

AC

Table of contents

Abbreviations

AGC	Adenine-guanine-cytosine kinase
Ala (A)	Alanine
AML	Acute myeloid leukemia
APK	Atypical protein kinase
Arg (R)	Arginine
Asn (N)	Asparagine
Asp (D)	Aspartic acid
ATP	Adenosine tri-phosphate
Bp	Base pair
BRCA	BReast CAncer
CAK	Cdk-activating kinase
CAMK	Calcium/calmodulin-dependent kinase
cAMP	Cyclic adenosine monophosphate
CDC	Cell division cycle
CDK	Cycline dipendent kinase
cGMP	Cyclic guanosine monophosphate
Chk	Checkpoint kinase
CK1	Cell kinase 1
CK2	Casein kinase 2
$CK2\alpha^{336}$/$CK2\alpha^{del}$	CK2α deleted at residue Ser336
$CK2\alpha^{pm}$	CK2α phosphomimetic mutant
$CK2\alpha^{wt}$	CK2α wild type full-length
$CK2\alpha'^{del}$	CK2α' starting from the amino acid 3 of the wt
$CK2\alpha'^{long}$	CK2α' with the 14-amino acids tail of the MCS
$CK2\alpha'^{wt}$	CK2α' wild type
$CK2^{del}$	CK2 holoenzyme with the deleted form of the CK2α
$CK2^{pm}$	CK2 holoenzyme with the phoshomimetic mutant of CK2α
$CK2^{wt}$	CK2 holoenzyme with the wild type full-length CK2α
CLK	CDC-like kinase
CMGC	CDK, MAPK, GSK3 and CLK kinases

Abbreviations

C-spine	Catalytic spine
Cys (C)	Cysteine
Da	Dalton
DLS	Dynamic Light Scattering
DMAT	2-Dimethylamino-4,5,6,7-tetrabromo-1H-benzimidazole
DMSO	Dimethyl sulfoxide
DNA	Deoxyribonucleic acid
dNTP	deoxyribonucleotide triphosphate
DRB	5,6-Dichloro-1-β- D –ribofuranosylbenzimidazole
DTT	Dithiothreitol
EC	Enzyme Commission
EDTA	Ethylenediaminetetraacetic acid
ELK	Eukaryotic Like Kinase
EPK	Eukariotic protein kinase
ESRF	European Synchrotron Radiation Facility
FPLC	Fast Protein Liquid Chromatography
Gln (Q)	Glutamine
Gly (G)	Glycine
GSK	Glycogen synthase kinase
GST	Glutathione S-transferase
His (H)	Histidine
Ile (I)	Isoleucine
IPTG	Isopropyl β-D-1-thiogalactopyranoside
IRK	Insulin receptor kinase
Kb	Kilobase
LB	Luria-Bertani
Leu (L)	Leucine
LSP	Local spatial pattern
Lys (K)	Lysine
MAPK	Mitogen-activated protein kinase
MAT1	Menage a trois 1
MCS	Multiple Cloning Site)
MDM 2	Mouse double minute 2
Met (M)	Methionine

MM	Multiple myeloma
OD	Optical density
OGT	O-N-Acetylglucosamine transferase
ON	Overnight
PCR	Polymerase Chain Reaction
PDB	Protein data bank
PEG	Poly ethylenglycol
Phe (F)	Phenylalanine
PIM	Proviral integration of MMLV (Moloney-murine leukemia virus)
PIN 1	Peptidyl-prolyl cis-trans isomerase NIMA-interacting 1
Plk1	Polo-like kinase 1
PKA/C/G	Protein kinase A/C/G
Pro (P)	Proline
RGC	Receptor Guanylate Cyclase
RMSD	Root-mean-square deviation
R-spine	Regulatory spine
SDS-PAGE	Sodium Dodecyl Sulphate - PolyAcrylamide Gel Electrophoresis
SEC	Size exclusion chromatography
Ser (S)	Serine
TBB	4,5,6,7-tetrabromo-2-azabenzimidazole
TBI	[1,2,4]triazino[4,3-alpha]benzimidazole
TCEP	Tris(2-carboxyethyl)phosphine
TFIIS	Transcription factor S-II
Thr (T)	Threonine
TK	Tyrosine Kinase
TKL	Tyrosine Kinase Like
TLS	Translation/Libration/Screw
Trp (W)	Tryptophan
Tyr (Y)	Tyrosine
UDP	Uridine disphosphate
UV	Ultraviolet
Val (V)	Valine
wt	Wild type

Abstract

The subject of this thesis is the protein kinase CK2 which is a family of enzymes that in humans consists of two catalytic subunits, termed CK2α and CK2α', and one regulatory subunit, CK2β. CK2 is a highly conserved acidophilic Ser/Thr protein kinase, ubiquitously distributed in different cell compartments. CK2 is a member of the superfamily of eukaryotic protein kinases (EPKs), meaning the catalytic subunit is related by sequence homology and structural features to the other 478 kinases of the superfamily.

CK2 shows some singular features like its high constitutive activity and the lack of an defined mode of regulation, which make CK2 unique with respect to the other kinases. With hundreds of substrates, this kinase is involved in several cellular events, resulting essential for the cell viability: CK2β gene knockout in mouse model is lethal even at single cell level, CK2α gene knockout are embryonic lethal at day 10.5 and CK2α' (expressed only in brain and testis) mouse knockout are viable with some defects in spermatogenesis. It participates in cell cycle progression, gene expression, cell growth, and differentiation and embryogenesis. Down-regulation of CK2 leads to apoptosis while abnormal over-activation has been found coupled to several diseases: the clinical relevance of CK2 is that high levels of the protein activity have been detected in a number of cancers, such as head and neck, renal, breast, prostate, lung, and kidney.

A wide spectrum of cell permeable, fairly specific ATP site directed CK2 inhibitors are currently available which are proving useful to dissect its biological functions and which share the property of inducing apoptosis of cancer cells with no comparable effect on their "normal" counterparts. One of these, CX-4945, has recently entered clinical trials for the treatment of advanced solid tumors, Castelman's disease and multiple myeloma.

CK2 is considered constitutively active enzyme and, unlike many other protein kinases, it does not require phosphorylation for activation. The mechanism of regulation of CK2 is not firmly established yet, however it is clear that it differs from those commonly utilized by other protein kinases.

Dozens of crystal structures of CK2 have been solved and highlighted the structural features of the main CK2 entities, the catalytic subunit CK2α, the regulatory subunit CK2β and the tetrameric $\alpha_2\beta_2$ CK2 holoenzyme. Even if the structural knowledge of CK2 is very extended, no high resolution 3D-structure are available for the C-terminal part of

CK2α, which has been deleted for the crystallization purpose. Moreover the structure of the CK2α' has been solved but no structural information are present for the tetrameric holoenzyme with this catalytic subunit.

To address this issue, one part of my PhD project focused on the production and the structural characterization of the full-length wild type CK2α and a phosphomimetic mutant in the tetrameric holoenzyme, in order to study the possible structural role of the C-terminus. Starting from the three holoenzyme structures solved we were able to determine some new holoenzyme structural features, in particular the new interface of interaction between the subunits within the tetramer and the so far unknown symmetry of the complex. Moreover we dealt with the development of a purification protocol of the CK2α'$_2$β$_2$ holoenzyme (and a chimeric CK2αα'β$_2$) in quantities appropriate for structural approaches.

The second part of the PhD focused on the structural characterization of a new potent dual inhibitor K164 which is specific for CK2 and Pim1; the crystal structure of the inhibitor in complex with the CK2α^{336} has been solved at 1.25 Å, which is the highest resolution ever reached for CK2.

Riassunto

Il soggetto di questa tesi è la protein chinasi CK2, una famiglia di enzimi che negli uomini è composta da due subunità catalitiche, CK2α e CK2α', e da una subunità regolatoria, CK2β. CK2 è una Ser/Thr protein chinasi acidofila altamente conservata nel mondo eucariote, presente in differenti compartimenti cellulari. CK2 è un membro della superfamiglia delle protein chinasi eucariotiche (EPKs), con la subunità catalitica correlata mediante omologia di sequenza e caratteristiche strutturali alle altre 478 chinasi della superfamiglia.

CK2 mostra alcune caratteristiche singolari, come la sua elevata attività costitutiva e la mancanza di un importante meccanismo di regolazione, il quale rende CK2 unica rispetto alle altre chinasi. Con centinaia di substrati, CK2 è coinvolta in numerosi processi biologici, risultando essenziale per la vitalità cellulare: il *knockout* del gene CK2β nel modello murino è letale anche a livello di singola cellula, il *knockout* del gene CK2α è letale al giorno 10.5 dello sviluppo embrionale e il *knockout* CK2α' (espresso solo nel cervello e testicoli) in topo è vitale con alcuni difetti di spermatogenesi. CK2 partecipa alla progressione del ciclo cellulare, all'espressione genica, alla crescita cellulare e alla differenziazione e all'embriogenesi. *Down-regulation* di CK2 porta all'apoptosi cellulare mentre una sovra-attivazione anomala è stata trovata accoppiata a diverse malattie: la rilevanza clinica di CK2 risiede nel fatto che alti livelli di attività della proteina sono stati trovati in diversi tipi di tumori, come alla testa e al collo, ai reni, al seno, alla prostata e al polmone.

Un ampio spettro di inibitori di CK2, permeabili alle cellule e specifici per il sito dell'ATP, sono attualmente disponibili e si stanno rivelando utili per analizzare le funzioni biologiche della proteina; queste piccole molecole sono in grado di indurre l'apoptosi delle cellule tumorali senza alcun effetto analogo sulle loro controparti "normali". Uno di questi inibitori, CX-4945, è recentemente entrato in studi clinici per il trattamento di tumori solidi avanzati, malattia di Castelman e mieloma multiplo.

CK2 è considerato un enzima costitutivamente attivo e, a differenza di molte altre protein chinasi, non richiede fosforilazione per l'attivazione. Il meccanismo di regolazione di CK2 non è stato ancora stabilito, tuttavia è chiaro che si differenzia da quelli comunemente utilizzati dalle altre protein chinasi.

Decine di strutture cristallografiche di CK2 sono state risolte e hanno evidenziato le caratteristiche strutturali delle principali entità di CK2: la subunità catalitica CK2α, la

subunità regolatoria CK2β e l'oloenzima tetramerico $CK2\alpha_2\beta_2$. Anche se la conoscenza strutturale di CK2 è molto estesa, non è disponibile alcuna struttura 3D a elevata risoluzione per la parte C-terminale di CK2α, che è sempre stata deleta per scopi di cristallizzazione. Inoltre, malgrado la struttura di CK2α' sia stata risolta, non sono presenti alcune informazioni strutturali per l'oloenzima tetramerico con questa subunità catalitica.

Per raggiungere questo obiettivo, una parte del mio progetto di dottorato si è focalizzata sulla produzione e sulla caratterizzazione strutturale di CK2α *wild type* (completa della parte C-terminale) e di un mutante fosfomimetico nell'oloenzima tetramerico, al fine di studiare il possibile ruolo strutturale del C-terminale. Partendo da tre strutture dell'oloenzima risolte abbiamo potuto determinare alcune nuove caratteristiche strutturali dell'oloenzima, in particolare la nuova interfaccia di interazione tra le subunità all'interno del tetramero e la simmetria del complesso, finora sconosciuta. Inoltre ci siamo occupati dello sviluppo di un protocollo di purificazione dell'oloenzima $CK2\alpha'_2\beta_2$ (e di una forma chimerica $CK2\alpha\alpha'\beta_2$) in quantità appropriate per approcci strutturali.

La seconda parte del dottorato si è focalizzata sulla caratterizzazione strutturale del complesso con un nuovo potente inibitore duale (K164) il quale è specifico per CK2 e Pim1; la struttura cristallina di $CK2\alpha^{336}$ in complesso con l'inibitore è stata risolta a 1.25 Å, che è la più alta risoluzione mai raggiunta per CK2.

1. Introduction

1.1. Protein kinase introduction and classification

The importance of protein phosphorylation as a regulatory mechanism was discovered by Krebs and Fisher nearly 50 years ago: they found that glycogen phosphorylase was activated by a reversible addiction of a phosphate group by a protein kinase (phophorylase kinase) (Krebs, 1998). The second protein kinase to be discovered was the cAMP-dependent protein kinase (PKA) in the 1968 (Walsh et al., 1968). With the advent of DNA cloning and sequencing in the mid-1970s, it rapidly became clear that a large family of eukaryotic protein kinases exists. After the completion of the human genome sequence it was possible to identify almost all the human protein kinases: the human kinome is composed by 518 kinases, 478 human EPKs and 40 APK, and they are encoded by the 1.7% of all human genes (Manning et al., 2002). Emphasizing the importance of phosphorylation is the estimate that one third of cellular proteins are phosphorylated (Ahn and Resing, 2001) and often at different sites (Cohen, 2000). The major part of the protein kinases belong to the EPKs superfamily and can be classified into 9 broad groups, divided in families and subfamilies (Table 1.1). The classification is based primarily on kinase domain similarity, deduced from pairwise and multiple sequence alignments and phylogeny; knowledge on sequence similarity, domain structures outside the catalytic domains and known biological functions were used to refine the classification (Manning et al., 2002 b).

Table 1.1 Kinase distribution by broad groups in human

Group	Families	Subfamilies	Human kinase
AGC	14	21	63
CAMK	17	33	74
CK1	3	5	12
CMGC	8	24	61
STE	3	13	47
TK	30	30	90
TKL	7	13	43
RGC	1	1	5
Other	37	39	83
aPKs	14	22	40
Total	134	201	518

The **AGC** group protein kinases (named after the PKA, PKC, PKG) tend to be basic amino acid-directed enzymes, phosphorylating substrates at Ser/Thr lying very near Arg or Lys; this group contains many cytoplasmic serine/threonine kinases that are regulated by secondary messengers such as cyclic AMP (PKA) or lipids (PKC).

The **CAMK** group protein kinase also tend to be basic amino acid-directed; many but not all of the kinases members of this group are known to be activated by Ca^{2+}/calmodulin binding to a small domain located near the catalytic domain (Calmodulin/Calcium regulated kinases).

CK1 group (Cell Kinase 1) is a small group of kinases very similar to each other in sequence but very different from the structural point of view from the other ePKs, with several conserved motifs which are modified in the CK1 group.

CMGC group (named after another set of families CDK, MAPK, GSK3 and CLK) is composed by Ser/Thr protein kinases which mainly phosphorylate residues lying near a Pro-rich environments and involved in cell-cycle control, stress response, splicing and metabolic control. Part of this group are for example the CDKs (Cycline dipendent kinases) and CK2 family which fail to conform the proline-directed specificity showing instead a strong preference for Ser residues located NH_2-terminal to a cluster of acidic residues.

TK group (Tyrosine Kinase) includes a large number of enzymes with quite closely related kinase domains that specifically phosphorylate on Tyr residues. This group is very young from the evolutionary point of view and it is absent from plants and unicellular

organism. Due to the fact that their function is related to the transmission of extracellular signal into the cell, half of TKs are cell receptor and many of the others are close to the surface of the cell.

TKL group (Tyrosine Kinase Like) is composed by kinases relatively weakly related to each other, and all are also similar to members of the TK (Tyrosine Kinase) group, though they generally lack the TK-specific motifs of the TK group and whose activities are generally on serine/threonine substrates.

RGC group (Receptor Guanylate Cyclases) are single-pass transmembrane receptors with an extracellular active guanylate cyclase domain and a cytoplasmatic catalytically inactive kinase domain. The guanylate cyclase domain makes the second messenger cGMP, and the intracellular kinase domain appears to have a regulatory function (Hanks and Hunter, 1995).

1.2. Structural features of kinases

We discuss the classification of the protein kinases in 9 broad groups and how they differ from each other in this nomenclature; because now we have a significant "structural" kinome available, composed of over 150 protein kinases (Taylor and Kornev, 2011), in this paragraph I will analyze the general unique structure features of the EPKs superfamily. All the kinases of the EPKs superfamily are characterized by a conserved kinase core: this core is composed by a bi-lobal protein of approximately 250 amino acids. The catalytic cleft is positioned in the middle of the protein, where the two lobes convert to form a deep cleft where the adenine ring of the ATP is bound and the δ-phosphate points at the outer edge of the cleft. Catalysis is mediated by opening and closing of the active site cleft allowing for transfer of the phosphate and then release of the nucleotide (Taylor et al., 2012).

The N-terminal lobe (N-lobe) is composed of 5 anti-parallel beta sheet and one single conserved αC-helix (between β strand 3 and 4); β strand 1 and 2 are linked by a gly-rich loop which stays on top of the adenine ring and blocks the δ-phosphate of the ATP on a correct conformation for the catalysis. β strand 3 interacts with the αC-helix by a coupling between a conserved Lys residue (Lys72 in PKA and Lys68 in CK2) and a conserved Glu residue in the helix (Glu91 in PKA and Glu81 in CK2) when the kinase is in an active state.

In contrast the C-terminal lobe (C-lobe), covalently linked to the N-lobe by the so-called hinge region, is mainly composed of alpha helix with four-stranded beta sheet leaning on the top of the lobe. And these beta sheets contain the other two conserved residues fundamental for the catalysis: the catalytic base of the catalytic loop (Asp164 in PKA and Asp156 in CK2) and the conserved motif Asp-Phe/Trp-Gly (DFG in PKA and DWG in CK2) where a conserved Asp residue (Asp184 in PKA and Asp175 in CK2) binds to the catalytic magnesium ion (Figures 1.1 and 1.2).

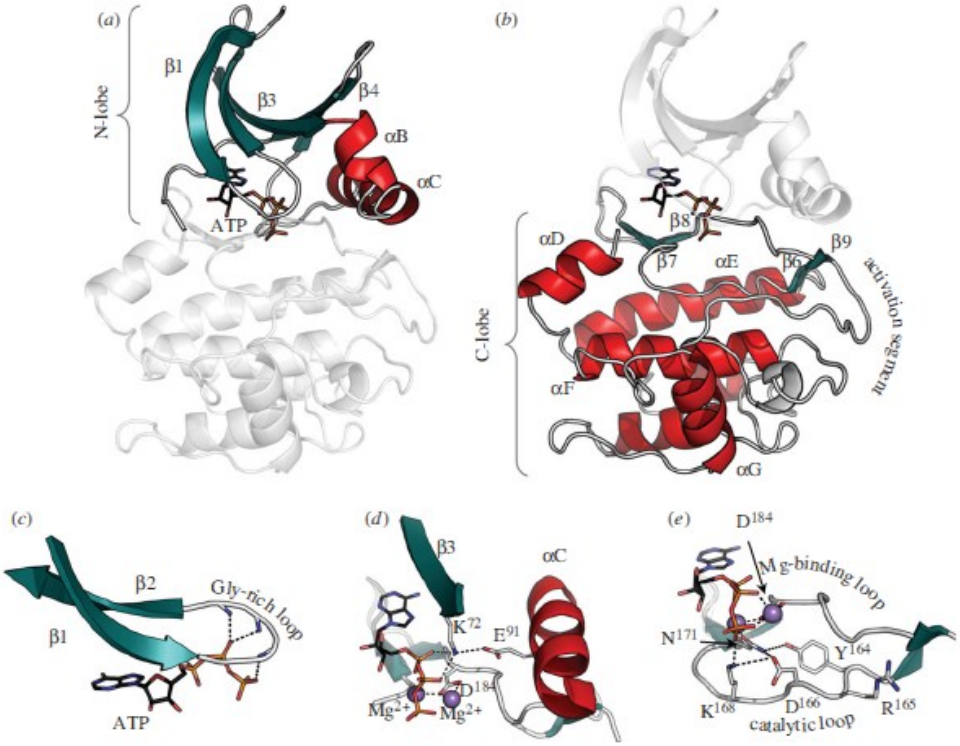

Figure 1.1 *Conserved core of the eukaryotic protein kinases. The bottom panels (c–e) highlight functional motifs in the N-lobe (a) and the C-lobe (b) using PKA as a prototype for the EPK family. Helices are shown in red; β-strands in teal.* ***(a)*** *The N-lobe contains five β-strands and a large αC-helix.* ***(b)*** *The C-lobe is mostly helical with a large activation segment. A four-stranded β-sheet rests on the helical core and forms one surface of the active site cleft. ATP is bound in the cleft between the two lobes.* ***(c)*** *The phosphates of ATP are positioned by a conserved glycine-rich loop between the β1- and β2-strands.* ***(d)*** *Conserved residues Lys72 from the β3-strand, Glu91 from the αC-helix, and Asp164 from the DFG motif in the activation segment where Mg^{2+} ions are show as purple balls.* ***(e)*** *The catalytic loop also contains a set of catalytically important residues: Asp166, Lys168, Asn171 (Taylor et al., 2012).*

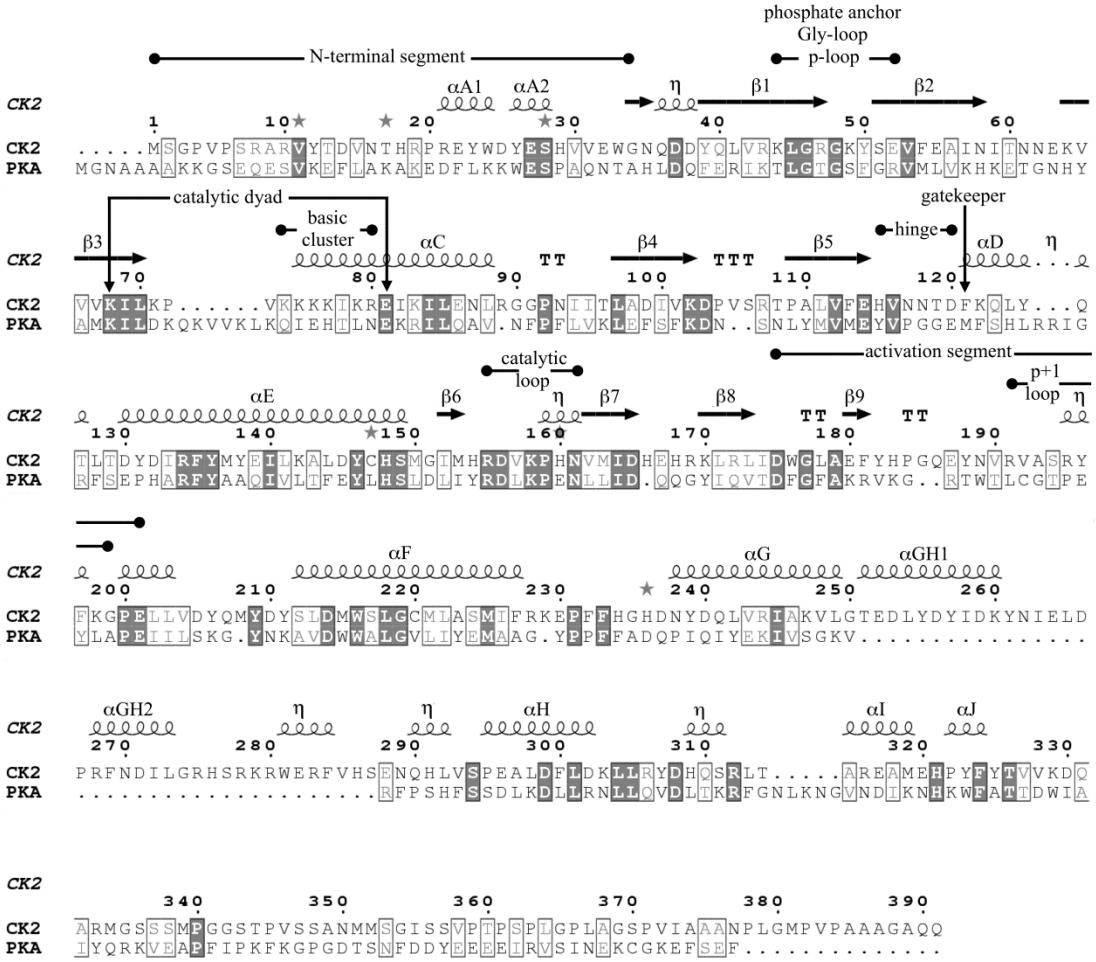

Figure 1.2 *Structure-based sequence alignment (by 3D-Coffee) of human CK2, PDB 3NSZ, and human PKA, PDB 3AGM (enhanced by ESPript Web-server). Elements of the CK2 secondary structure are indicated (α=α-helix; β=β-strand; η=3_{10}-helix; T=Turn). Conserved and homologues residues are indicated in white on a black background and in contoured boxes, respectively. Numbering refers to the human CK2 sequence. The secondary structure of the C-terminal tail of CK2 (from residue 333) is unknown (NIefind et al., 2012).*

In the last two decades hundreds of EPKs representing various functional and binding states have been published and this allow to determine additional conserved structural elements. A rigorous comparison between many protein kinase structures revealed that the conserved catalytic core is built around a stable yet dynamic hydrophobic core, made up of three essential elements: a single hydrophobic helix that spans the large lobe (αF- helix) and two hydrophobic spines which connect the N-lobe and the C-lobe and that are each made up of non-contiguous residues from both lobes (Taylor et al., 2012).

The spine concept arises from a new approach of sequence comparison based on the

novel “local spatial pattern” (LSP) alignment procedure (Kornev et al., 2006). The first application led to the detection, by the analysis of only solvent accessible residues, of an hydrophobic spine composed of two residues of the N-lobe and two residues of the C-lobe (in PKA: Leu106, Leu95, Phe185 and Tyr164). This spine connects the two lobes in a non-covalent manner and, because this spine is broken in the inactive kinases, was later renamed “regulatory spine” (or “R-spine”).

When the LSP approach was used to compare all residues of all the published kinases, another hydrophobic spine, that runs parallel to the R-spine, became visible (Kornev et al., 2008). Unlike the R-spine this spine is always opened and it is completed only by the adenine ring of the ATP; this spine was therefore called “catalytic spine” (or “C-spine”). Both spines are anchored to the αF- helix (Figure 1.3).

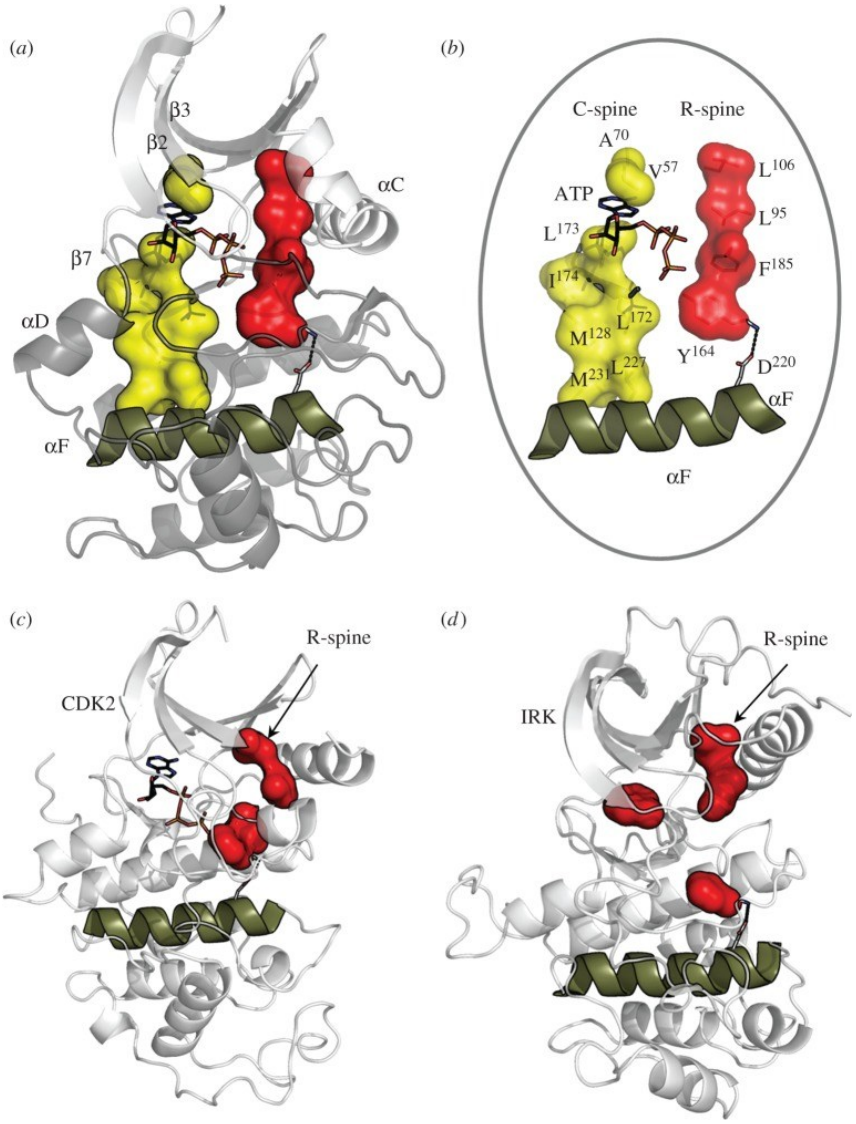

Figure 1.3 *Hydrophobic spines define the internal architecture of the EPKs. (a) Two hydrophobic spines span the two lobes of the kinase core and provide a firm but flexible connection between the N- and C-lobes. (b) The regulatory spine (R-spine) contains four residues from different kinase subdomains and is anchored to the αF-helix by conserved Asp220. The catalytic spine (C-spine) is completed by ATP. (c,d) In the inactive state, the R-spine is typically disassembled. Disassembly of the R-spine can be achieved in different ways: by movement of the αC-helix like in cyclin-dependent kinase 2 (CDK2) (c) or by movement of the activation segment like in insulin receptor kinase (IRK) (d) (Taylor et al., 2012).*

1.3. CK2

1.3.1 Introduction

The correct regulation of protein phosphorylation is fundamental for the correct function of the cellular signaling pathways, and loss of regulation in these pathways underlies many human diseases, including cancer (Hanahan and Weinberg, 2000). CK2 is a small family of protein serine/threonine kinases that is overexpressed in multiple forms of cancer and has oncogenic proprieties in mice and cultured fibroblasts (Litchfield, 2003).

Originally discovered in 1954 (Burnett and Kennedy, 1954), CK2 is a family of enzymes that in humans consists of two catalytic subunits, termed CK2α and CK2α', and one regulatory subunit, CK2β (St-Denis and Litchfield, 2009).

CK2 is fundamental for cell viability: regulatory CK2β gene knockout in mouse model is lethal even at single cell level (Buchou et al., 2003), CK2α gene knockout are embryonic lethal at day 10.5 (Lou et al., 2008) and CK2α' (expressed only in brain and testis) mouse knockout are viable with some defects in spermatogenesis (Xu et al., 1999).

CK2 is a member of the superfamily of eukaryotic protein kinases (EPKs), meaning the catalytic subunit is related by sequence homology and structural features to the other 478 kinases of the family in a way as described before. However CK2 shows some incredible features like its high constitutive activity and the lack of an acute mode of regulation, which make CK2 unique with respect the other kinases (Pinna, 2002).

At the beginning acidic phosphoproteins, like casein, were used as artificial substrates for CK2 but only in the 1980ies was found that negatively charged residues near the phosphorylatable serine or threonine was fundamental for CK2 substrate recognition (Pinna et al., 1984). The first physiological substrates of CK2 was discovered more than 20 years after its identification: CK2 was discovered to be one of the enzymes responsible for the phosphorylation of the "glycogen synthase 5" (GSK5) and "Troponin-T kinase" (Pinna, 1994).

The minimal consensus sequence for CK2 phosphorylation was published in 1988 to be S/T-X-X-D/E (Marchiori et al., 1988) and now the number of proteins phosphorylated by CK2 amount to more than 300 substrates (Meggio and Pinna, 2003). This number seems to underestimate the whole "CK2 phosphoproteome" if we consider

that consensus sequence analysis performed on a database of 10.899 naturally phosphorylated sites reveal that 2.275 of these (>20%) display the unique acid pattern of CK2 (Salvi et al., 2009).

Due to this broad substrate spectrum CK2 belongs to EC class 2.7.11.1 (Scheer et al., 2011), i.e. to the non-specific serine/threonine protein phosphotransferases.

In the introduction to the kinase superfamily, we saw how the mechanism of binding of an ATP molecule is conserved within the kinases and this is because ATP is the typical cosubstrate of an EPK; interestingly CK2 is able to use, alternatively to the ATP, a GTP molecule as cosubstrate (Rodnight and Lavin, 1964). This double specificity entails structural features in the binding site peculiar to CK2.

1.3.2 CK2 cell cycle

CK2 has been reported to be fundamental for cell viability and it is involved in every stage of cell cycle progression (Table 1.2) phosphorylating different proteins crucial to the successful production of daughter cells (Litchfield, 2003).

Table 1.2 Cell cycle's phases description.

State	Abbreviation	Description
Quiescent/ senescent	G_0	In this phase the cell has left the cell cycle, and it's in a quiescent state.
Interfase	G_1	Also called the "growth phase", cell starts the synthesis of new proteins required for the new cell and for the DNA replication. The G_1 checkpoint controls that everything is correct for the DNA duplication (under the control of p53 and consequentially p21)
	S	In this phase the DNA is replicated in two copies.
	G_2	After the DNA synthesis, the cell continues to grow and the G_2 checkpoint ensures the cell is ready for the mitosis (under favourable conditions phosphatase cdc25 activates the CyclineB/CDK1 complex)
Cell division	M	In this phase the cell starts the division in two daughter cells. There's another checkpoint in the middle of the mitosis for the correct cell division.

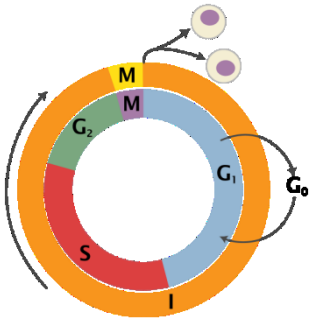

In mammalian cells, the inhibition of CK2 with specific inhibitor or CK2 antibodies can all stop the cell cycle progression, meaning that mammalian cells require CK2 for G_0/G_1, G_1/S, and G_2/M transitions (Lorenz et al., 1993; Lorenz et al., 1994; Pepperkok et al., 1994).

Cdks are the main characters in the cell cycle progression, and they are controlled by an extremely precise activation-deactivation mechanism: Cdk4/Cyclin D at the G_1/S transition, and Cdk1/Cyclin B at the G_2/M transition (Nasmyth, 1996). The Cdk-activating kinase (CAK) is an enzyme complex composed of Cdk7, Cyc H and MAT 1 and it activates the mentioned kinases in the appropriate times: this activator is regulated by the CK2 phosphorylation itself and the activity is modulated by this phosphorylation.

Another well studied CK2 substrate involved in cell cycle regulation is the tumor suppressor protein p53. P53 is a transcription factor which can induce the cell cycle arrest and eventually the programmed cell death (apoptosis) (Sherr and McCormick, 2002). The phosphorylation of p53 by CK2 comes in response to a UV radiation DNA damage, and increase the p53 activity enhancing its DNA binding and transcriptional activation (Kapoor and Lozano, 1998). In normal cells, p53 is constantly produced and degraded and the degradation is induced by MDM-2 protein; MDM-2 protein is also a CK2 substrate and its phosphorylation leads to a decreased capability to induce p53 degradation favouring the cell cycle arrest (Hjerrild et al., 2001). Moreover the inhibition of CK2 with TBB (4,5,6,7-tetrabromo-2-azabenzimidazole) leads to cell cycle arrest and apoptosis induced by p53, confirming CK2 involvement in this mechanism.

CK2 is phosphorylated itself in a cell cycle-dependent manner by the Cdk1 at Ser 209 of the CK2β (which the function is unknown) (Litchfield et al., 1991), and at four residues located at the C-terminal domain of CK2α (Thr 344 and 360 and Ser 362 and 370) (Bosc et al., 1995). The presence of this phosphorylation sites indicates that CK2 has a specific role in mitosis and, even if the phosphorylation doesn't affect the CK2 activity, could be a binding site for different interacting proteins targeting CK2 towards favourable substrates or away from unfavourable substrates during the mitotic progression (St-Denis and Litchfield, 2009). There aren't any structural data about this C-terminal tail of CK2α, because all the 39 structures deposited in the PDB database lack this portion of protein, but it has been reported that the disruption of these phosphorylation sites by mutating in alanine residues, prompt to mitotic catastrophe: this means that CK2 has also a crucial role in mitosis progression (St-Denis et al., 2009). For example it has been demonstrated that Pin1, a peptidyl-prolyl isomerase which catalyzes the cis-trans isomerization of

proline residues adjacent to phosphorylated serine or threonine and which is believed to have a central role in mitosis, can bind CK2α via its phosphorylated C-terminal tail (Messenger et al., 2002). This interaction could actually catalyze isomerization of the prolines, but is known that it modulates CK2 activity.

As in G_1/S transition, CK2 is involved in the p53-mediated DNA damage checkpoint in G_2 and many different proteins involved are reported to be CK2 substrates like checkpoint kinases Chk1 and Chk2, Topoisomerase II, BRCA and Plk1 (St-Denis and Litchfield, 2009); by the way, the role of CK2 in the DNA damage response in G_2/M remains unknown.

On the other hand, CK2 has been reported to be an important pro survival enzyme because the overexpression of CK2 is protective for drug-induced apoptosis and cell lines which show drug-resistant phenotype often overexpress CK2 (Di Maira et al., 2008). As a consequence the chemical inhibition of CK2 is able to induce apoptosis in cancer cells and makes CK2 a putative target for cancer treatment. In particular CK2 is involved in protein protection from caspase cleavage: the sequence consensus of CK2 recognition (S/T-X-X-Acidic) for phosphorylation is very similar to the consensus recognized by protein caspases which act at the level of an aspartic residue. So phosphorylating proteins at serine or threonine close to an aspartic acid can protect the proteins from caspase recognition and the apoptosis is avoided (Tozser et al., 2003). In addition CK2 can also directly regulate the caspase activity for example by means of phosphorylating caspase 9 and protecting it from caspase 8 cleavage, or phosphorylating caspase 2 and preventing its dimerization/activation (McDonnell et al., 2008; Shin et al., 2005). Taken together, all of these implications of CK2 in cell cycle regulation and apoptosis make clear that a down regulation of CK2 may cause drastic and important consequences in the cell ending with high probability in an oncogenic phenotype. More deeply CK2 is not itself an oncogene, which is a gene that has the potential to cause cancer and usually it's mutated and overexpressed in certain types of cancer cells, but has a role on ensuring survival of a wide variety of cancer where its high activity is not due to genetic modification but to the alteration of the global chemical environment inside the cell; and in this direction, it has been proposed that different kind of tumors became somehow "addicted" to CK2 (Ruzzene and Pinna, 2010). While CK2 is expressed in all cells, normal or transformed, its level and possibly its substrates significantly differ and this suggests that tumor cells rely more deeply on CK2 activity for their survival pathway than normal cells do. The number of tumor and cancer cells that crucially depend on CK2 levels for their survival is

continuously growing (Table 1.3):

Table 1.3 Cell lines which show a high level of activity of CK2.

Neoplasia	**Cell type**
T-cell leukemia	Jurkat, CEM , HPB-ALL, TAIL-7, primary cells
Burkitt lymphoma	Raji
MM	OPM2, U266, RPMI 8226, primary cells
BCR/ABL-positive lymphoblastic leukemia	PLC1, B1, B2
AML	NB4, HL60, primary cells
NPM/Alk-positive ALCL	Karpas299, SR786, SUDHL 1
Murine leukemia	P388
Osteosarcoma	U2OS
Ovarian carcinoma	2008
Prostate carcinoma	PC-3, LNCaP, DU-145, ALVA-41
Colon carcinoma	HCT8, HCT116, HT29 ,DLD-1, SW-480
Hepatocellular carcinoma	HepG2, Hep3B
Endometrial cancer	IK, RL95, primary cells
Rabdomiosarcoma	JR1, Rh30, RD
Pancreatic cancer	MiaPaCa2, DanG
Cervical cancer	HeLa
Breast cancer	MCF-7, NF639, ZR-75, SKBr-3, Hs578T, MDA231
Squamous cell carcinoma	SCC-15
Lung carcinoma	A549, H1299

Based on Ruzzene and Pinna 2010.

What makes CK2 atypical from the other kinases is that it is not implicated in "hierarchical" signaling cascades but it rather plays a "lateral" role acting in different "longitudinal" pathways: due to this involvement in different pathways it is difficult to determine which are essential and which are more "complementary". So CK2 must be considered as a "master kinase" which has the ability to integrate and consolidate different biological mechanism.

The scenery is even more complicated due to the lack of a clear mechanism of regulation for CK2. CK2 has been considered for decades a "constitutive active" kinase and this adjective has found structural meanings in all of the structures published in the database. In the next chapter I will discuss all of the peculiar structural features of CK2 and how the biological activity of CK2 finds its answer in the crystal structure.

1.3.3 Structural Biology of CK2

CK2 has in the cell a tetrameric architecture composed of a CK2β_2 dimer and two catalytic subunits CK2α or α' which can also combine giving a chimeric holoenzyme (CK2$\alpha_2\beta_2$ CK2$\alpha'_2\beta_2$ or CK2$\alpha\alpha'\beta_2$). The structural analysis of CK2 started in the 1990ies and now in the database are present more than 60 structures of different CK2 subunits. The more studied are the CK2α and the CK2β and only two structures are present for the CK2α' and for the CK2 holoenzyme.

1.3.3.1 CK2 catalytic subunit

CK2 catalytic subunit has the canonical bilobal shape of an EPK, with the N-lobe composed of β-sheet and only one conserved α helix, and the C-lobe predominantly composed by α helix. We can actually divide the N-lobe in two different regions composed of the conserved αC-helix and the layer of five stranded antiparaller β-sheet. In this region is present a second binding site for CK2α, composed of an hydrophobic cleft within the β-sheet layer, and it was found to be the interface region for the regulatory β subunit for the first time in a structure of catalytic maize enzyme in complex with the C-terminal tail of the CKβ subunit (Battistutta et al., 2000) (Figure 1.4).

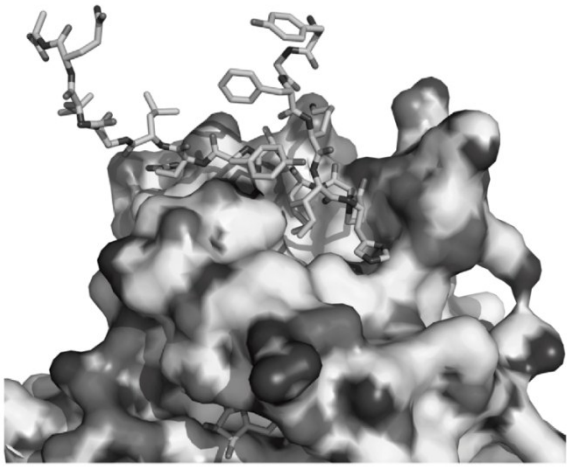

Figure 1.4 *Close-up view of the secondary (allosteric) binding site occupied by the β peptide [181-203], in the N-terminal lobe of the α-subunit (shown as surface). This is the site of major interaction between the α and the β subunits in the tetrametric $\alpha_2\beta_2$ holoenzyme (Niefind et al., 2012).*

In order to have the binding, a small loop between the β-sheet 4 and 5 (loop β4β5) has to assume a stretched conformation instead of a close one. The binding of the β subunit is incompatible with the close one and it was proposed that the opening of this loop could have a functional importance as a driving force for the interaction (Raaf et al., 2008). This hypothesis was confuted by a recent work (Papinutto et al., 2012) were we

showed that both of the conformations can occur without any apparent correlation with the occupation of the secondary binding site.

Under the β-sheet layer there's the nucleotide binding site: the Lys68 and the Glu81 are conserved residues among all the EPKs and they are part of the β3 strand and of the αC-helix respectively and they're involved in the interaction with the α and β phosphate group of the ATP (Figure 1.5).

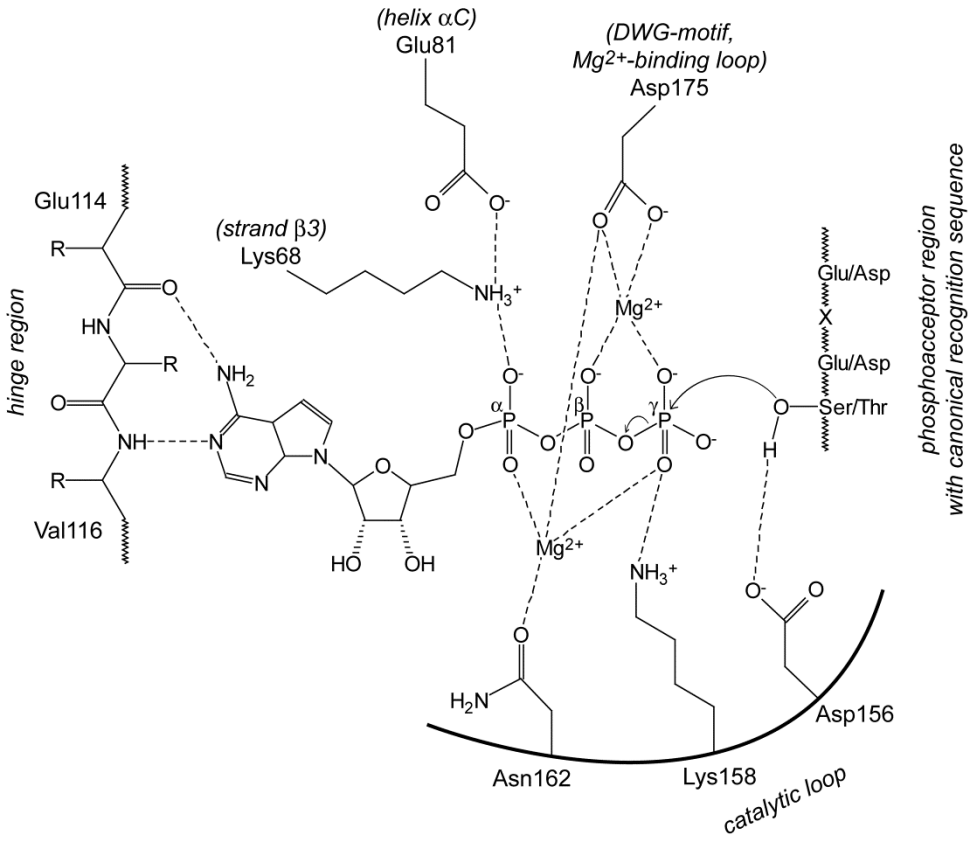

Figure 1.5 *Schematic drawing of the coordination of ATP within the active site and of the catalytic key residues. Important hydrogen bonds and coordinative bonds with the two magnesium ions are indicated by dashed lines. Water molecules completing the Mg^{2+} coordination shells are left out. The sequence numbers refer to CK2α. The phosphoacceptor region shows the minimal recognition sequence of CK2α substrates (Niefind et al., 2012).*

The aromatic ring of the ATP (or GTP) is surrounded and stabilized by the residues Val66 (part also of the C-spine) from strand β3, Val45 from strand β1, Val53 from strand β2 and Phe113 from strand β5 which create a hydrophobic compartment. This hydrophobic well is fundamental also for the design of CK2 inhibitors with high specificity and for their binding. The C-lobe of the catalytic subunit is crossed by the large and conserved αF-helix which is the basis for the two hydrophobic spines that link

the two lobes.

Another important region in the C-lobe is the “activation segment”. This element distinguishes EPKs from ELKs (Eukaryotic Like Kinase, which are prokaryotic kinase), and arises during the evolution answering to the necessity of a strictly regulation mechanism. Actually the activation segment plays a fundamental role in this context: it is formed by the magnesium binding loop (DFG/DWG motif), the “activation loop” and the P+1 loop. In many EPKs the activation loop can assume two different conformations, one fully active and the other inactive, by large rearrangement of the structure, usually due to a phosphorylation of one or more residues of the loop. In CK2 no phosphorylation site is present on the loop and no conformational change was observed within the more than 60 structures of CK2α published to date (Niefind et al., 2009). A more detailed structural analysis of all of the structures of CK2α confirmed that the activation loop is always in a conformation that is very similar to the fully active state of the nearest kinases in the EPKs (CDKs and MAP kinases). This is due to intense contact between the N-terminal domain and the activation loop giving a final structure where the αC-helix, the activation segment and the N-terminal domain is free from plasticity. One of the structural reasons for the impossibility of the activation loop to undergo a huge conformational change is an hydrogen bond across the β8–β9 joining loop between Trp176-NE1 and Leu173-O. In this way, the active state of the activation segment is stabilized by an internal constraint in addition to the contact with the N-terminal region (Niefind et al., 1998). Moreover the Trp176 goes more deeply in the hydrophobic core of the protein, and it makes 37 non-covalent contacts with the atoms of the environment, stabilizing the active conformation. Interestingly CK2α and CK2α' are the only kinases of the EPKs with a Trp instead of a Phe in the DFG/DWG triplet; a recent analysis on the active state of the EPKs found that this phenylalanine (DFG) is part of the R-spine, and that the spine is completed and fully active only with the phenylalanine in the DFG-in conformation. In the CK2α (or α') this conformation is the only possible, due to structural contacts listed before, and this strengthens the constitutively active character of the protein (Figure 1.6).

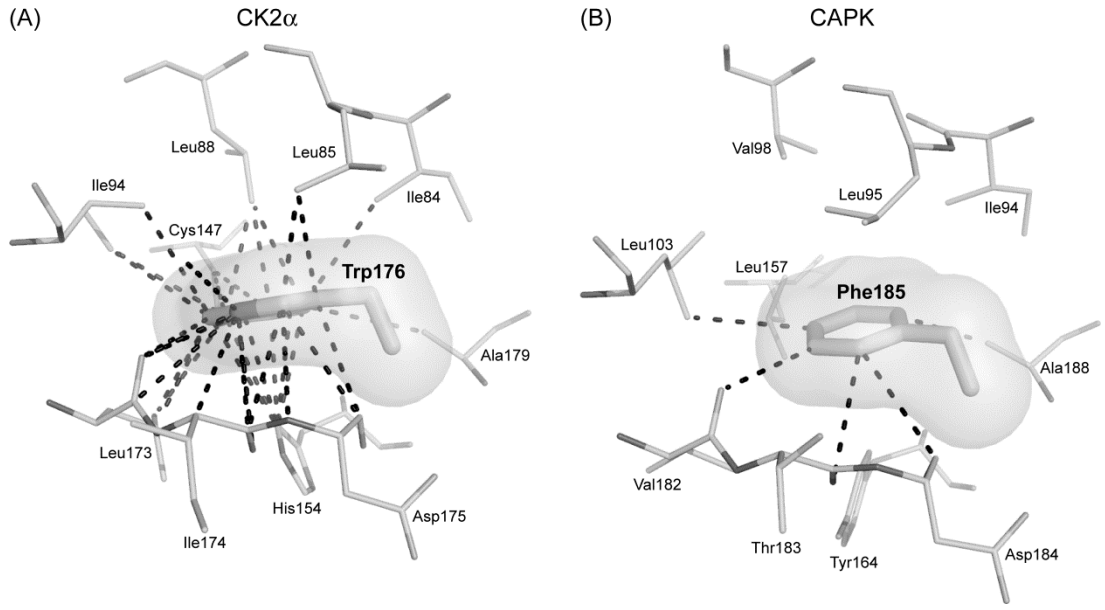

Figure 1.6 *The central side chain of the DFG-motif – a member of the regulatory spine and its atomic contacts to neighbouring residues. The atomic contacts are drawn by dashed lines with a cutoff of 4 Å.* ***(A)*** *CK2α (from maize) with the unique mutation of the DFG-motif to DW*^{176}*G. More than 30 atomic contacts are indicated, among them a 3-Å-hydrogen bond from the Trp176 side chain to the peptide carbonyl oxygen of Leu173.* ***(B)*** *PKA with a canonical DFG-motif in the "DFG-in" conformation. A comparison of the two panels reveals the intensive embedding of the Trp176 side chain into its hydrophobic environment (Niefind et al., 2012).*

Interesting and important region of the catalytic subunit is the so called *hinge/αD helix* which is responsible for the double dual-cosubstrate specificity. The hinge region connects the two lobes of the protein and supplies the hydrogen bonding counterparts for the binding of the adenine and guanine base of ATP or GTP. The hinge region is able to adopt two different conformations, an open and a close one, with the open conformation creating lot of space in the region of nucleotide binding site, giving the possibility of a dual-cosubstrate specificity due to an "hydrogen bond frame shift" of the two ligands (Figure 1.7).

This open conformation of the hinge region, reported for all the structures of maize CK2α, CK2α' and many structures of human CK2α, is unique in all the EPKs structures published to date. In this conformation the conserved R-spine is not correctly assembled because the Phe121 (equivalent to the C-spine member Met128 of PKA) is not stabilized by hydrophobic interaction with the other components of the R-spine and prefers an open conformation. But the hinge region of CK2α shows an untypical structural plasticity and it has been reported that also a close conformation is possible (Raaf et al., 2008b) and in this close conformation the R-spine is completely and correctly assembled in a EPK-canonical way (Battistutta and Lolli, 2011). So which is the "correct conformation" of the

hinge region? A recent analysis of 7 new structures of CK2α, proposed that there's not a clear correlation between all these flexible regions of the protein and that probably in solution there is an equilibrium between the two main conformations and a variety of subpopulation concerning the side chains (Papinutto et al., 2012) (Figure 1.7).

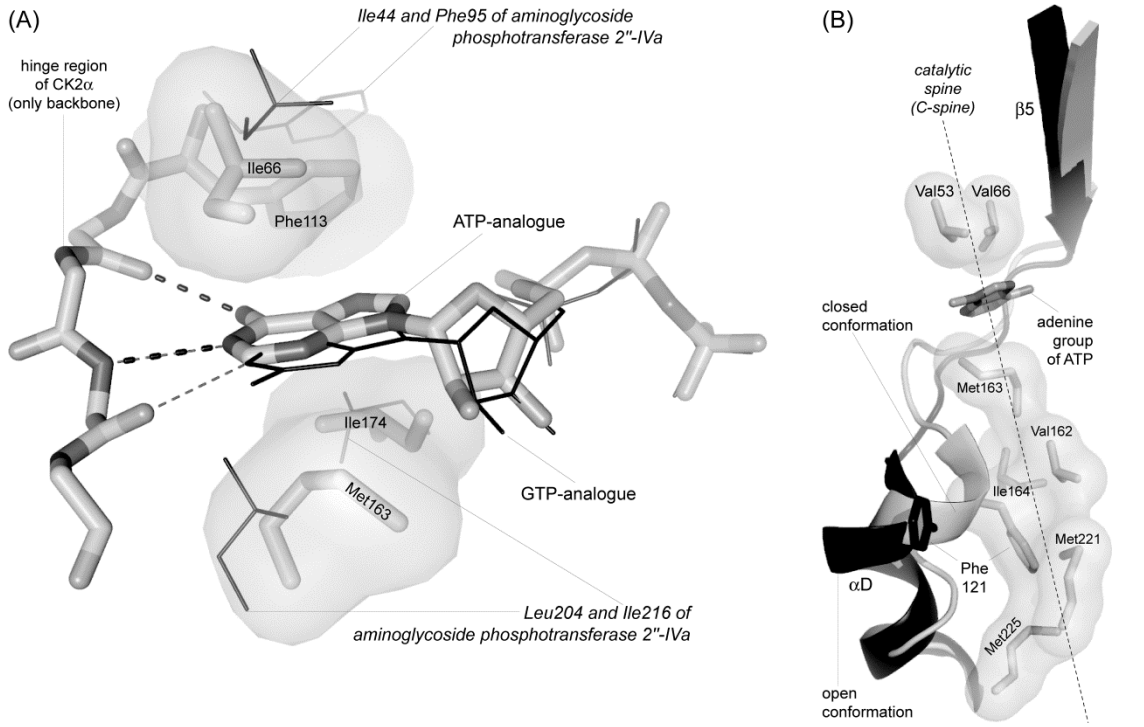

Figure 1.7 *The hinge/helix αD region:* ***(A)*** *Maize CK2α in complex with either an ATP- or a GTP-analogue. Hydrogen bonds between the purine bases and the hinge region important for binding and recognition are indicated by dashed lines. Bulky side chains that determine the "purine-base binding plane" are drawn embedded in a molecular surface. For comparison the equivalent side chains of aminoglycoside phosphotransferase 2"-IV, an enzyme with a similar dual-cosubstrate specificity like CK2 were drawn with small black bonds.* ***(B)*** *The hinge/helix αD region of human CK2α with an open (black) and with a closed conformation (grey). The catalytic spine residues of human CK2α covered by a molecular surface. Phe121 is equivalent to the CAPK-C-spine member Met128 and can adopt the EPK-canonical position only in the context of the closed conformation of the hinge/helix αD region (Niefind et al., 2012).*

Another unique feature of human CK2 paralogs (CK2α and CKα') is the C-terminal extension: this C-terminal extension is different in sequence and length and it was hypothesized to be the source of functional differentiation and regulation between CK2α and CK2α'. To strengthen this hypothesis it has been reported that the C-terminal tail of CK2α has four phosphorylation sites, phosphorylated in a cell cycle manner by Cdk1 (Bosc et al., 1995), and has also a glycosylation site (Tarrant et al., 2012) in contrast to human CK2α'. None structural information is available for the CK2α C-terminal tail because it undergoes to spontaneously degradation, or it has been truncated by

mutagenesis from crystallization trials. The only structural information for the C-terminal tail of CK2α is given by the crystal structure of the complex between the O-linked β-N-acetylglucosamine and the G^{341}GSTPVSSANM352 portion of the C-terminal tail of human CK2α. The OGT is an enzyme which catalyze the transfer of an N-acetylglucosamine group from uridine disphosphate (UDP) N-acetylglucosamine to serine side chains of protein and peptide substrates, among them to Ser347 from the C-terminal segment of human CK2α (Tarrant et al., 2012). In the complex the peptide assumes a bent conformation and is well ordered in the crystal structure (Figure 1.8).

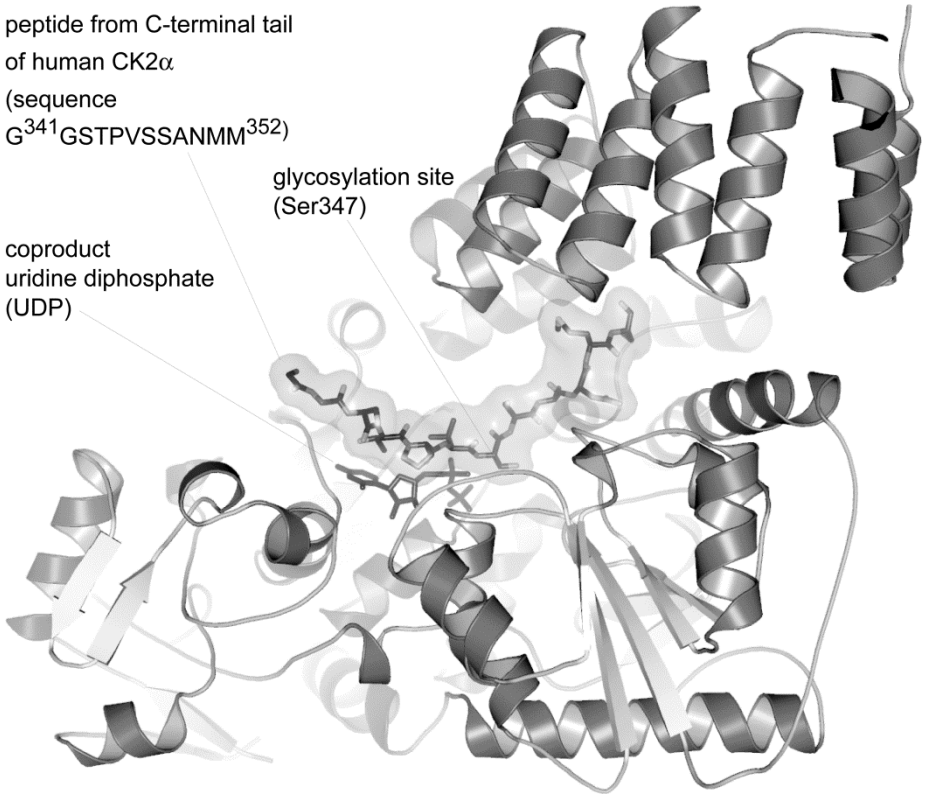

Figure 1.8 *Ternary complex structure of human O-acetylglucosamine transferase (OGT) with uridine disphosphate (UDP) and a peptide substrate derived from the (otherwise disordered) C-terminal tail of human CK2α. UDP is the coproduct of the OGT-reaction after transfer of the acetylglucosamine moiety to a serine side chain of a substrate (Niefind et al., 2012).*

1.3.3.2 CK2 regulatory subunit

The regulatory subunit is an obligate dimer and only in this form has a structural stability and a functional competence (Canton et al., 2001). The monomer of CK2β can be divided in two structural sub-domains: domain I (N-terminal domain) and domain II (C-terminal domain). The domain I is composed mainly by α-helix (αA, αB, αC, αD and

αE) where αD (40 Å long) and αE form a “L” structure, as stem and base respectively. Another important region of the domain I is the “acidic groove” composed by elements from αC (Asp51), αD (Asp70, Glu73, Glu77) and the loop connecting the two helix named “acidic loop” (Asp55, Glu57, Asp59, Glu60, Glu61, Glu63, Asp64) (Chantalat et al., 1999). This acidic cluster has been reported to be able to bind polyamines like spermine (Leroy et al., 1995), polycationic molecules that are able to stimulate the CK2 activity in vitro. A similar up-regulating effect has been detected with mutational studies on this region, where negative charge was reduced by substituting charged residues with alanine resides. For years it has been proposed that the acidic loop could have a down-regulatory effect on the CK2 holoenzyme activity; but this hypothesis was always weakened by the distance reported in the CK2 crystal structure between the catalytic cleft and the acidic loop. (Niefind et al., 2001) Only recently a new crystal structure of the holoenzyme seems to have clarified the mechanism of how CK2 can undergoes to an autoinhibitory polymerization mediated by the acidic loop (Lolli et al., 2012). The domain II is composed of three-stranded beta sheet and one single α-helix (αF). In this domain 4 conserved cysteines (Cys109, Cys114, Cys137 and Cys140) are involved in a Zn^{2+} binding motif, which is very similar to the zinc-binding site of the transcriptional elongation factor TFIIS. To avoid aggregation problems with the full length β-subunit, the last 35 amino acids were deleted for obtaining the crystal structure of the dimer; these residues are implicated in the CK2α binding as proved by mutational studies (Boldyreff et al., 1993) and are able to bind also to the maize catalytic subunit (Battistutta et al., 2000) (Figure 1.4). These 35 amino acids don't make any contact with the body of the monomer and they cross the entire dimer in contact with the other monomer up to Tyr188 where it makes a deviation forming two-stranded antiparallel β-sheet (β4 and β5) fundamental for the CK2α binding (Figure 1.9). In the last structure published of the holoenzyme (PDB code 4DGL) the entire C-terminal tail, until residue Arg215, has been defined for the first time, and it is in contact in the crystal with some residues of the catalytic cleft coming from a neighboring tetramer (Lolli et al., 2012).

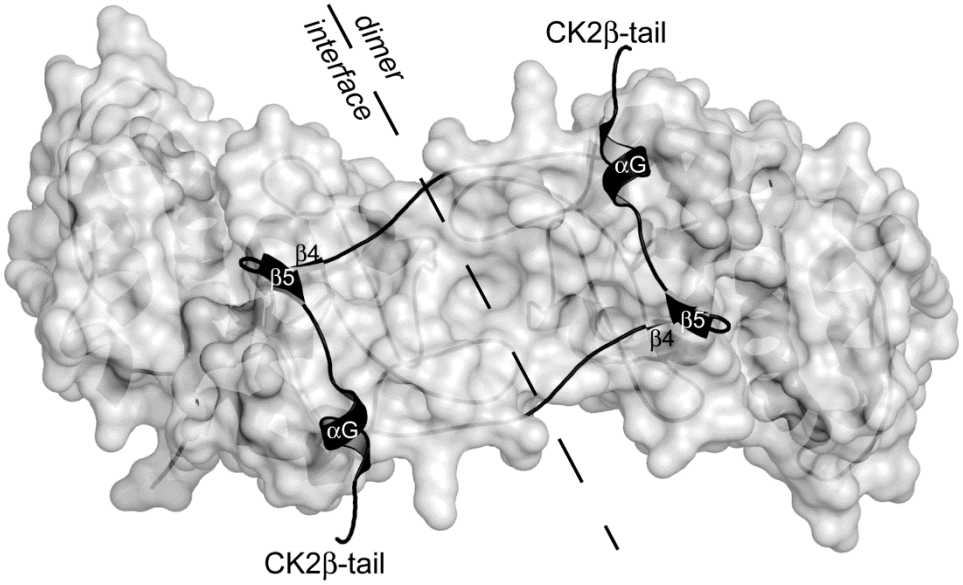

Figure 1.9 *CK2β tail (black) penetrating the dimer interface and being attached to the CK2β body of the neighbouring subunit. The CK2β body dimer is covered with a molecular surface (Niefind et al., 2012).*

1.3.3.3 CK2 holoenzyme

In vivo the fully functional form of CK2 is considered the $\alpha_2\beta_2$ holoenzyme, a heterocomplex of 140 kDa composed of two catalytic α-subunits and two regulatory β-subunits. Only two structures for the holoenzyme are available dated 2001 (PDB code 1JWH) (Niefind et al., 2001) and 2012 (PDB code 4DGL) (Lolli et al., 2012), and they represent the only structural knowledge about the α/β interaction to date:

- a central β_2 dimer recruiting two catalytic α-subunits on opposite sites;
- the global architecture has a butterfly shaped enzyme;
- the two α-subunits attached to the β_2 dimer do not touch each other;
- the C-terminal tail of the β-subunit is the main element involved in the α/β interface;
- the α interface is located in the outer part of the N-lobe β-sheet.

The formation of the holoenzyme causes only minor conformational changes between CK2β-bound and unbound CK2α, leaving unaltered the structural determinants for an effective catalysis, already present in the isolated α-subunit (Lolli et al., 2012), in accordance to the constitutive active enzyme. So the structure of the holoenzyme doesn't explain how the CK2β is able to modulate the activity of the CK2α and if there is a regulation mechanism hidden behind this interaction.

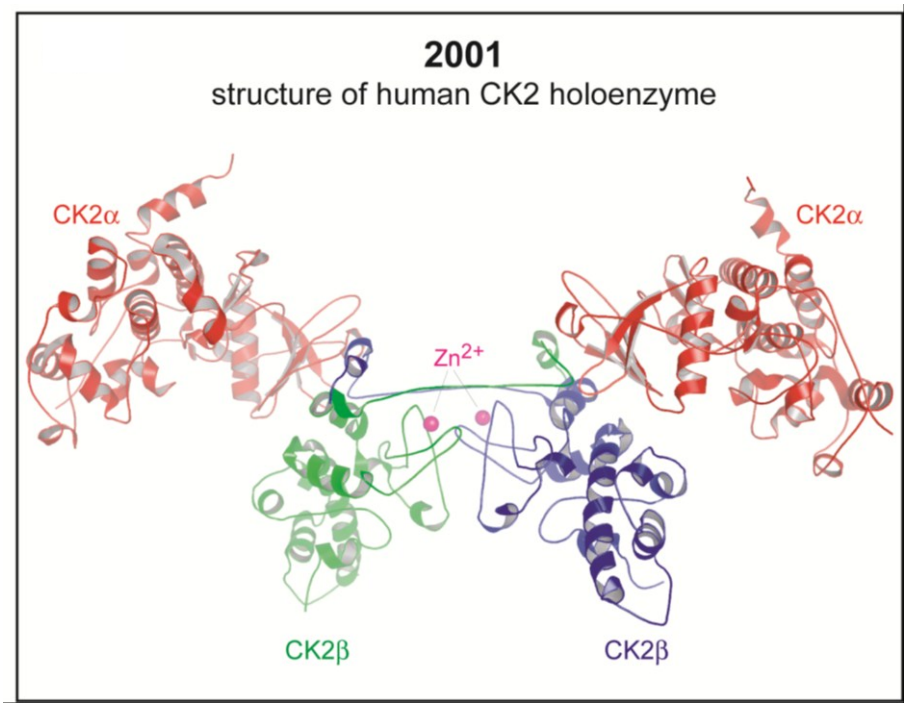

Figure 1.10 *Structure of a heterotetrameric human CK2 holoenzyme complex (Niefind et al., 2001; PDB 1JWH) and disclosing the fact that the CK2α/CK2β interface is formed by three protomers, namely one CK2α subunit and both CK2β chains (Niefind et al., 2012).*

From the structures of the holoenzyme it is clear that both of the CK2β monomers cooperate to form the α/β interface giving a final heterotrimeric contact (Niefind et al., 2001): as said before, the main interaction element is the C-terminal tail of one CK2β monomer which gives a total interaction area of 490 $Å^2$ (1JWH) (603 $Å^2$ for 4DGL). But this is complemented by about 340 $Å^2$ (415 $Å^2$ for 4DGL) arisen from the contact with the other CK2β monomer. This last contact involves elements from the body of the regulatory subunit, mainly from αF-helix and in minor parts from αD-helix and is fundamental to increase the total interaction area to a main value of 830 $Å^2$ (1018 $Å^2$ 4DGL). This value draws the attention of the scientists to the total interaction area required for a stable or transient complex; in particular it was hypothesized that this relatively small interaction area was sufficient only for a non-permanent protein/protein complex (Niefind et al., 2001) which is in contrast to the reported strong denaturation condition to dissociate the complex. The main residues involved in the interaction are the Tyr188 and Phe190 as proved by mutational experiments (Laudet et al., 2007) and by the structure 4DGL which shows how the Phe190 fills the hydrophobic cavity of the α-catalytic subunit (Lolli et al., 2012). As reported before, CK2 has been considered for years a "constitutive active" enzyme due to the lack of clear mechanism of regulation for

the kinase. One of the first methods of regulation proposed for CK2 comes from the tendency of CK2 to form regular aggregates under certain conditions (Glover, 1986). In 1986 Glover found that aggregation of Drosophila CK2 at low ionic strength results from a polymerization of the enzyme to form linear filaments. The forces that stabilize the polymer were in contrast with the forces that stabilize the tetramer (stable up to 1M NaCl). The results were confirmed in 1995 by Valero and co-workers (Valero et al., 1995) and they were able to distinguish three different form of CK2 composed by the single protomer, a ring-like structure and a filamentous form. Another interesting feature of CK2 which could be involved in the regulation of the enzyme is that CK2 is found extensively autophosphorylated in vivo, when obtained from cells (Litchfield et al., 1991). The autophosphorylation sites are βSer2 and βSer3 and mutation in alanines of the acidic residues of the acidic loop prompt to a inhibition of the autophosphorylation and to an hyperactivation of the enzyme (Pagano et al., 2005). All of these singular features of CK2 are elegantly described by a structural point of view, in the last structure of the holoenzyme published in 2012 (Lolli et al., 2012): in this article autophosphorylation and the tendency to form aggregates of CK2, are in accordance with the trimeric organization of the butterfly shaped tetramers found in the crystal packing of the 4DGL structure. In this trimeric organization the autophosphorylation sites are really close to the catalitic cleft of CK2α coming from neighboring tetramers, the surface of interaction within the three tetramers is very extended and composed mainly of electrostatic interaction (in accordance with the low ionic strength-dependence of polymerization) and the ring like shape and the piling organization within the crystal can well describe the different oligomeric forms found with electron microscopy images. The beta subunits play a crucial role in this super-molecular organization, because the main contact within the tetramer is the acidic loop-basic stretch interaction between different tetramers. In this polymeric organization CK2 is supposed to be completely inactive due to steric hindrance of the catalytic cleft of CK2α, by different elements coming from neighboring CK2β; this inhibition by polymerization has been also discussed in the past (Poole et al., 2005) with the conclusion that CK2 in vivo might be a “constitutive inactive” kinase that is stimulated by alterations of the ionic status and by polycationic activators. So recently the idea of a “constitutive active” kinase is changing with the new data about the auto-inhibitory polymerization, but some points remain open to discussion: the small CK2α/CK2β interface and the asymmetry found in both of the CK2 structures keep open the question whether the tetramer is a stable complex or a non-obligate complex or simply

a transition state between isolated CK2α and CK2β subunits and order super-molecular aggregates (Figure 2.22).

1.3.4 CK2 inhibition

The interest in developing small molecules that can act as kinase inhibitor has grown enormously since the first project started by Novartis 25 years ago, not only in the pharmaceutical industry but also in the academic research. In fact these small molecules can be useful also for studying many cellular pathways, like signal transduction, cell cycle regulation, development, apoptosis and others (Hemmings et al., 2009). Nowadays protein kinases (codified by the 2% of the genome) are the second most important drug targets after the G-protein-coupled receptor, and they represent the 20-30% drug discovery project in pharmaceutical companies (Hemmings et al., 2009). Targeting kinases with drug inhibitor molecules is not interesting just because kinases are usually related to cancer development, but also because they are implicated in different kind of pathologies as well: for example kinases are implicated in the inflammatory response, autoimmune disease and neurodegenerative disease.

As described before, CK2 is essential for viability and it is implicated in different kind of biological pathways, so it can be considered a potential drug target for cancer therapy on the basis of different evidences: CK2 activity is elevated in several cancer cells, it is a potent suppressor of apoptosis promoting the survival of the cell and it promotes the multi-drug resistant phenotype (Battistutta, 2009). Recently CK2 has been discovered to be involved in neurodegenerative disease like Alzheimer's disease and Parkinson's disease but also in viral infection, because virus uses CK2 for the phosphorylation of some fundamental exogenous proteins, and in inflammation and cardiovascular diseases; for these reasons the development of CK2 inhibitors acts in different pharmacological fields, with a multi-potential perspective.

Within the kinase family there is a conservation of many different structural elements, and part of this is the ATP binding site; to complicate the scenario there are other proteins inside the cell that are able to bind ATP. Another problem is the high concentration of ATP inside the cell (1-10 mM) that competes with the inhibitors for the binding to the kinase. Fortunately even if the catalytic cleft is globally conserved from the structural point of view, small differences at the level of single amino acids substitutions

are able to confer the possibility of an efficient and selective drug design with the result that many ATP-competitive kinase inhibitors (more than 130) are now in clinical trials (Fabbro et al., 2012). The selectivity of an inhibitor is therefore fundamental and it is actually the most difficult issue to achieve; anyway it has been proposed that the absolute selectivity for one single target is not a mandatory requirement for kinase inhibitor that aims to become a useful target. This is due to the fact that in cancer the pathways that promote proliferation and survival, are regulated not by a single kinase but by different kinases, comprising CK2, and therefore inhibiting different kinases at the same time seems a promising approach for cancer treatment. This concept of "one drug - many targets" having some non-specific effect on other kinases, has recently attracted the attention not only for inhibitor of kinases but also for other kind of drugs (Imming et al., 2006).

1.3.4.1 ATP-competitive inhibitors

The ATP-binding site of protein kinase can be divided into three hydrophobic (adenine region and hydrophobic region I and II) and two hydrophilic regions (sugar pocket and phosphate binding region) (Fig. 1.21). ATP-competitive inhibitors are divided in two different classes: Type I and Type II. The Type I inhibitors target the protein in its active conformation (DFG-in conformation of the activation loop) and bind preferentially in the hydrophobic region of the adenine. These kinds of inhibitors are actually the most common inhibitors currently available for kinase inhibition and also for CK2. Type I inhibitors usually interact with the hinge region of the kinase and make hydrogen bounds with the backbone of the residues miming the interaction with the amino group of the adenine ring of the ATP. Type II inhibitors on the other hand bind to the inactive state of the protein kinase (DFG-out conformation of the activation loop) but have also contacts with the hinge region of the kinase (Battistutta, 2009).

1.3.4.2 Structural aspect of inhibition by Type I ATP-competitive inhibitors

CK2 bears most of the common sequence and structural features conserved during the evolution and found in most of the other kinases of the human kinome. The only two differences found in the primary sequence for the CK2 are the missing of a conserved third glycine in the phosphate-anchor loop, residues 46-51 GXGXøG (usually the ø is a

tyrosin or a phenylalanine like for the Pim kinase) and the substitution of the conserved DFG triplet, at the beginning of the activation segment, with a tryptophan (W176) instead of the phenylalanine. Another important feature of the primary sequence of CK2 is the presence of a basic cluster at the beginning of the helix αC (resides 74-80) where 6 of the 7 amino acids are basic residues.

CK2 is an constitutive active kinase, because of its unique structural features, so only the active conformation of the kinase can be tagged with ATP-competitive inhibitors and as a consequence only the Type I inhibitor are available for CK2. They establish direct polar interaction with a limited, conformationally rigid, portion at the N-terminal part of the hinge/αD region (backbone of residues Glu114 and Val116) and/or with the deeper part of cavity, principally with some conserved water and with the lysine 68. A recent analysis of the flexible region of the protein showed that ligands that don not use the hinge/αD region for the binding to the protein would, at least in principle, bind in the same way to the CK2 with an open (like CK2 maize enzyme) or close conformation of the hinge region. This concept has been demonstrated for two CK2 inhibitors like emodin (1,3,8-trihydroxy-6-methyl-antraquinone) and for quinalizarin (1,2,5,8-tetrahydroxy-anthraquinone) (Figure 1.11), which have been crystallized with an open and a close conformation of the hinge/αD region: both of the inhibitors bind in the same way to the kinase with an open or close conformation of the hinge/αD region (Papinutto et al., 2012). The overall structure of the protein is only marginally affected by the binding of the inhibitor, with the C-lobe of the protein poorly influenced by the complex formation, and with N-lobe of the protein which has a much higher degree of flexibility in particular on the phosphate anchor loop. The other regions which have a structural plasticity are the His160, the hinge/αD region and the stretch from residues 102 to residues 108 comprising the external loop between strands β4 and β5 (β4-β5 loop) (Papinutto et al., 2012).

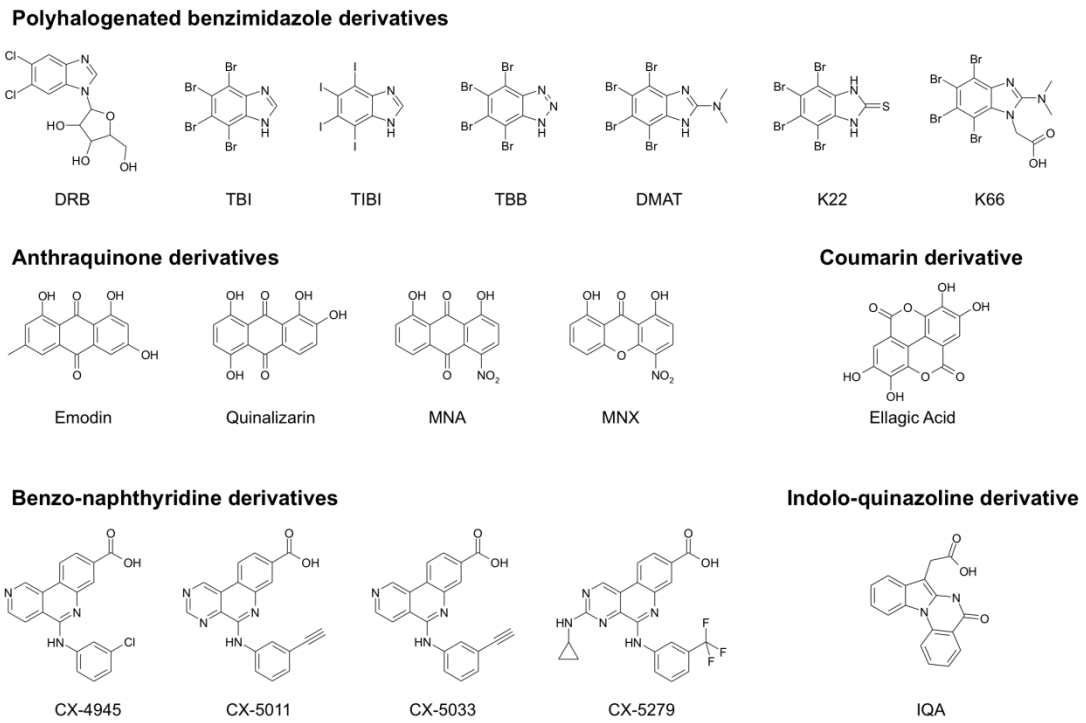

Figure 1.11 *Structural formulas of the principal CK2 inhibitors, grouped by chemical classes (Niefind et al., 2012).*

The binding site of CK2 is composed of the residues Leu85, Val95, Leu111, Phe113, and Ile174 (hydrophobic region I), Val53, Ile66, Val116 and Met163 (adenine region) and Val45 and Tyr115 (hydrophobic region II) (Figure 1.12); this hydrophobic surface of the CK2 binding pocket is fundamental for the hydrophobic interactions and van der Waals contacts with the small ligand, which give the most important energetic contribution to the binding.

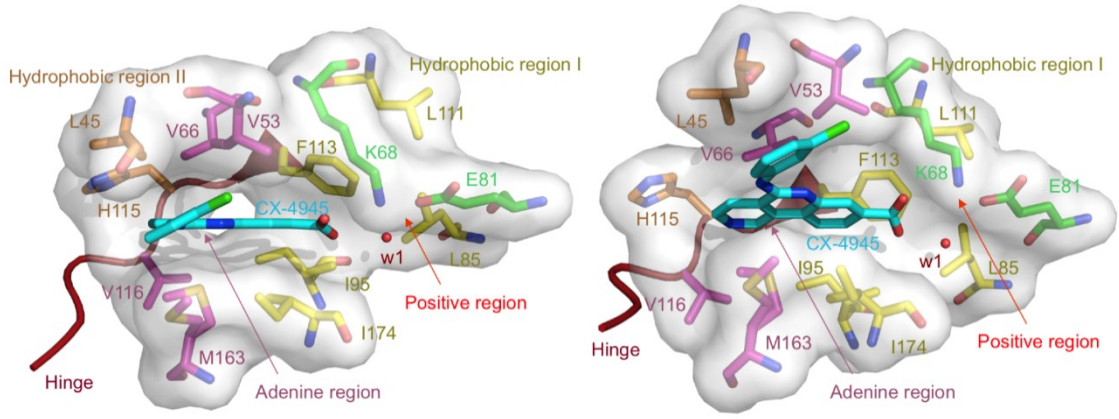

Figure 1.12 *Main structural features of the CK2α ATP-binding site shown in two different orientations. The active site is occupied by the CX-4945 inhibitor (cyan). Residues of the three hydrophobic regions common to the "kinase pharmacophore" are shown in yellow (hydrophobic region I, in the deepest part of the cavity), in orange (hydrophobic region II, at the entrance of the cavity) and in magenta (adenine region). Other important elements of the CK2α pharmacophore are the hinge region (dark red) and the area with a positive electrostatic potential near the salt bridge between Lys68 and Glu81, where the fully conserved water molecules w1 is located. These two regions are the main polar anchoring points for CK2 inhibitors (Niefind et al., 2012).*

The binding pocket of CK2 is smaller with respect to the other kinases, and this is due to the presence of some bulky side chains like Val66 and Ile174, which in the other kinases is replaced with a less cumbersome amino acids like alanine and leucine. For instance, the inhibitor TBB (4,5,6,7-tetrabromo-1-benzotriazole) binds in a different way to CDK2, which is a kinase belonging to the closely related CMGC group of the kinase family, with respect to CK2. This difference in binding is precisely due to the fact that the binding site of CDK2 is larger than CK2 because of the presence of alanine instead of the isoleucine 66 and 174, and as a consequence TBB shows an remarkable affinity for CK2 (Figure 1.13). In particular in these kind of tetra-halogenobenzo derivates the bulkiness of the four halogen atoms is essential for the potency of the inhibitor with an increasing value upon the replacement of chlorine with bromine and even more with iodine.

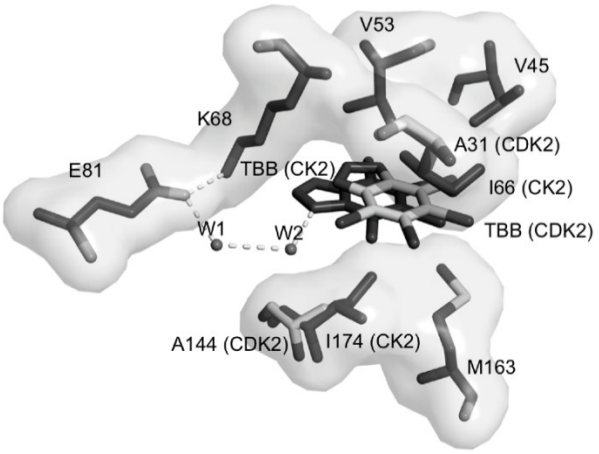

Figure 1.13 *TBB binds to CK2 (light grey) and CDK2 (dark grey) with different poses. Bulky CK2 residues Ile66 and Ile174 are substituted with two alanines (31 and 144) in CDK2, whose active site results larger. The different shapes of the active sites determine the two diverse binding modes of TBB to the kinase (Niefind et al., 2012).*

An analysis of the electrostatic potential inside the catalytic site, revealed that there's a positive charged region located in the deeply area of the cavity near the hydrophobic region I and the salt bridge between Lys68 and Glu81; for this reason if in the inhibitor is present a negatively charged moiety, like the acidic triazole ring of the TBB or the CX compounds, it tends to cluster in this region of the ATP-binding site. Another important feature of the deeper part of catalytic cleft is the presence of a conserved water molecule, called water molecule 1 (W1), which is present in all the CK2 crystal structures published to date. It makes hydrogen bounds with the amidic NH of Trp176, with carboxylic oxygen of Glu81 and with another conserved water molecule (W2) which can be eventually replaced by a portion of a certain ligand (Emodin or CX compounds) (Figure 1.12).

In general to be a good ATP-competitive inhibitor of CK2 a small ligand should have: an appropriate hydrophobicity to pass quickly from the aqueous phase to the hydrophobic site, an excellent shape complementary with the small and unique active site of CK2 and, most importantly, the capability to establish electrostatic interaction with the positive area near the W1 and hydrogen bounds with the possible anchoring points in the hinge region (Val116 and Glu114).

To be useful as biochemical tools and to be considered compounds with pharmacological potential inhibitors must be cell permeable and active in cells. CX-4945, CX-5011, and CX-5279 all display cell permeability and high efficacy as antiproliferative

agents when tested on a variety of cancer cells (Pierre et al., 2011). Polyhalogenated benzimidazole (or triazole or pyrazole) derivatives, namely DMAT, TBB, TBI are all cell permeable and were among the most frequently used CK2 inhibitors for *in vivo* studies. However, there are other types of inhibitors, despite of their potency *in vitro*, which the practical use *in vivo* is hindered by deliverability problems, limiting their pharmacological potential and the possibility to use them as biochemical tools.

The new concept of "one-drug many-targets" has been recently applied also for CK2 in the identification of difurandicarboxylic acid derivatives as potent dual inhibitors of this protein kinase and PIM kinases, two structurally and functionally related kinases. Crystal structures of CK2 and PIM1 complexes suggested that the basis of the selectivity of this class of compounds mainly relies on the narrower ATP-binding site of both CK2 and PIM1, and particularly on the presence of two conserved isoleucine (Ile174 and Ile95 in CK2, Ile185 and Ile104 in PIM1) (Lopez-Ramos et al., 2010).

1.3.4.3 Non-ATP-competitive inhibitor (Type III Inhibitor)

This kind of compounds do not target the active site of the protein but they're able anyway to down regulate the activity of the kinase; examples of allosteric inhibitors, which display no contact with the hinge region, have been proposed also for CK2. The first Type III inhibitor for CK2 which was crystallized with CK2 is DRB: despite its ATP-competitive activity, a second molecule of DRB was found in the hydrophobic cavity near the loop β4-β5, which is the main interacting zone for the CK2β for the holoenzyme formation. The binding of the DRB shows a non-competitive inhibitory effect that was discriminated from the ATP-competitive one (Raaf et al., 2008b), but more interesting the identification of this new binding site is important also for the possibility to selectively interfere with the assembly of the tetrameric enzyme (Figure 1.14).

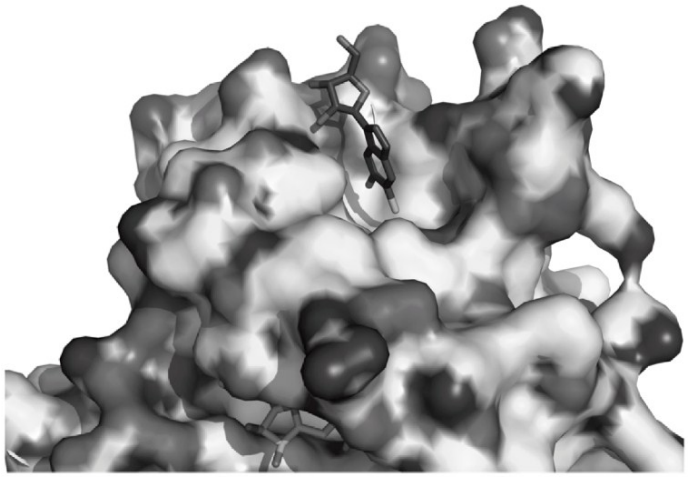

Figure 1.14 *Close-up view of the secondary (allosteric) binding site occupied by inhibitor DRB, in the N-terminal lobe of the α-subunit (shown as surface) (Niefind et al., 2012).*

Another recent example of non-ATP compound was design on the basis of the α/β interface of CK2, and it is composed of a cyclized peptide containing the sequence Arg186-His193 of the CK2β. This cyclic peptide is able to inhibit the formation of the holoenzyme and to affect the substrate preference (Laudet et al., 2007). Due to the lack of the crystal structure of this compound with the CK2α the exact mode of binding is unknown but presumably it binds in the same way of the CK2β C-terminal tail and also in the same area of interaction (like the linear peptide and the DRB). The DRB with the human CK2α and the linear peptide of the β-subunit are not the only molecules found in this allosteric site; in particular structures of human CK2α with other small ligands like PEG or ethylenglycol (Papinutto et al., 2012) or glycerol (Raaf et al., 2008b) have been reported. None of these structures shows significant conformational changes inside the active site that can be related to a modulation, either negative or positive, of the catalytic activity of the isolated CK2α and to date there are no clear explanation for the structural effects of the binding to the secondary "allosteric" site.

The design of specific inhibitor of the α/β interaction is fundamental for the study of the assembly of the CK2 tetramer, inhibiting it *in vivo* and could be used as a tool in the study of the substrates which phosphorylation is dependent on the presence of CK2β.

1.4. Aim of the project

Most of the knowledge related to the structural characteristics of CK2 has come from studies within the last fifteen years and the interest in this enzyme has expanded, as shown by the increasing number of publications within recent years. Despite the increasing interest in this protein, a substantial amount of research is needed to understand its mechanism of regulation in human physiology. The structural characterization is an essential step to understand how CK2 is regulated in all of the biological processes, which have been reported to be related with the kinase.

Even if the structural knowledge of CK2 is very extended, very little is known about the C-terminus of CK2α and no high resolution 3D-structure is available for the full-length sequence. This region is supposed to be very flexible and non-structured in solution but it has been reported that CK2 can be phosphorylated in a cell cycle dependent manner at residues located in this C-terminal portion.

Moreover no 3D structure of the tetrameric holoenzyme with the catalytic subunit CK2α' is present in the literature. The paralog isoform of the catalytic subunit CK2α', present in humans and higher animals, is very similar in sequence to the CK2α up to position 330, while the C-terminal segments differ completely in length and sequence. The knowledge on CK2α' is much lower than the paralog isoform CK2α; the main reasons are the reported solubility problems that occur after the expression in hosts cells like *E. coli* or insect cells.

To this purpose the first part of the PhD project focused on the production and crystallization of a stable full-length CK2α phosphomimetic mutant and a tetrameric holoenzyme with the same catalytic subunit, in order to study the possible structural role of the C-terminus. Using the same protocol we worked on the production and crystallization of other forms of tetrameric holoenzyme with the wild type full-length CK2α and with its C-terminus deleted form.

The second part of the project concerned with the development of a protocol for the production of the holoenzyme with the CK2α' subunit and the physiological chimeric holoenzyme composed of CK2α and CK2α'. We started with the full-length mouse CK2α' conjugated with the GST tag which may increase expression and solubility of the recombinant fusion protein.

A part of my PhD project focused on the interaction between CK2 and small ligand which can compete with the ATP for the binding to the kinase. In collaboration with the

laboratories of Professor Pinna and Professor Moro, we studied the interaction between the CK2α336 (deleted at residue Ser336) and a potent and selective Type I ATP-competitive inhibitor, called K164. We worked on the crystallization condition of the apo form of $CK2\alpha^{336}$ which was fundamental for the obtaining of the structure of the complex between the ligand and the kinase.

2. CK2α phosphomimetic mutant and CK2 holoenzyme $CK2\alpha_2\beta_2$

2.1 CK2α phosphomimetic mutant

2.1.1 Methods

2.1.1.1 Overview

We know that CK2α subunit undergoes to phosphorylation by Cdk1 in a cell cycle dependent manner; the four phosphorylation sites are located in the C-terminal tail of the protein namely at Thr344 and 360 and Ser362 and 370. The only structural information present in the literature about the C-terminal tail is the structure of the O-GlcNAc transferase in complex with a peptide substrate composed of the c-terminal tail of the CK2 341PGGSTPVS*SANM352 (Figure 1.8).

The C-terminal tail of CK2 is absent in all the structures published in the database because it was deleted by mutagenesis or by auto-proteolysis; the reason of this deletion is that the C-terminal tail is flexible in solution and shows a high degree of degradation which can give after the purification a non-homogeneous sample not suitable for the crystallization. For this reason, the first problem to overcome was obtaining a full-length protein with a low degree of degradation.

To investigate if the phosphorylation of the four residues could have a structural role at the level of the CK2α monomer or at the level of the holoenzyme, we mutated the four residues in four glutamic acids to mimic the negative charges of the phosphate group.

```
CK2α            MSGPVP-SRARVYTDVNTHRPREYWDYESHVVEWGNQDDYQLVRKLGRGKYSEVFEAINI 59
CK2α'           MPGPAAGSRARVYAEVNSLRSREYWDYEAHVPSWGNQDDYQLVRKLGRGKYSEVFEAINI 60
                *.**.. ******::**: *.*******:** .**************************

CK2α            TNNEKVVVKILKPVKKKKIKREIKILENLRGGPNIITLADIVKDPVSRTPALVFEHVNNT 119
CK2α'           TNNERVVVKILKPVKKKKIKREVKILENLRGGTNIIKLIDTVKDPVSKTPALVFEYINNT 120
                ****:*****************:*********.***.* * ******:*******::***

CK2α            DFKQLYQTLTDYDIRFYMYEILKALDYCHSMGIMHRDVKPHNVMIDHEHRKLRLIDWGLA 179
CK2α'           DFKQLYQILTDFDIRFYMYELLKALDYCHSKGIMHRDVKPHNVMIDHQQKKLRLIDWGLA 180
                ******* ***:********:********* ****************:::**********

CK2α            EFYHPGQEYNVRVASRYFKGPELLVDYQMYDYSLDMWSLGCMLASMIFRKEPFFHGHDNY 239
CK2α'           EFYHPAQEYNVRVASRYFKGPELLVDYQMYDYSLDMWSLGCMLASMIFRREPFFHGQDNY 240
                *****.****************************************:******:***

CK2α            DQLVRIAKVLGTEDLYDYIDKYNIELDPRFNDILGRHSRKRWERFVHSENQHLVSPEALD 299
CK2α'           DQLVRIAKVLGTEELYGYLKKYHIDLDPHFNDILGQHSRKRWENFIHSENRHLVSPEALD 300
                *************:**.*:.**:*:***:******:*******.*:****:*********

                                                        *
CK2α            FLDKLLRYDHQSRLTAREAMEHPYFYTVVKDQARMGSSSMPGGSTPVSSANMMSGISSVP 359
CK2α'           LLDKLLRYDHQQRLTAKEAMEHPYFYPVVKEQS---------------------------- 333
                :**********.****:*********.***:*:

                * *       *
CK2α            TPSPLGPLAGSPVIAAANPLGMPVPAAAGAQQ 391
CK2α'           -----QPCADNAVLSSG------LTAAR---- 350
                     * *...*::::.      :.**
```

Figure 2.2.1 *Multiple sequence alignment of selected CK2 alpha and alpha prime ClustalW tool, EMBL-EBI. C-terminal tail is highlighted in the squares and C-terminal peptide in complex with O-GlcNAc transferase is highlighted in yellow.*

2.1.1.2 Mutagenesis

Single-site mutagenesis was performed using QuickChange® Site-Directed Mutagenesis kit (Stratagene) and PfuTurbo® DNA polymerase.

Table 2.1 Oligonucleotide primers used for mutagenesis

Single-site mutagenesis	Primers	base	Tm (°C)
T360E-S362E	5' gggatttcttcagtgccaGAGcctGAacccctttggacctctggc 3' ccctaaagaagtcacggtCTCggaCTtggggaacctggagaccg	44	79.3
T344E	5' ccaggggcagtGAgcccgtcagcagc 3' ggtcccccgtcaCTcgggcagtcgtcg	27	79.8
S370E	5' ggacctctggcaggcGAaccagtgattgctgc 3' cctggagaccgtccgCTtggtcactaacgacg	32	79.8

MIX: 2.5 µl reaction buffer, 2 µl of plasmid containing the sequence of CK2α, 4.5 µl of each primers (4.5 pmol), 0.5 µl of dNTPs, 11.0 µl of H_2O, 0.5 µl of PfuTurbo DNA polimerase (2.5 U/µl). After 16 PCR cycles we add 1 µl of Dpn I restriction enzyme (10 U/µl) for the digestion of non-mutated DNA.

The mutations have been inserted in the order of table above and after every mutagenesis we sequenced the DNA.

2.1.1.3 Protein expression

E. coli BL21(DE3) cells, harboring the plasmid pT7-CK2α phoshomimetic, were grown overnight (ON) at 37 °C in LB medium (10 g/l tryptone, 5 g/l yeast extract, and 10 g/l NaCl) supplemented with 50 μg/ml ampicillin. LB medium was inoculated with this ON culture (ratio 1:10) and grown at 37 °C, in a suitable shaker. Protein expression was induced at an OD_{600} of 0.6 by adding 1 mM IPTG and prolonged for 4-5 h at 30 °C under vigorous shaking. Bacteria were harvested by centrifugation at 5000 g for 30'.

2.1.1.4 Protein purification

In order to obtain a stable CK2α full-length protein we proceeded with a very fast protocol of purification with two purification steps performed in the same day; in this way the protein passed from the bacterial cytoplasm to the final buffer C (with a purity of ≈ 95%) and storage at -80 °C in only 8 hours avoiding C-terminal degradation. Bacteria were suspended in buffer A [25 mM Tris-HCl (pH 8), 350 mM NaCl, 1 mM dithiothreitol (DTT)] supplemented with protease inhibitors (Roche) and lysed with a French press (Thermo Spectronic) at high pressure.

The lysate was centrifuged to remove cell debris at 27000 g for 30' and filtered with 0.22 μm syringe filter. After the filtration the sample is loaded onto an affinity column performed on a Äkta FPLC chromatographic system (GE Healthcare) using a HiTrap Heparin HP 5ml (GE Healthcare) equilibrated with buffer A. After extensive washing with buffer A, the protein was eluted with a gradient of NaCl with buffer B [25 mM Tris-HCl (pH 8), 1 M NaCl, 1 mM DTT]. Fractions containing the protein were pooled and further purified by size exclusion chromatography using a Superdex 75 prep-grade 26/60 column (GE Healthcare) equilibrated with buffer C [25 mM Tris-HCl (pH 8.5), 500 mM NaCl, and 1 mM DTT].

2.1.1.5 Protein crystallization

Crystallization trials using commercial kits (Qiagen, Molecular Dimensions and Hampton Research) based on sparse matrix, grid screen, and/or ionic sampling, were

performed by vapour diffusion (with the sitting drop method) techniques, using the Oryx8 automatic system (Douglas Instrument). CK2α phosphomimetic mutant was concentrated to 15 mg/ml for crystallization purposes. Thin and fragile crystals were grown at 20 °C, using the following precipitant solution: 0.2 M ammonium acetate, 0.1 M tri-sodium citrate pH 5.6, 30% w/v PEG 4000.

2.1.1.6 Data collection, structure determination, and refinement

The data set at 3.3 Å resolution was collected at the ELETTRA-Synchrotron beamline XDR1, (Trieste, Italy). Data sets were measured at 100 K using the precipitant solution, including 10% glycerol as cryoprotectant. Crystals belonged to space group $P4_32_12$, with unit cell parameters reported in Table 2.2. Diffraction data were processed with XDS (Kabsch 2010) and reduced and merged with SCALA included in the CCP4 suite (Evans, 2005). For structure determination, molecular replacement (Phaser CCP4) (McCoy et al., 2007) was performed with the coordinates of the $CK2\alpha^{del}$ from PDB ID 3BQC. The model was then refined alternating several cycles of automatic refinement with REFMAC (CCP4) (Murshudov et al., 1997) and manual model building with Coot (Emsley and Cowtan, 2004).

2.1.2 Results

2.1.2.1 Mutagenesis

In order to mimic the negative charges of the four phosphorylated residues at the C-terminal tail of the CK2α (Thr344, Thr360, Ser362, Ser370), we mutated the four residues in glutamic acids by single-site mutagenesis; the success of the experiment was confirmed by DNA sequencing after each PCR. The primary sequence of the CK2α clone after the third experiment of mutagenesis confirmed the presence of the four mutations (the mutated codons that encode for glutamic acids are highlighted in yellow):

```
                                                          344
CK2α mut          GGACCAGGCTCGAATGGGTTCATCTAGCATGCCAGGGGGCAGTGAGCCCGTCAGCAGCG
                  ||||||||||||||||||||||||||||||||||||||||||||  ||||||||||||||
CK2α wt           GGACCAGGCTCGAATGGGTTCATCTAGCATGCCAGGGGGCAGTACGCCCGTCAGCAGCG

                                              360   362
CK2α mut          CCAATATGATGTCAGGGATTTCTTCAGTGCCAGAGCCTGAACCCCTTGGACCTCTGGCA
                  |||||||||||||||||||||||||||||||   |||  ||||||||||||||||||
CK2α wt           CCAATATGATGTCAGGGATTTCTTCAGTGCCAACCCCTTCACCCCTTGGACCTCTGGCA

                     370
CK2α mut          GGCGAACCAGTGATTGCTGCTGCCAACCCCCTTGGGATGCCTGTTCCAGCTGCCGCTGG
                  |||  ||||||||||||||||||||||||||||||||||||||||||||||||||||||
CK2α wt           GGCTCACCAGTGATTGCTGCTGCCAACCCCCTTGGGATGCCTGTTCCAGCTGCCGCTGG

CK2α mut          CGCTCAGCAGTAA
                  |||||||||||||
CK2α wt           CGCTCAGCAGTAA
```

Figure 2.2 *Multiple sequence alignment of CK2α^{wt} and CK2α^{pm}.*

2.1.2.2 Protein Expression and Purification

CK2α^{pm} (CK2α phosphomimetic mutant) was successfully expressed mainly in soluble forms in *E. coli* BL21(DE3) (Figure 2.3 lane 3).

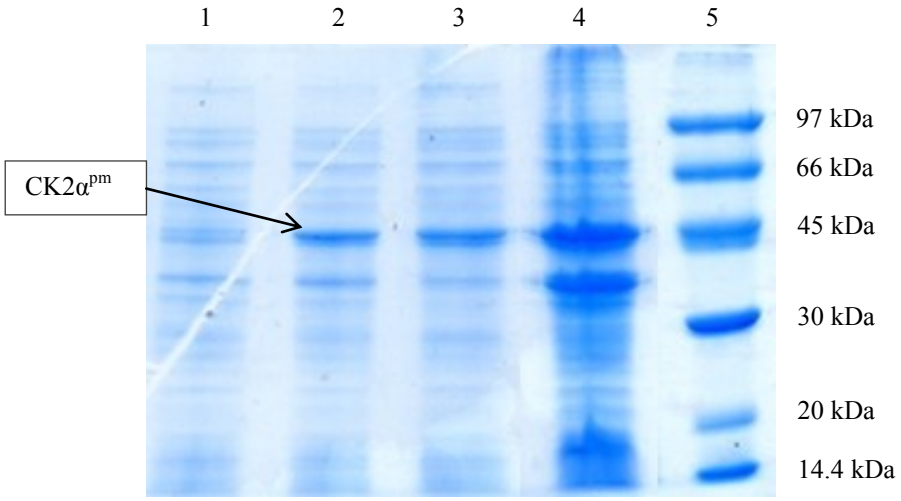

Figure 2.3 *Coomassie-stained SDS-PAGE of expression in BL21(DE3) of CK2α^{pm}. Lane 1: not induced bacterial cells. Lane 2: IPTG induced cells. Lane 3: soluble portion of bacterial lysate. Lane 4: insoluble fraction of bacterial lysate. Lane 5: low molecular weight protein markers in kDa.*

The soluble fraction of CK2α^{pm} protein was purified by an affinity step using a HiTrap Heparin column. The elution of the protein from the column was performed weakening the electrostatic interactions between CK2α and heparin molecules with a NaCl gradient.

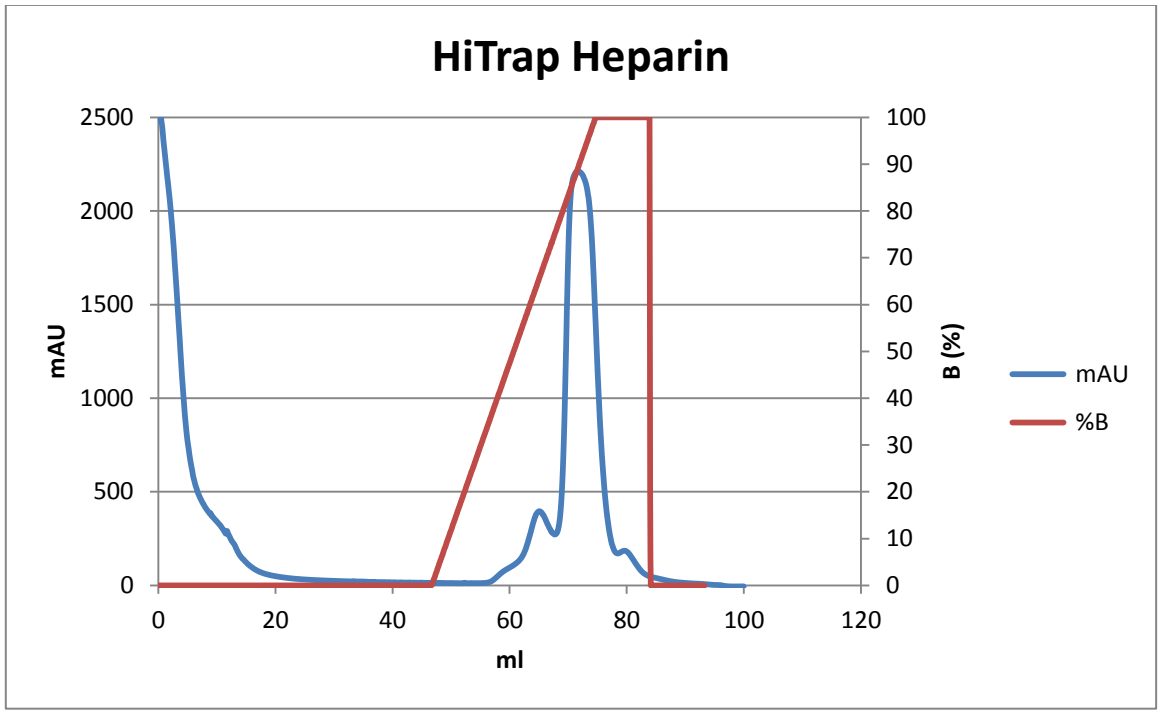

Figure 2.4 *Elution profile of affinity chromatography of CK2α^{pm} on column: HiTrap Heparin (GE Healthcare) equilibrated with buffer A [25 mM Tris-HCl (pH 8), 350 mM NaCl, 1 mM DTT]. Elution performed with increasing percentage of buffer B [25 mM Tris-HCl (pH 8), 1 M NaCl, 1 mM DTT].*

Fractions of the main peak were loaded in a coomassie-stained SDS–PAGE for identify the protein of interest (Figure 2.5). The fractions of the main peak showed a considerable level of impurities and also a probable degradation form exactly under the band of 45 kDa, which corresponds to the CK2α^{pm}. To obtain a pure and homogenous sample we collected only the fractions corresponding to the first half of the main peak which showed a lower degree of contaminations. These fractions were than pooled in a second purification step represented by a size exclusion chromatography using a Superdex 75 prep-grade 26/60 column (GE Healthcare) equilibrated with buffer C, the final buffer of the purification.

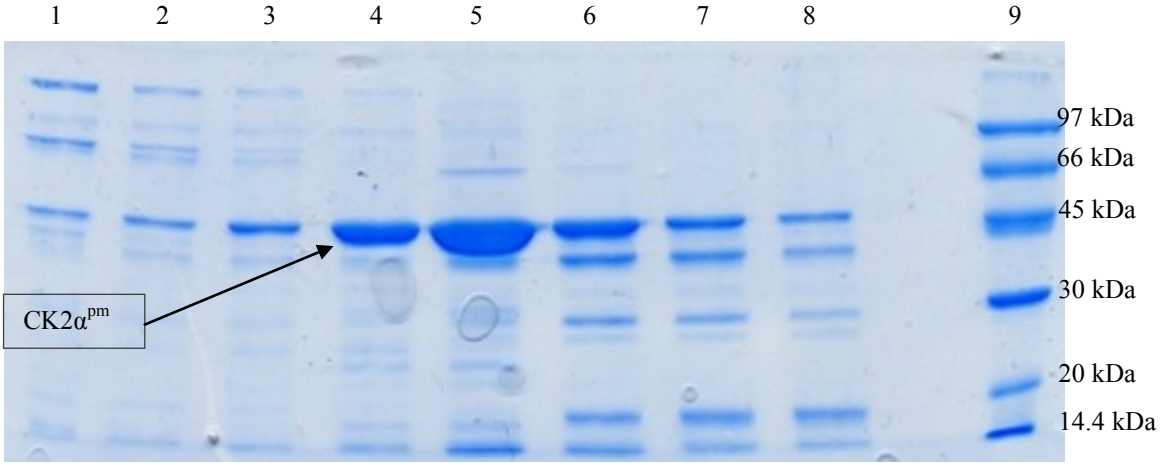

Figure 2.5 *Coomassie-stained SDS–PAGE after affinity chromatography. Lanes 1-8 correspond to fractions of the main peak of the chromatogram and lane 9 corresponds to low molecular weight protein markers in kDa.*

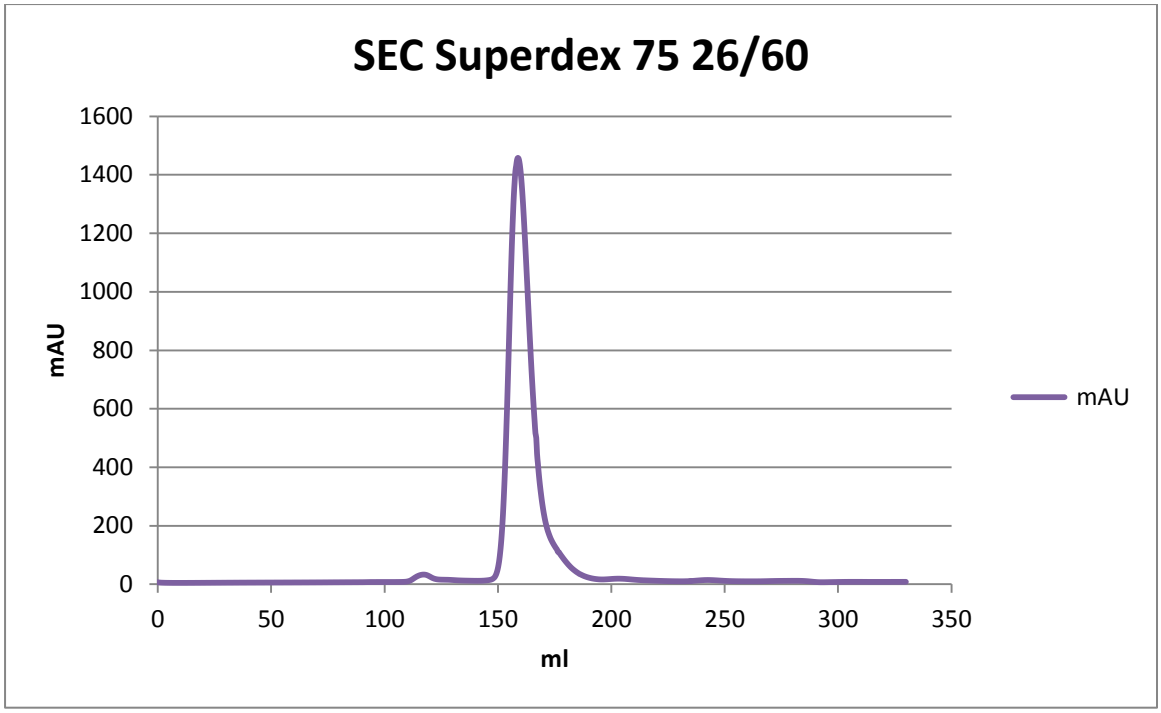

Figure 2.6 *Elution profile of size exclusion chromatography with a Superdex 75 prep-grade 26/60 column (GE Healthcare) equilibrated with buffer C [25 mM Tris-HCl (pH 8.5), 500 mM NaCl, and 1 mM DTT]*

The elution profile of the size exclusion chromatography showed a single slightly-tailed peak; like for the step before, we loaded the fractions of the main peak in a coomassie-stained SDS–PAGE for evaluate the purity level of the sample after the size exclusion chromatography.

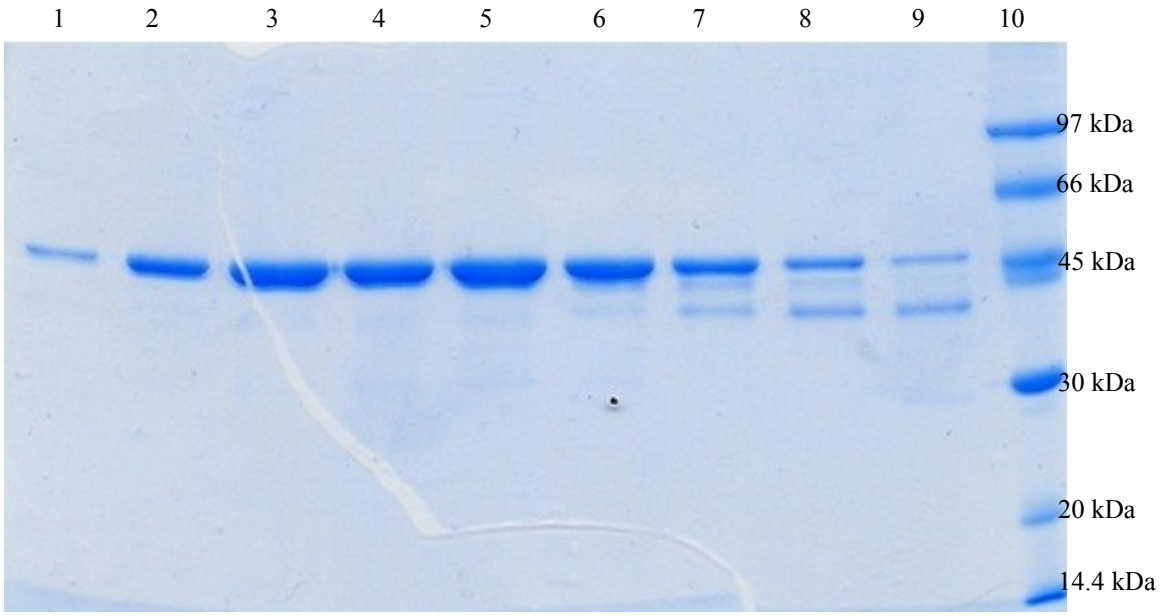

Figure 2.7 *Coomassie-stained SDS–PAGE after size exclusion chromatography. Lanes 1-9 correspond to fractions of the main peak of the chromatogram and lane 10 corresponds to low molecular weight protein markers in kDa.*

After the size exclusion chromatography the purity of the sample was high enough for the crystallization purpose. Under the main 45 kDa band, especially in the tail of the peak, there are some bands which correspond to degradation forms of the protein; even if we performed the purification with a fast protocol a small amount of protein underwent to proteolysis, probably losing the mutated C-terminal tail. We collected the fractions with a high purity of the sample, discarding the degraded forms, and the $CK2\alpha^{pm}$ was concentrated to 15 mg/ml by ultrafiltration to a final yield of 12 mg per liter of culture.

2.1.2.3 Protein crystallization

We knew that $CK2\alpha^{del}$ gives good diffracting crystals under an optimized precipitant solution with 0.1 M Tris-HCl (pH 8.5), 0.2 Lithium Sulphate and 32% w/v PEG 4000 in $P2_1$ space group, and less-good diffracting form with 0.1 MES pH 6.5, 0.2 Ammonium Sulphate and 22% w/v PEG 5000 MME in $P4_32_12$ space group; because in $CK2\alpha^{pm}$ we have 55 amino acids more than in the deleted form, we started from a sparse matrix screening, trying to obtain a new crystal packing with the entire visible C-terminal tail. After sever trails and optimization cycles we obtained a stick-shaped crystal under the following precipitant solutions: 0.2 Ammonium Acetate, 0.1 Tri-Sodium Citrate (pH 5.6) 30% w/v PEG 4000.

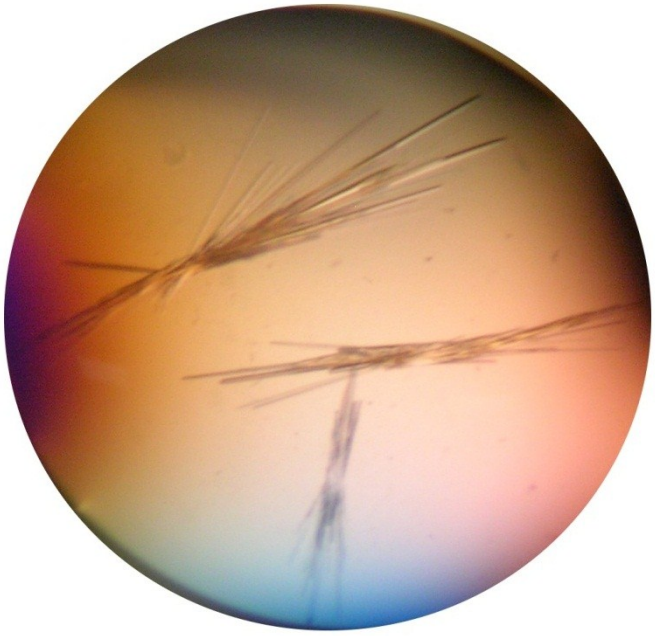

Figure 2.8 *Crystals of $CK2\alpha^{pm}$ in 0.2 Ammonium Acetate, 0.1 Tri-Sodium Citrate (pH 5.6) 30% w/v PEG 4000.*

Even if the crystals of CK2α^{pm} were very fragile and very difficult to manipulate we were able to collect a data set at the ELETTRA-Synchrotron beamline XDR1 (Trieste, Italy).

2.1.2.4 Structure determination

The structure was solved by molecular replacement using the structure of the CK2α^{del} 3BQC. Statistics on data collections and refinement are reported in table 2.2. CK2α^{pm} crystallized in the space group $P4_32_12$, like the CK2α^{del} with precipitant solution at pH 6.5 mentioned above; we were not able to obtain a new crystal form of the enzyme, and the overall structure of the enzyme within the crystal packing is identical to the published CK2α^{del}. Even if the quality of the data was not ideal and the refinement is not finished yet, the information found in the structure was sufficient for our purpose.

Table 2.2 Data collection and refinement statistics

Data collection statistics	**ELETTRA beamline XDR1, λ=1 Å**
Cell dimensions a, b, c (Å) α, β, γ (°)	 126.74 126.74 124.27 90.00 90.00 90.00
Total number of observations	83931 (10862)
Total number of unique	15571 (2192)
Resolution (Å)	56.68 (3.30)
R_{merge} (%)	0.355 (1.054)
R_{meas} (%)	0.393 (1.172)
I/σ(I)	4.9 (1.8)
Completeness (%)	98.8 (97.9)
Multeplicity	5.4 (5.0)
Refinement statistics	
R_{work} (%)	0.25971
R_{free} (%)	0.30963

The values in brackets are referred to the highest resolution shell.

2.1.2.5 CK2α^{pm} structure

From the data collected we were able to solve and analyze the first structure of CK2α^{pm} with the entire C-terminal tail. The following considerations can be taken after the analysis of the data:

- We were able to crystallize the full-length form CK2α with four mutations on the C-terminal tail;
- The packing within the crystal is the same of the other published CK2α^{del} in

$P4_32_12$ and the overall folding of the kinase is identical to the other $Ck2\alpha^{del}$ structures;

- Although the electronic density is well defined in the major part of the structure, the last 59 residues are not visible and there is not free more electron density after the residue Ala332; so the C-terminal tail remains flexible and not visible in the crystal structure.

Moreover, the not-so-good data collected, relating to maximum resolution and statistics, means a not homogenous sample within the crystal. This is probably due to the presence of the entire C-terminal tail which is flexible and disordered in solution and within the crystal. Even if we were not able to find a structural role for the entire phospho-mutant C-terminal tail, we optimized a fast purification protocol for obtain the full-length form of the CK2α enzyme; we used this for the further CK2 holoenzyme purifications, because we wanted to understand whether the C-terminal tail could had a structural significance within the holoenzyme form.

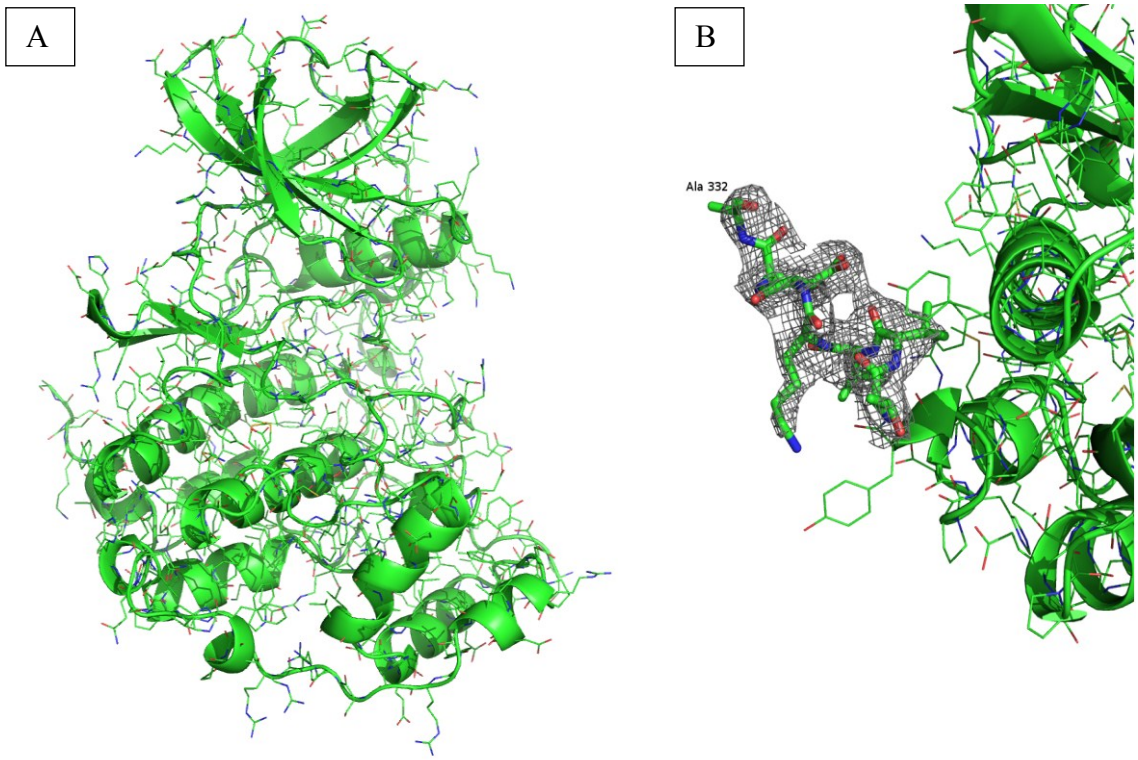

Figure 2.9 (A) *Overall structure of the* $CK2\alpha^{pm}$ *in tetragonal crystal system* ***$P4_32_12$*** *.* ***(B)*** *Detail of the electron density of the C-terminal tail: no more free electron density after the residue Ala332.*

2.2 CK2 holoenzyme CK2$\alpha_2\beta_2$

2.2.1 Methods

2.2.1.1 Overview

The holoenzyme form of the protein kinase CK2 is composed of two catalytic α (or α') subunits and two regulatory β subunits organized in a tetrameric form. Two structures are present in the database showing the architecture of the complex and how the subunits interact between each other; both of these structures lack completely the C-terminal tail of the α subunit. What we wanted to know was whether the C-terminal tail, which is flexible in solution and undergoes rapidly to auto-proteolysis during the purification, could have a structural role in the tetrameric holoenzyme. Again the first step was to find a way to obtain a stable CK2 holoenzyme with the entire C-terminal tail and then try to crystallize it. We actually were able to produce a stable form of the enzyme, with the same fast procedure of purification, and we crystallized three different forms of CK2 holenzyme namely the CK2 holoenzyme with the wild type full-length CK2α ($CK2^{wt}$), the CK2 holoenzyme with the phoshomimetic mutant of CK2α ($CK2^{pm}$) and the CK2 holoenzyme with the deleted form of the CK2α ($CK2^{del}$).

2.2.1.2 Protein expression

E. coli BL21(DE3) cells, harboring the plasmid pT7-CK2β were grown overnight (ON) at 37 °C in LB medium (10 g/l tryptone, 5 g/l yeast extract, and 10 g/l NaCl) supplemented with 50 μg/ml ampicillin. LB medium was inoculated with this ON culture (ratio 1:10) and grown at 37 °C, in a suitable shaker. Protein expression was induced at an OD_{600} of 0.6 by adding 1 mM IPTG and prolonged for 4-5 h at 30 °C under vigorous shaking. Bacteria were harvested by centrifugation at 5000 g for 30'.

2.2.1.3 Protein purification

Bacteria were suspended in buffer A [25 mM Tris-HCl (pH 8), 300 mM NaCl, 0.4 mM (tris(2-carboxyethyl)phosphine) (TCEP)] supplemented with protease inhibitors EDTA free (Roche) and lysed with a French press (Thermo Spectronic) at high pressure.

The lysate was centrifuged to remove cell debris at 27000 g for 30' and filtered with

0.22 μm syringe filter. After the filtration we added CK2α^{wt}, CK2α^{pm} or CK2^{del} (250 μl at 15 mg/ml for 2.5 l of CK2β culture) and we left the lysate incubate for 10 minutes at 4 °C. After the formation of the complex the sample is loaded onto an affinity column performed on a Äkta FPLC chromatographic system (GE Healthcare) using a HiTrap Heparin HP 5ml (GE Healthcare) equilibrated with buffer A. After extensive washing with buffer A the protein was eluted with a gradient of NaCl with buffer B [25 mM Tris-HCl (pH 8), 1 M NaCl, 0.4 mM TCEP]. Fractions containing the protein were pooled and further purified by size exclusion chromatography using a Superdex 200 prep-grade 26/60 column (GE Healthcare) equilibrated with buffer C [25 mM Tris-HCl (pH 8.5), 500 mM NaCl, and 0.2 mM TCEP]. The two step of purification were performed in the same day getting the sample always in ice to avoid the auto-proteolysis of the C-terminal tail as previously described for the CK2α^{pm}.

2.2.1.4 Dynamic light scattering

DLS data were recorded on a Zetasizer NanoS instrument (Malvern Instruments Ltd.) at 20 °C, using a quartz cuvette and 20 μl of sample. Protein solutions were filtered using 0.22 μm filters. The data were recorded and analyzed with the Dispersion Technology Sofware (Malvern).

2.2.1.5 Analytic gel filtration analysis

Gel filtration chromatography can be used to calculate the molecular weight of a protein from its elution volume. Performed on an Äkta FPLC chromatographic system (GE Healthcare) we used a Superdex 200 10/300 GL column which is a prepacked gel filtration column for high-resolution, semipreparative and analytical separations of biomolecules. Superdex 200 has a separation range for molecules with molecular weights between 10000 and 600000 Da. We used thyro Globulin (699 kDa), Ferritin (440 kDa), Catalase (232 kDa), BSA (67 kDa), Oval Bumin (43 kDa) and Ribonuclease (13.7 kDa) for the calculation of a calibration line.

2.2.1.6 Protein crystallization

Crystallization trials using commercial kits (Qiagen, Molecular Dimensions and Hampton Research) based on sparse matrix, grid screen, and/or ionic sampling, were

performed by vapour diffusion (with the sitting drop method) techniques, using the Oryx8 automatic system (Douglas Instrument). CK2 holoenzymes were concentrated to 8 mg/ml for crystallization purposes. Crystals were grown at 20 °C, using the following precipitant solution: 0.2 M ammonium citrate, pH 6.5, 20% w/v PEG 3350.

2.2.1.7 Data collection, structure determination, and refinement

The three data set were collected at the ELETTRA-Synchrotron beamline XDR1, (Trieste, Italy) and at European *Synchrotron* Radiation Facility beamline ID23-2 *gemini* (ESRF Grenoble, France). Data sets were measured at 100 K using the precipitant solution, including 20% glycerol as cryoprotectant. Full length CK2 crystals, phosphomutant or wild type, belonged to space group $P2_1$ and the crystal of the deleted of CK2 belonged to the space group C2, with unit cell parameters reported in Table 2.3. Diffraction data were integrated with XDS (Kabsch, 2010) and reduced and merged with SCALA included in the CCP4 suite (Evans, 2005). For structure determination, Rigid Body Refinement (CCP4) was performed with the coordinates of the wt CK2α from PDB ID 3BQC and with the coordinates of CK2β subunit PDB ID 3EED for the β_2 dimer. The model was then refined alternating several cycles of automatic refinement with REFMAC (CCP4) (Murshudov et al., 1997) and manual model building with Coot (Emsley and Cowtan, 2004). Finally also the TLSs (Translation/Libration/Screw parameterization) were added. Statistics of the refinements and final models are reported in Table 2.3.

2.2.2 Results

2.2.2.1 Protein expression and purification

For obtain a stable form of the holoenzyme ($CK2^{wt}$, $CK2^{pm}$ or $CK2^{del}$) we expressed the CK2β in *E. coli* BL21(DE3) and we added previously purified CK2αs ($CK2\alpha^{wt}$, $CK2\alpha^{pm}$ or $CK2\alpha^{del}$) to the filtrated lysate; after the incubation under ice for 10 minutes we loaded the sample in a HiTrap Heparin column for the first affinity purification step. The elution of the protein from the column was performed in the same way described for the $CK2\alpha^{pm}$, with a gradient of NaCl; in this way only the CK2β dimer which had formed a stable complex with the CK2α subunit would bind to the column due to the affinity between the catalytic subunit and the heparin molecules.

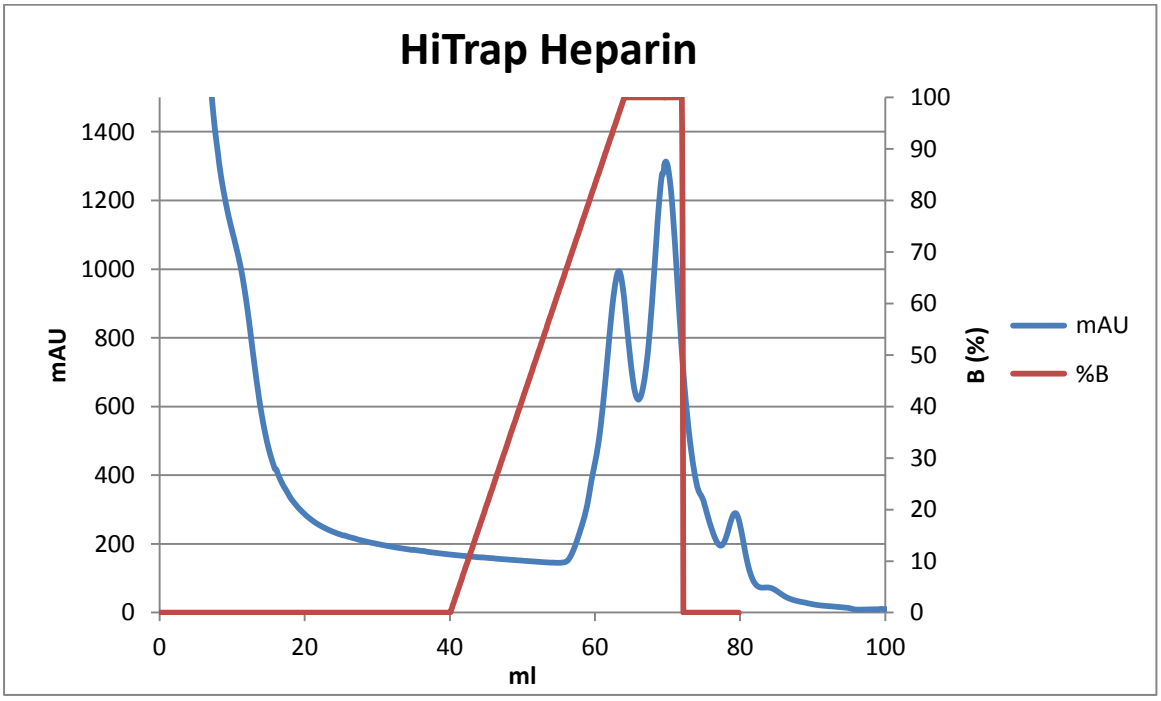

Figure 2.10 *Elution profile of affinity chromatography of CK2 holoenzyme on column: HiTrap Heparin (GE Healthcare) equilibrated with buffer A [25 mM Tris-HCl (pH 8), 300 mM NaCl, 0.4 mM TCEP]. Elution performed with increasing percentage of buffer B [25 mM Tris-HCl (pH 8), 1 M NaCl, 0.4 mM TCEP].*

The chromatogram reported regards the elution profile for the holoenzyme with the $CK2\alpha^{pm}$ form, but the same trend was found for the other holoenzyme complexes. Fractions of the main peak were loaded in a coomassie-stained SDS–PAGE:

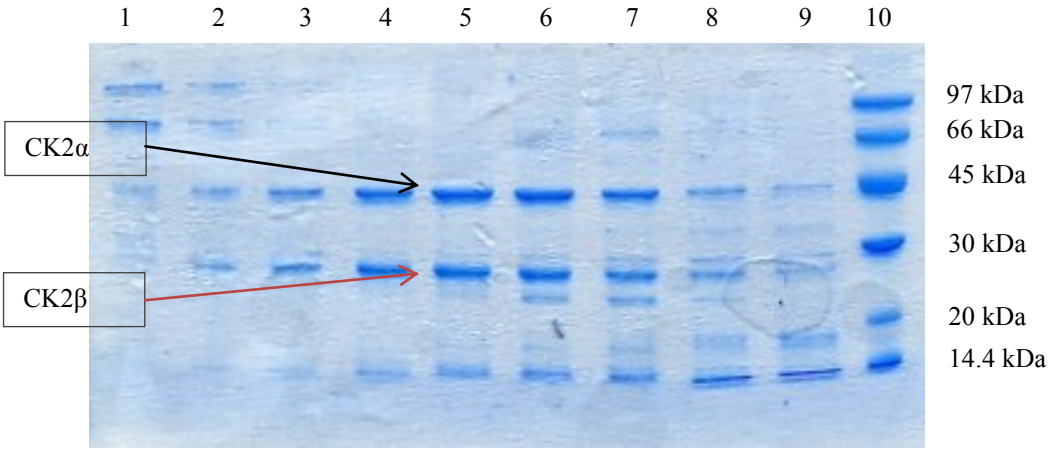

Figure 2.11 *Coomassie-stained SDS–PAGE after affinity chromatography. Lanes 1-9 correspond to fractions of the second main peak of the chromatogram and lane 10 corresponds to low molecular weight protein markers in kDa.*

The SDS-PAGE confirmed that the complex between CK2α and CK2β2 was formed, because they are both present in the gel, and that CK2α was able to bind to the heparin molecules without interfering with the bounded $CK2\beta_2$ dimer. As in the purification of the single $CK2\alpha^{pm}$, this first step of purification was not sufficient for getting a pure sample and lots of impurities were present in the fractions of the main peak; so we proceeded with a second size exclusion chromatographic step:

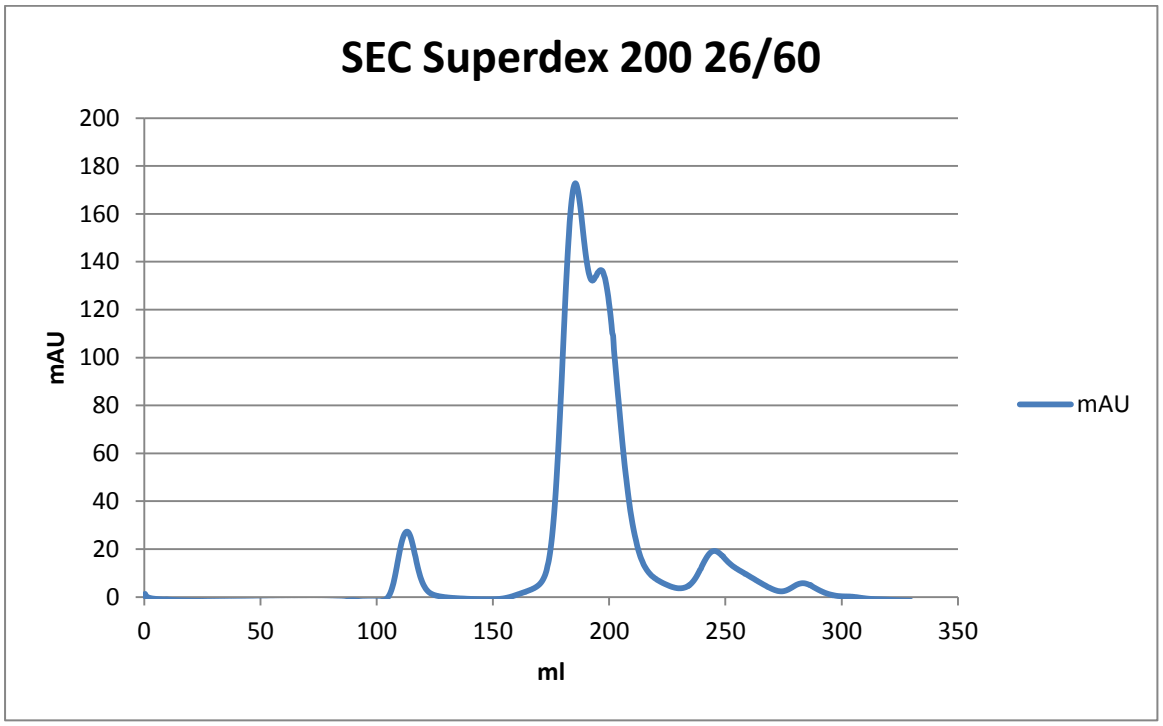

Figure 2.12 *Elution profile of CK2α2β2 from size exclusion chromatography with a Superdex 200 prep-grade 26/60 column (GE Healthcare) equilibrated with buffer C [25 mM Tris-HCl (pH 8.5), 500 mM NaCl, and 0.2 mM TCEP]*

The elution profile of the CK2 holoenzyme showed two peaks; to understand whether the proteins that cause the peaks were CK2α and CK2β we loaded the fractions of two peaks in a Coomassie-stained SDS–PAGE.

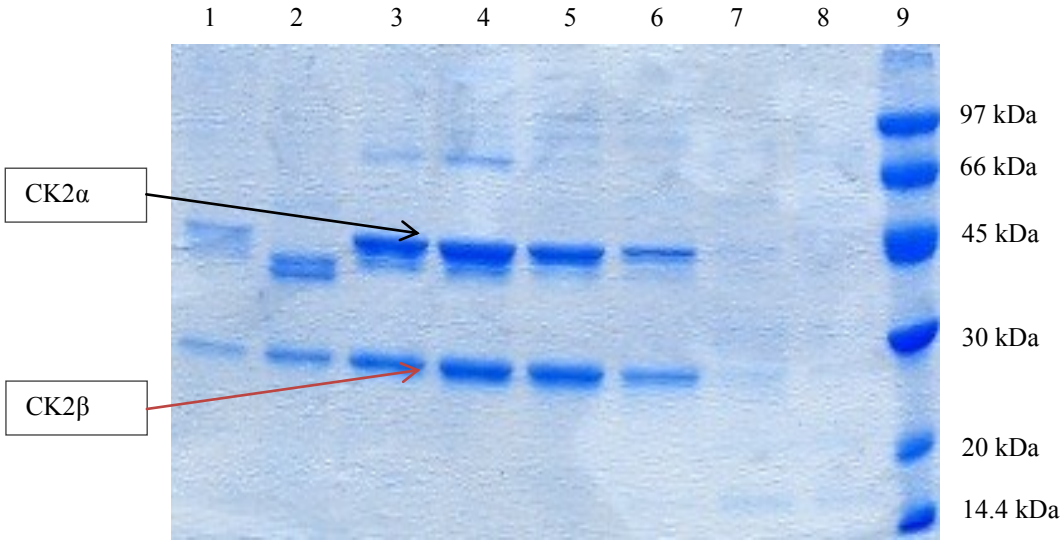

Figure 2.13 *Coomassie-stained SDS–PAGE after size exclusion chromatography. Lanes 1-8 correspond to fractions of the main peak of the chromatogram and lane 9 corresponds to low molecular weight protein markers in kDa.*

From the SDS-PAGE we could confirm that the two peaks were composed of CK2α and CK2β proteins bounded together because both of them were present in all of the fractions. The size exclusion crhomatogrphy separates the proteins by their molecular weights and we knew that CK2β_2 can bind at most two CK2αs; in this case it seemed that there were two different forms of CK2 holoenzymes, composed both of CK2α and CK2β subunits, that segregates at two different elution volumes due to their different molecular weights. Firstly, we tried to separate the two species (“first peak” and “second peak”) and reloaded in the same size exclusion chromatography to understand whether there was a dynamic equilibrium between the two CK2 forms. From the chromatogram reported in figure 2.7 we understood that the two species are stable and do not interconvert in each other when they are isolated. The stability of the two CK2 holoenzyme forms permitted us to work on the characterization of the two macromolecules, in particular using techniques that could be useful to elucidate whether this double peak was due to different form of aggregation or to a different stoichiometry of binding between CK2 subunits.

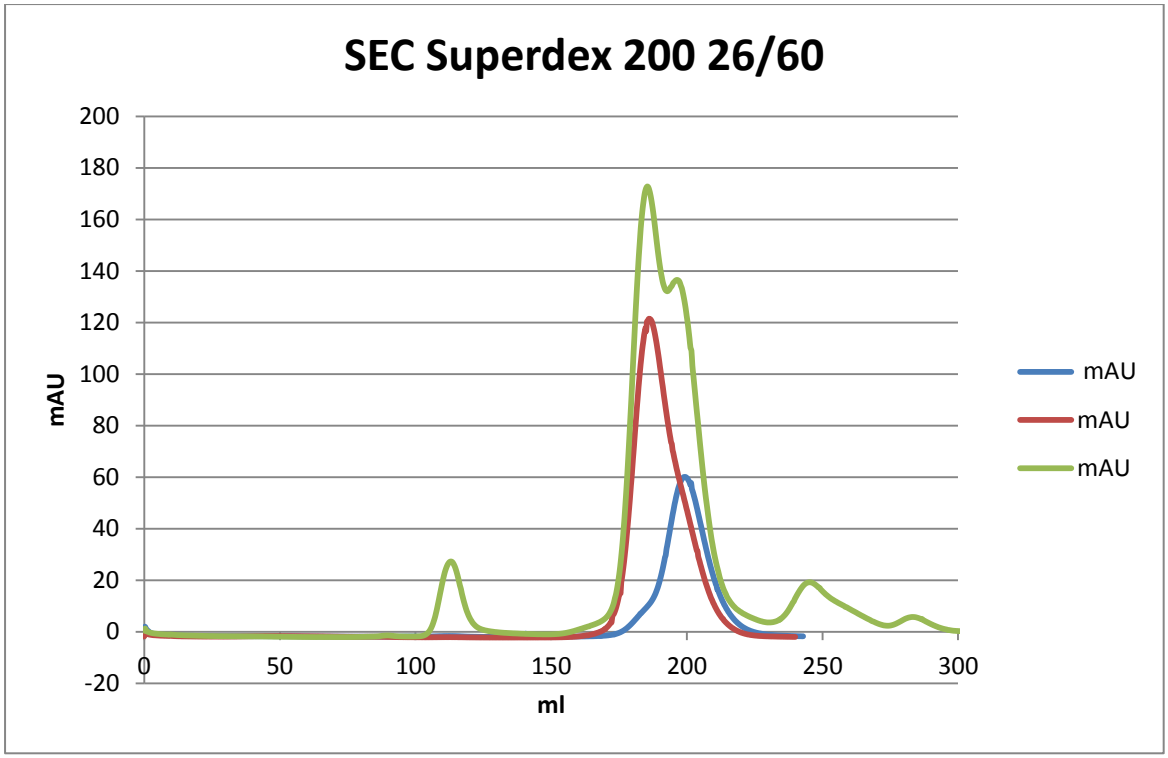

Figure 2.14 *Elution profile of size exclusion chromatography with a Superdex 200 prep-grade 26/60 column (GE Healthcare); in blue the "second peak" reloaded in the column, in red the "first peak" reloaded in the column and in green the double in peak reported for comparison.*

2.2.2.2 Dynamic light scattering

For the quantification of the molecular weight and for the analysis of the protein behavior in solutions, the two species were analyzed by Dynamic Light Scattering (DLS). The particle size distribution by intensity of the two CK2 forms is reported in Figure 2.15; the main form in solution for the "first peak" is the monomeric form while for the "second peak" high molecular weight aggregates are present in addition to the monomeric form. The presence of these aggregates is usually a symptom of a not good behavior of the sample in solution and usually indicates that the sample is not suitable for crystallization purpose. From the DLS analysis we got information about the size of the two spices; in particular the "first peak" has a calculated diameter of 12 nm which corresponds circa to a 220 kDa molecule and the "second peak" has a calculated diameter of 9 nm which corresponds to a 120 kDa molecule. DLS analysis confirmed the data of the first size exclusion chromatography that the two species are stable in solution and one ("first peak") has a diameter, and so as a consequence a molecular weight, bigger than the other one ("second peak").

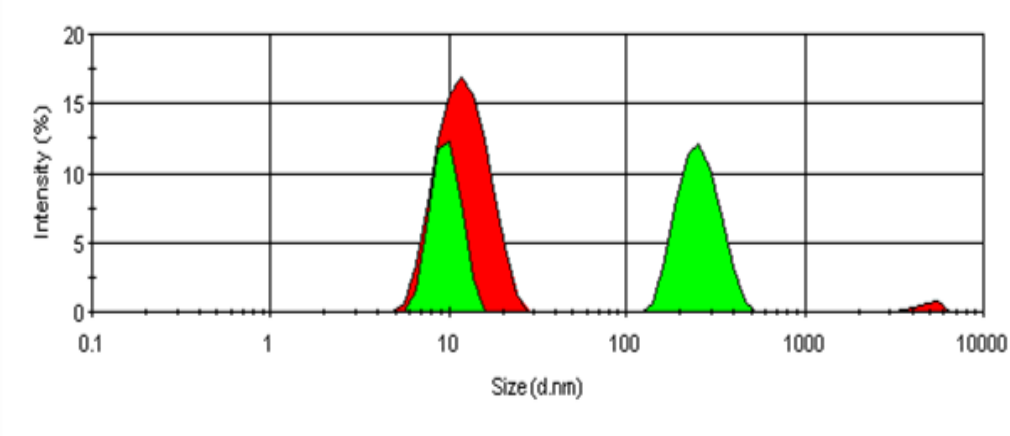

Figure 2.15 *Particle size distribution by intensity of (RED) CK2 holoenzyme "first peak" and of (GREEN) CK2 holoenzyme "second peak". The proteins concentration was 1 mg/ml in 25 mM Tris-HCl, 500 mM NaCl and 0.2 mM TCEP (pH 8.5).*

2.2.2.3 Analytic gel filtration analysis

To have a more precise valuation of the molecular weight of the two species we performed an analytic gel filtration chromatography with a Superdex 200 10/300 GL column which is a prepacked gel filtration column for high-resolution analytical separations of biomolecules. We used a mixture of six different proteins as standards to calculate the calibration line:

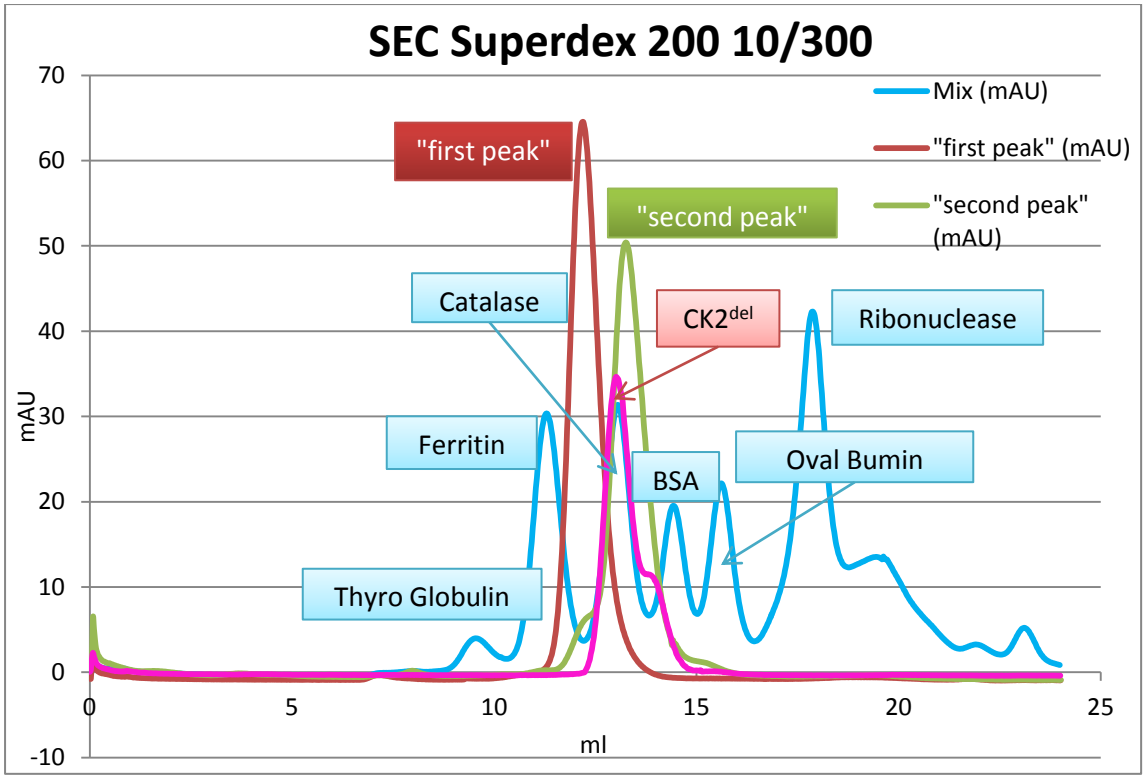

Figure 2.16 *Elution profile of analytical size exclusion chromatography with a Superdex 200 10/300 column (GE Healthcare); in cyan the elution profile of the mix of standards composed of Thyro Globulin (699 kDa), Ferritin (440 kDa), Catalase (232 kDa), BSA (67 kDa), Oval Bumin (43 kDa) and Ribonuclease (13.7 kDa), in red the elution profile of the "first peak", in green the elution profile of the "second peak" and in magenta the elution profile of the CK2^{del} with the two species still mixed together.*

From the calibration line calculated we were able to evaluate the following molecular weights for the two CK2 holoenzyme forms:

- CK2 full-length (CK2^{wt} or CK2^{pm})
  - 230 kDa for the "first peak"
  - 137,5 kDa for the "second peak"
- CK2^{del}
  - 154 kDa for the "first peak"
  - 111 kDa for the "second peak"

We noticed that there was a great difference between the calculated molecular weight for the CK2 holoenzyme with the C-terminal tail (CK2^{wt} and CK2^{pm}) and the CK2 holoenzyme without it (CK2^{del}); the C-terminal 55 amino acids have a molecular weight of 5.16 kDa and could unlikely explain the gap between the "first peaks" where the difference in terms of calculated molecular weight was 76 kDa (230 kDa and 154 kDa). Another interesting thing was the difference of molecular weights between first and

second peak of the full-length CK2 holoenzyme: 93 kDa couldn't be easily explained by the addition of a single CK2α (45 kDa) or a $CK2\beta_2$ dimer (50 kDa). The explanation of this phenomenon come from the molecular weight difference between first and second peak of the $CK2^{del}$ holoenzyme: in this case the gap was 44 kDa and it could well fit with the molecular weight of a single $CK2\alpha^{del}$ molecule (40 kDa). We than hypothesized that the "first peak", for both full-length CK2 and $CK2^{del}$ holoenzyme, could correspond to the tetrameric form of the kinase $CK2\alpha_2\beta_2$, and the "second peak" could correspond to a trimeric form, namely $CK2\alpha\beta_2$. This hypothesis was confirmed by the addiction of free CK2α' to the "second peak" of the full-length CK2 holoenzyme: the result was a shifting of the elution volume to a value equivalent of the "first peak" (Figure 3.16). The meaning of this effect was that in the purification we didn't saturate all the $CK2\beta_2$ binding site for the CK2α, with a consequent double population of saturated tetrameric holoenzyme $CK2\alpha_2\beta_2$ ("first peak") and an incomplete trimeric form of $CK2\alpha\beta_2$ ("second peak"). Moreover we understood that the 55 amino acids of the C-terminal tail were able to increase the hydrodynamic volume of the full-length protein with an effect analogous to an apparent increase in the MW of 76 kDa with respect to the deleted form; this fact is probably due to the reported great flexibility of the C-terminal tail in solution.

After these considerations we continued working with only the tetrameric form of the protein and we proceeded with the crystallization trials.

2.2.2.4 Protein crystallization

Like for all of the new proteins we started from crystallization trials using commercial kits based on sparse matrix with the Oryx8 automatic system (Douglas Instrument): with the robot we are able to make a crystallization plate in 20 minutes testing 96 different precipitant conditions at two different protein concentrations. All of CK2 holoenzymes were concentrated to 8 mg/ml for crystallization purposes. After more than 300 precipitant solution tested, we were able to individuate three best promising conditions which gave crystals of different sizes and shapes; figures below were taken from crystallization drops made by hand after 3 days of incubation mixing 1 µl of precipitant solution and 1 µl of protein solution concentrated to 8 mg/ml.

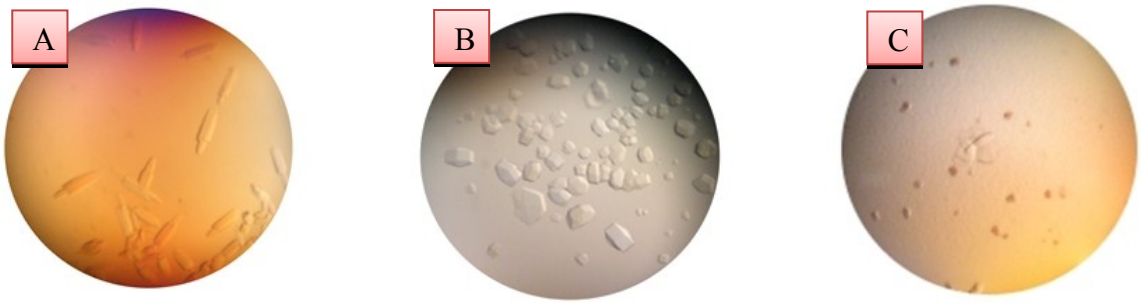

Figure 2.17 *Crystals of CK2 holoenzyme obtained with precipitant solutions* ***A*** *[0.2 M NaCl, 0.1 Hepes (pH 7.5), 10% v/v isopropanol],* ***B*** *[0.2 NaCl, 0.1 M Na/K (pH 6.2), 50% v/v PEG 200] and* ***C****[0.2M d-Ammonium Citrate (pH 5.5), 20% w/v PEG 3350].*

All of the crystals above were tested at the ELETTRA-Synchrotron beamline XDR1, (Trieste, Italy) with a resolution limit of 12 Å for condition A, 6 Å for condition B and 4 Å for condition C. After the *high-throughput* screening we then started with the optimization procedure of the three best conditions; after several cycles of optimization we were able to individuate the best precipitant solution for obtaining a big and resistant CK2 holoenzyme crystal, which was composed of 0.2 M d-Ammonium Citrate (pH 6.5), 20% w/v PEG 3350. This precipitant solution permitted us to crystalize (even if with some adjustments in precipitant's concentrations) and solve the crystal structure of all the three forms of holoenzyme produced $CK2^{wt}$, $CK2^{pm}$ and $CK2^{del}$. In Figure 2.18 the photo of the crystal of the $CK2^{pm}$, taken at the European *Synchrotron* Radiation Facility beamline ID23-2 *gemini* (ESRF Grenoble, France), which was the first full-length CK2 holoenzyme crystallized, collected and which structure was solved.

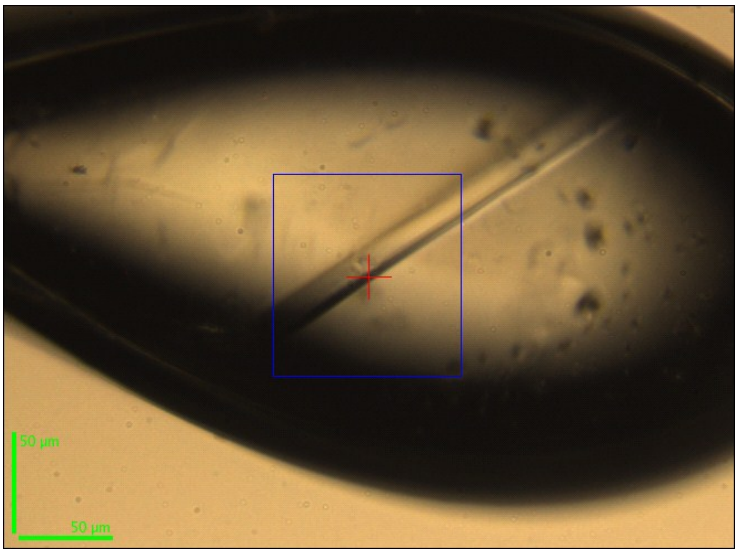

Figure 2.18 *Crystal of* $CK2^{pm}$ *holoenzyme obtained with precipitant solution 0.2 M d-Ammonium Citrate (pH 6.5), 20% w/v PEG 3350, taken at the European Synchrotron Radiation Facility beamline ID23-2 gemini (ESRF Grenoble, France)..*

2.2.2.5 Data collection, structure determination, and refinement

We collected the dataset of the $CK2^{pm}$ at European *Synchrotron* Radiation Facility beamline ID23-2 *gemini* (ESRF Grenoble, France) while the dataset or $CK2^{wt}$ and $CK2^{del}$ were collected at the the ELETTRA-Synchrotron beamline XDR1, (Trieste, Italy): the microfocus beamline of the ID-23 permitted us to achieve the 3.1 Å resolution for the $CK2^{pm}$, while for the other two holoenzymes the resolution is lower with 3.79 Å for the $CK2^{wt}$ and 4 Å for the $CK2^{del}$. The CK2 holoenzyme crystallized in monoclinic space groups ($P2_1$ in the presence of the full-length CK2α for $CK2^{wt}$ and $CK2^{pm}$ and C2 with truncated form of CK2α for $CK2^{del}$). The crystal packing is very similar and the differences are to be ascribed to the additional space required for the CK2α C-terminus ($CK2^{wt}$ and $CK2^{pm}$) (Figure 2.19). In particular in the space group $P2_1$ two molecules for asymmetric unit are present, while in the space group C2 only one molecule for asymmetric unit.

Table 2.3 Data collection and refinement statistics

	$CK2^{pm}$	**$CK2^{wt}$**	**$CK2^{del}$**
Data collection statistics	ESRF beamline ID23-2 , λ=1 Å	ELETTRA beamline XDR1, λ=1 Å	ELETTRA beamline XDR1, λ=1 Å
Cell dimensions a, b, c (Å) α, β, γ (°)	P 1 21 1 142.316, 57.958, 86.188 90.00, 102.42, 90.00	P 1 21 1 141.575, 58.085, 185.568 90.00 102.33 90.00	C 1 2 1 210.310, 58.340, 140.600 90.00 118.66 90.00
Total number of observations	278220 (40507)	80645 (7523)	28630 (4193)
Total number of unique	52811 (7775)	25159 (3590)	11387 (1680)
Resolution (Å)	181.90 – 3.10	181.35 – 3.79	123.40 - 4
R_{merge} (%)	0.162 (0.643)	0.229 (0.337)	0.182 (0.574)
R_{meas} (%)	0.179 (0.715)	0.265 (0.427)	0.229 (0.723)
I/σ(I)	10.2 (2.6)	4.1 (2.2)	4.3 (1.9)
Completeness (%)	97.9 (98.7)	85.9 (85.0)	88.4 (89.8)
Multeplicity	5.3 (5.2)	3.2 (2.1)	2.5 (2.5)
Refinement statistics			
R_{work} (%)	0.23	0.29	0.25
R_{free} (%)	0.26	0.32	0.26

The values in brackets are referred to the highest resolution shell.

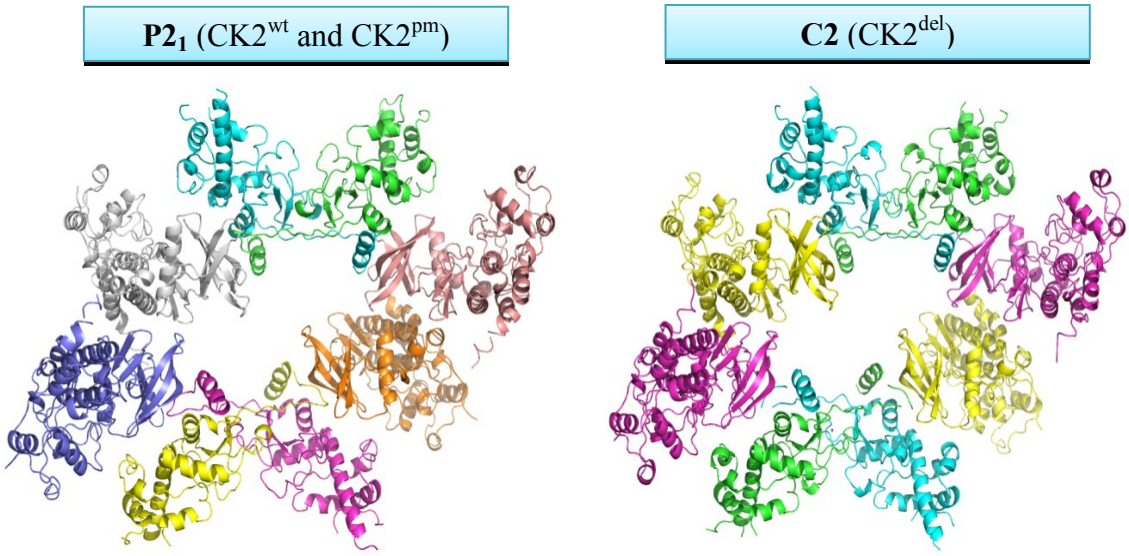

Figure 2.19 *Crystal packing in monoclinic crystal system $P2_1$ ($CK2^{wt}$ and $CK2^{pm}$) and C2 ($CK2^{del}$).*

2.2.2.6 CK2 holoenzyme in monoclinic crystal systems

In the two structures containing the full-length CK2α subunit ($CK2^{wt}$ and $CK2^{pm}$) no appreciable density is present for the C-terminal tail. Like in the structure of the monomer $CK2\alpha^{pm}$, the C-terminal tail appears to be flexible and disordered in solutions and it is not visible in the crystal structure; the only effect that we were able to notice, due to the presence of the C-terminal tail, was the different crystal packing between the proteins with the 55 amino acids tail ($P2_1$ for $CK2^{wt}$ and $CK2^{pm}$) and without (C2 for $CK2^{del}$). This fact confirms that the fast protocol for the purification of the full-length CK2α permitted us to obtain a non-degraded form of the protein we were able to obtain a stable full-length CK2 holoenzyme and to crystallize it; unfortunately the structural role of the C-terminal tail remains unknown but we surely added some important information that will be useful for the complete understanding of the CK2 regulation mechanism.

As reported in the introduction, among protein kinases, CK2α displays a unique flexibility in its hinge region that can assume two major conformations (open or close) (Figure 2.20B). In the numerous structures of the isolated CK2α subunit, both the open and close conformations have been reported. In the available structures of the CK2 holoenzyme, the hinge region was found in the open conformation, even when a mutation (Y125R in 4DGL) was inserted in order to interfere with such conformation. More precisely, in the close conformation F121 occupies a hydrophobic cavity that is instead

partially filled by Y125 in the open. Here we observe that in the structure containing the truncated CK2α ($CK2^{del}$), the hinge region is kept open. In $CK2^{wt}$ and $CK2^{pm}$, poor electron density defines the hinge region that appears to be highly flexible and possibly oscillating between the two conformations. Whether this phenomena is related to the presence of the C-terminal tail, which could interact with the hinge region and force it to oscillate between an open and close conformation, is difficult to say and may lead to speculations. We conclude that in the CK2 holoenzyme the open conformation of the hinge region is preferred over the closed one, which is instead more difficult to stabilize and isolate, and that in the presence of the full-length CK2α the hinge region oscillates between the two conformations.

In the interaction area between CK2α and CK2β, we found in all of the three structures that the CK2β phenylalanine 190 adopts a different conformation with respect to the one published in 2001 (1JWH). This conformation is the same found in the last CK2 holoenzyme structure (4DGL) and validate this new conformation: the CK2β Phe190 fills the hydrophobic cavity of CK2α subunit, while in the old structure the Phe190 was exposed to the solvent (Figure 2.20 C, D). This new conformation of the Phe190 strengthens the interaction between CK2α and CK2β making it more stable with a more pronounced hydrophobic character.

As reported before the CK2 holoenzyme crystallized in monoclinic space groups ($P2_1$ for $CK2^{wt}$ and $CK2^{pm}$, C2 for $CK2^{del}$) and, apart from small differences in the crystal packing due to the presence of the C-terminal tail in the full-length CK2 holoenzymes, the tetrameric architecture is virtually identical in all monoclinic structures (average RMSD = 1.4 Å); but a structural and comparative analysis with the published crystal structures (1JWH and 4DGL) in the hexagonal crystal system, made it clear that our structures were different (average RMSD = 2.5 Å) (Figure 2.21 A).

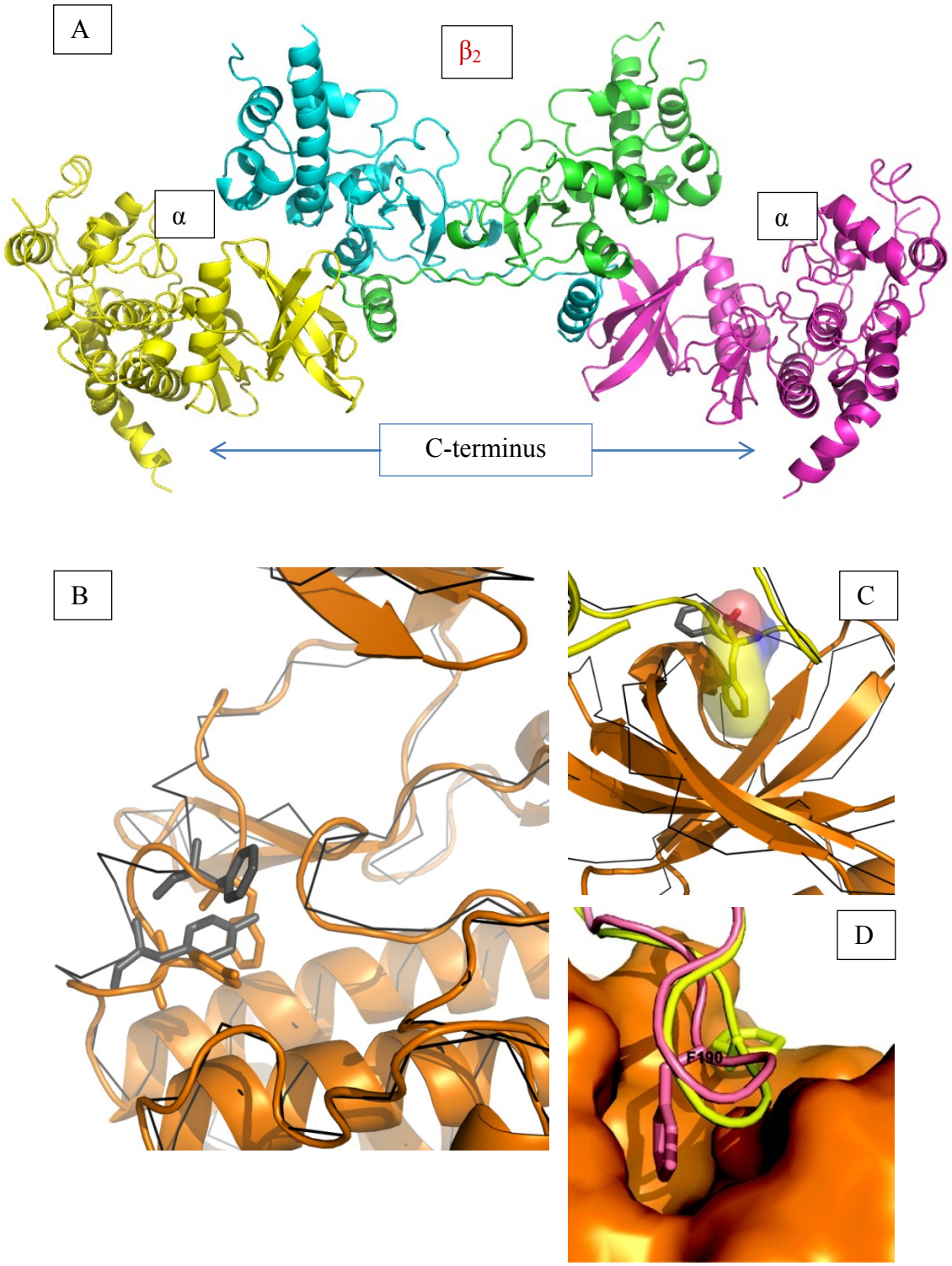

Figure 2.20 (A) *Crystal structure of the CK2 tetrameric holoenzyme in monoclinic system.* ***(B)*** *Double conformation of the hinge region with open conformation in black ($CK2^{del}$) and the close conformation in orange (in $CK2^{wt}$ and $CK2^{pm}$ there is an equilibrium between the two conformations).* ***(C)*** *Phenylalanine 190 (yellow) adopts a different orientation from the 1JWH structure (black) in the contact area between CK2α (orange) and CK2β (yellow).* ***(D)*** *Detail of the CK2α-CK2β interaction interface where the new CK2β Phe190 (highlighted in purple) fills the cavity of CK2α (in orange) with respect to the old conformation where the Phe190 leans on the outer interface (yellow).*

In the previously published 1JWH and 4DGL structures the $\alpha_2\beta_2$ tetramer is asymmetric in the position of the α-chains with respect to the central stable β_2 dimer, with two different α/β interfaces. In the description of the first CK2 crystallographic structure (1JWH), a relative rotation of 16.4º at one of the two α-β_2 interfaces around an axis lying at the outer β-sheet surface of the N-terminal CK2α domain was reported (Figure 2.21 B). For this reason at one side of the β-dimer, the first α chain binds through an extended interface (960 $Å^2$), while the other "rotated" interface on the opposite side is much smaller (770 $Å^2$) (Figure 2.21 C). The authors reported an average interface of 832 $Å^2$ and compared it with the average interface sizes of 1722 $Å^2$ for permanent and of 804 $Å^2$ for non-obligate protein complexes. They concluded that CK2 is a transient hetero-complex that, despite its spontaneous and stable nature in vitro, can dissociate in vivo.

Unlike in space group $P6_3$, in monoclinic crystals tetramers show a different, symmetric architecture, and two very similar α/β interfaces (average RMSD = 2.5 Å). The new symmetric architecture is due to the movement of the C-terminal lobe of a single α-chain, pivoting around the hinge region, towards the β-subunit (counter clockwise rotation in Figure 2.21 D). The asymmetric "distortion" of the structures in space group $P6_3$ is caused by the insertion of the acidic loop of one symmetric β-subunit (residues 55-64) and of the C-terminus of another symmetric β-subunit in between of the two lobes of the α-chain (Figure 2.21 E). The same crystallographic contacts are not present on the opposite side of the tetramers, leaving the other α-subunit and its interface with the β dimer undistorted and similar to what found in symmetric tetramers in monoclinic crystals. Structures presented here display that the CK2 holoenzyme is much more stable than what predicted before. First, they all confirmed the tracing of residues 194-207 of the β-subunit (increasing the interface area with the α-subunit), reported in the 4DGL structure and corrected in respect to the 1JWH structure. Then, α/β interfaces are now very similar with a mean value of 1081 $Å^2$. They are mostly hydrophobic, as indicated by the P-values of the solvation energy gain below 0.5 (around 0.1-0.15) (Krissinel and Henrick, 2007). As a matter of fact, relatively small interfaces in kinase complexes considered stable are not unusual. We compare CK2 (interface area >1000 $Å^2$) with the closely related Cyclin-dependent kinases. Interface for the Cdk9/CycT complex is 960 $Å^2$, similarly also to the Cdk4/CycD complex (1125 $Å^2$). These data are more in accordance with the very low dissociation constant of the tetrameric holoenzyme, whose value of 3.7 nM is typical of strong protein complexes. Moreover the CK2 holoenzyme is stable to up to 5 M urea (data not shown) and its dissociation is concomitant with

denaturation of the α-subunit.

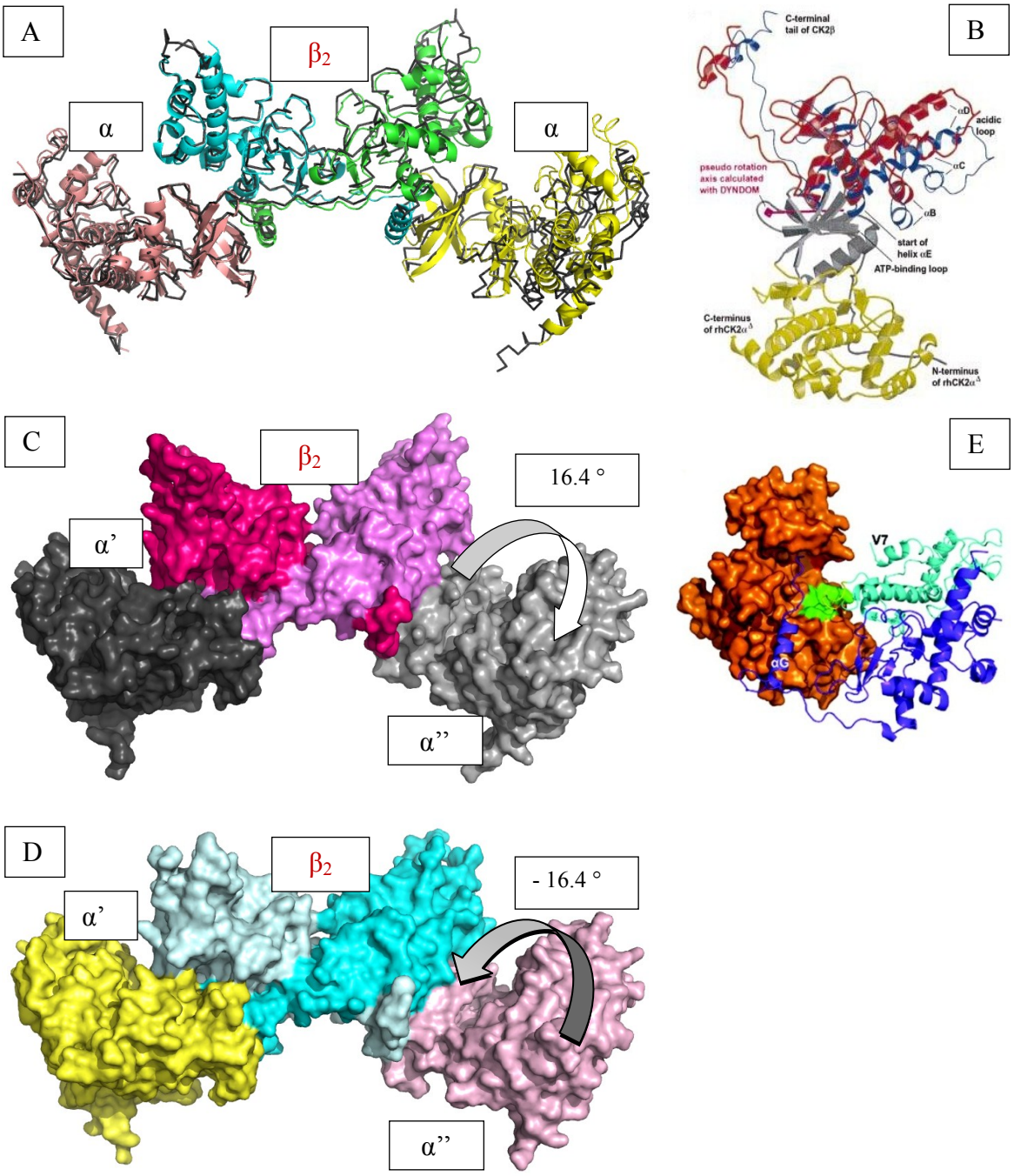

Figure 2.21 (A) *Superposition of crystal structure of CK2 tetramer in monoclic crystal system (colored) with CK2 tetramer in hexagonal crystal system (black).* ***(B)*** *Superposition of the two α-subunits of the tetramer in hexagonal system, showing the rotation axis lying at the outer β-sheet surface of the N-terminal CK2α domain.* ***(C)*** *Surface representation of the CK2 tetramer in hexagonal crystal system showing the rotation of 16.4° of the C-terminal lobe of the α'' subunit (gray), with two different interfaces of interaction between α'-β_2 (black and pink/purple) and α''-β_2 (gray and purple/pink).* ***(D)*** *Symmetric CK2 tetramer in the monoclinic system with identic interaction area α'-β_2 (yellow and cyan/blue) and α''-β_2 (pink and blue/cyan).* ***(E)*** *The asymmetric "distortion" of CK2 tetramer of the hexagonal system caused by the insertion of the acidic loop of one symmetric β-subunit (cyan) and of the C-terminus of another symmetric β-subunit (dark blue)*

in between of the two lobes of the α-chain (orange).

The presence of relatively small interfaces in the stable CK2 holoenzyme could have a functional significance, and be associated to a certain plasticity necessary to respond and adapt to external events like binding to other proteins. In Cdk9/CycT complex, for instance, binding to the HIV-TAT protein causes an 8.5º rotation of Cdk9 relative to CycT. This is not the case in the Cdk2/CycA complex, whose large interface (1834 $Å^2$) keeps the complex very rigid and not affected by the binding of additional proteins, as observed in the Cdk2/CycA/p27 complex. The distortion observed in the structure of the asymmetric holoenzyme can represent an example of what can happen when the enzyme interacts with some substrates. This structural plasticity of the holoenzyme, that is its aptitude to be temporary distorted from the more stable symmetric state, could also correlate with the property to interact with many different partners. Non interacting α and β subunits have been observed in cells (Theis-Febvre et al., 2005). This is not necessarily to be ascribed to an intrinsic hypothetical weakness of the complex, that disagree with the reported K_d value, the stability of the holoenzyme in vitro and with the crystallographic data reported here. As a consequence we hypothesized that the CK2 tetramer formation is an obligate protein complex instead of a transient protein complex and that once the complex is formed the subunits cannot return to the free monomer state. This view of the CK2 holoenzyme formation fits well with the recently proposed mechanism of regulation by an auto-inhibitory polymerization (Lolli et al., 2012) and can be describe as follow: the free monomer α-subunits and the β_2-dimer interact together to give the stable and symmetric CK2$\alpha_2\beta_2$ tetramer. This symmetric butterfly shaped holoenzyme is the fully active form of the protein. In the cellular environment, the CK2$\alpha_2\beta_2$ tetramers cooperatively self-organize in trimeric rings thus favouring the autophosphorylation of β, which in turn stabilizes the trimeric interaction. Due to a significant structural complementarity, trimers can pile one over another, giving rise to a polymerized form of CK2 that constitutes the latent, fully inactive form of this kinase. As for most protein kinases, CK2 activity is restored only upon necessity, in this case by a depolymerization process originating fully functional free symmetric tetramers. When CK2 activity is not necessary any more, the tetramer can come back to the trimer organization, to restore the pull of latent and inactive CK2.

Instead, it can be hypothesized that association of the CK2 holoenzyme can be prevented in vivo by mechanisms such as the intervention of β-competitive-α-interacting

or α-competitive-β-interacting proteins, by differential α and β localization or transport mechanisms or by unbalanced expression (Theis-Febvre et al., 2005). Tetramer dissociation could be also induced by specific regulatory mechanisms. However, whether such regulatory switches exist is still debated.

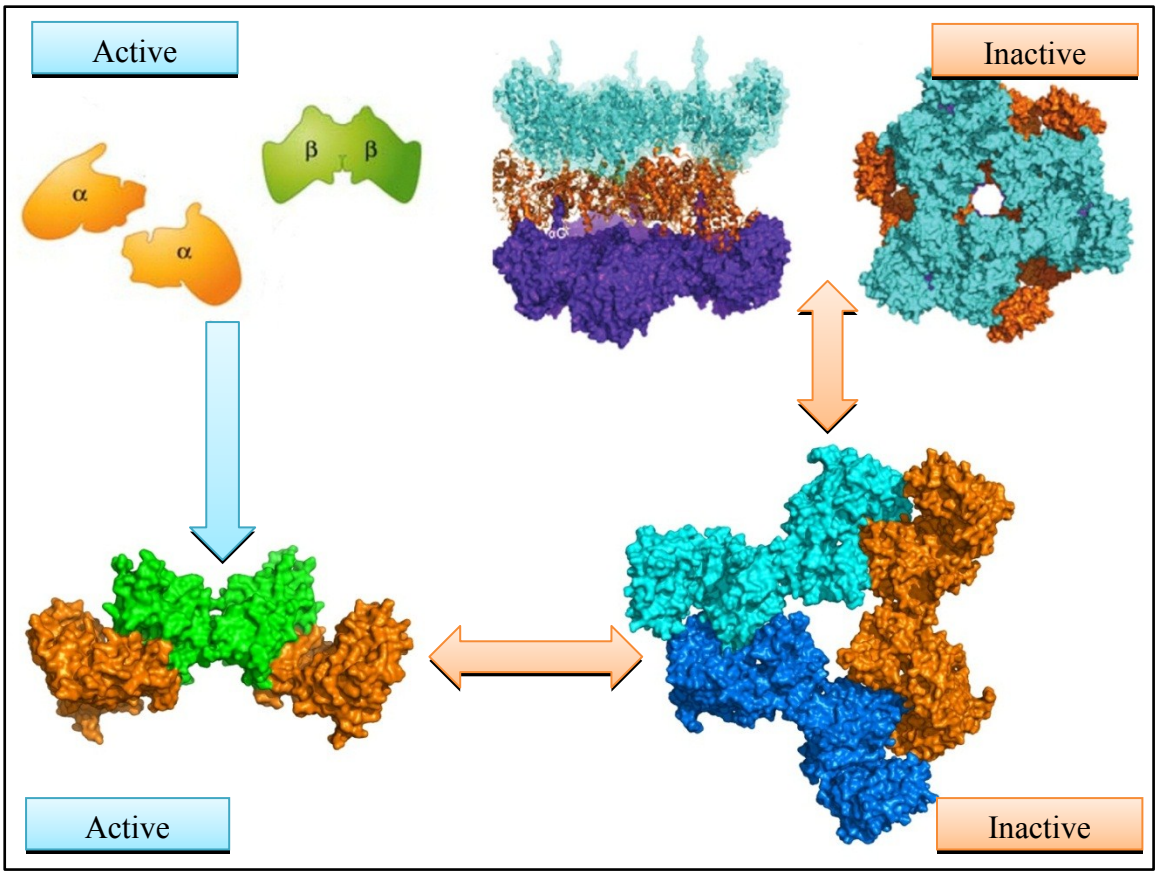

Figure 2.22 *Schematic representation of the regulation mechanism proposed for CK2. Once the CK2 tetramer is formed by the stable interaction by regulatory β_2-dimer (green) and α subunits (orange) it is in the fully active form; than it can undergo to auto-inhibitory polymerization mechanism first by forming trimer (inactive) and second by pilling organization of the trimers (inactive). This process of polymerization is reversible and the activity of CK2 can be restored upon necessity via depolymerisation mechanism.*

The unbalanced expression of the two subunits, with β being predominant, could lead to trimeric α β_2 holoenzymes or to chimeric enzymes with the free β-subunits able to recruit the paralogue subunit α' (in brain and testis where this last is expressed) or other kinases (A-raf, c-mos and Chk1 have all been reported to interact with the α-subunit possibly using the same binding mode observed for CK2α) or non-kinase partners. Here we report that in vitro a stable and active $\alpha\beta_2$ holoenzyme can be produced and this is able to recruit the α'-subunit in a stable chimeric $\alpha\alpha'\beta_2$ holoenzyme.

We also propose that binding of α-subunits to β-dimers is purely non-cooperative. The absence of any binding synergism could be inferred from the fact that no major structural rearrangement can be noticed in free and CK2α-bound β-dimer.

2.3 Conclusions

With the final aim to study the possible structural role of the C-terminus of CK2α, which is usually deleted for crystallization purpose being easily degraded during the purification process, but it plays an active role during the cell cycle, we produced and crystallized a stable full-length CK2α phosphomimetic mutant ($CK2\alpha^{pm}$) and a tetrameric holoenzyme with the same catalytic subunit. Furthermore we produced, crystallized and solved the 3D structure of other two tetrameric holoenzymes, one with the wild-type full-length CK2α ($CK2\alpha^{wt}$), and one with the deleted form of CK2α ($CK2\alpha^{del}$).

The purified $CK2\alpha^{pm}$ was submitted to extensive crystallization trials but it was successfully crystallized only in the crystallization conditions known for the deleted form of the protein, with the same space group and with the same crystal packing. In addition, no extra electron density was visible for the last 59 residues, like in the case of the structure of the previously published deleted form.

Regarding the full-length tetrameric holoenzymes, they were submitted to extensive crystallization trials and we optimized a new, never published, condition for the crystallization. Unfortunately, again it was not possible to visualize the electron density of the C-terminal tail because in the structures of the full-length holoenzymes the C-terminus appears to be flexible and disorder. The main difference between the structures of the holoenzymes with the full-length CKα ($CK2\alpha^{pm}$ and $CK2\alpha^{wt}$) and with the deleted form of CK2α ($CK2\alpha^{del}$) is the space group: $P2_1$ for the full-length and C2 for the deleted CK2 holoenzyme. The crystal packing is very similar and the only difference has to be ascribed to the extra space required for the C-terminal tail. Our new tetrameric holoenzymes structures differ significantly with the previously published CK2 holoenzyme structures. In particular the latter appears to be an asymmetric complex while our structure confutes this conformation with a more stable and symmetric holoenzyme, which is more in accordance with the functional and biochemical data present in literature.

3. CK2 holoenzymes: CK2α'$_2$β$_2$ and CK2αα'β$_2$

3.1 Methods

3.1.1 Overview

After the crystallization of the CK2 holoenzyme with the CK2α subunits, we focused the attention to the paralog isoform of the catalytic enzyme CK2α'. The paralog isoform of the catalytic subunit CK2α', present in humans and higher animals, is very similar in sequence to the CK2α up to position 330, while the C-terminal segments differ completely in length and sequence. The thermostabilization of CK2α' by the interaction with CK2β is much less than in the case of the CK2α and this, in accordance with other evidences, means that the affinity between CK2α' and CK2β is significantly lower than that between CK2α and CK2β (Olsen et al., 2006). The knowledge on CK2α' is much lower than the paralog isoform CK2α; the main reasons are the reported solubility problems that occur after the expression in hosts cells like *E. coli* or insect cells. This problem was overcome with the genetic truncation of the C-terminal segment from Gln334 upwards (Nakaniwa et al., 2009) or by the single point mutation of the full-length protein where the Cys336 is mutated in Ser (Bischoff et al., 2011). We worked with the full-length mouse CK2α' conjugated with the GST tag which may increase expression and solubility of the recombinant fusion protein and is useful for the first step of affinity chromatography. After the sequencing of the fragment encoding for the mouse CK2α' we found that 14 amino acids coming from the MCS (Multiple Cloning Site) were present at the N-terminal tail of the protein, after the region encoding for the GST tag. At the beginning we decided to work with this long-form of the protein and try the level of expression and eventually the crystallization. After the difficulty in obtaining good diffracting crystals we decided to eliminate the 14 amino acids of the MCS at N-terminal tail firstly re-cloning the entire CK2α' in a new vector without the GST tag and secondly by inserting a new cleavage site exactly after the 14 amino acids. In the end we tried to purify and crystallize the CK2α'$_2$β$_2$ starting from three different clones:

1) GST-CK2α'$_2^{long}$ with the 14-amino acids tail at the N-terminal;

2) CK2α'$_2^{wt}$ without the 14-amino acids tail and without the GST tag;

3) GST-CK2α'$_2^{del}$ without the 14-amino acids tail at the N-terminal and starting from amino acid 3 of the wt sequence.

```
CK2α'_long  GST-trombine cleavage site-MATTHMDIGSGFPGIPGPAAGSRARVYAEVNSLRSREYWDYEAHVPSWGN 50
CK2α'_MOUSE                            --------------MPGPAAGSRARVYAEVNSLRSREYWDYEAHVPSWGN 36
CK2α'_HUMAN                            --------------MPGPAAGSRARVYAEVNSLRSREYWDYEAHVPSWGN 36
                                                     :**********************************

CK2α'_long                             QDDYQLVRKLGRGKYSEVFEAINITNNERVVVKILKPVKKKKIKREVKIL 100
CK2α'_MOUSE                            QDDYQLVRKLGRGKYSEVFEAINITNNERVVVKILKPVKKKKIKREVKIL 86
CK2α'_HUMAN                            QDDYQLVRKLGRGKYSEVFEAINITNNERVVVKILKPVKKKKIKREVKIL 86
                                       **************************************************

CK2α'_long                             ENLRGGTNIIKLIDTVKDPVSKTPALVFEYINNTDFKQLYQILTDFDIRF 150
CK2α'_MOUSE                            ENLRGGTNIIKLIDTVKDPVSKTPALVFEYINNTDFKQLYQILTDFDIRF 136
CK2α'_HUMAN                            ENLRGGTNIIKLIDTVKDPVSKTPALVFEYINNTDFKQLYQILTDFDIRF 136
                                       **************************************************

CK2α'_long                             YMYELLKALDYCHSKGIMHRDVKPHNVMIDHQQKKLRLIDWGLAEFYHPA 200
CK2α'_MOUSE                            YMYELLKALDYCHSKGIMHRDVKPHNVMIDHQQKKLRLIDWGLAEFYHPA 186
CK2α'_HUMAN                            YMYELLKALDYCHSKGIMHRDVKPHNVMIDHQQKKLRLIDWGLAEFYHPA 186
                                       **************************************************

CK2α'_long                             QEYNVRVASRYFKGPELLVDYQMYDYSLDMWSLGCMLASMIFRKEPFFHG 250
CK2α'_MOUSE                            QEYNVRVASRYFKGPELLVDYQMYDYSLDMWSLGCMLASMIFRKEPFFHG 236
CK2α'_HUMAN                            QEYNVRVASRYFKGPELLVDYQMYDYSLDMWSLGCMLASMIFRREPFFHG 236
                                       *******************************************:******

CK2α'_long                             QDNYDQLVRIAKVLGTDELYGYLKKYHIDLDPHFNDILGQHSRKRWENFI 300
CK2α'_MOUSE                            QDNYDQLVRIAKVLGTDELYGYLKKYHIDLDPHFNDILGQHSRKRWENFI 286
CK2α'_HUMAN                            QDNYDQLVRIAKVLGTEELYGYLKKYHIDLDPHFNDILGQHSRKRWENFI 286
                                       ***************:**********************************

CK2α'_long                             HSENRHLVSPEALDLLDKLLRYDHQQRLTAKEAMEHPYFYPVVKEQSQPC 350
CK2α'_MOUSE                            HSENRHLVSPEALDLLDKLLRYDHQQRLTAKEAMEHPYFYPVVKEQSQPC 336
CK2α'_HUMAN                            HSENRHLVSPEALDLLDKLLRYDHQQRLTAKEAMEHPYFYPVVKEQSQPC 336
                                       **************************************************

CK2α'_long                             AENTVLSSGLTAAR 364
CK2α'_MOUSE                            AENTVLSSGLTAAR 350
CK2α'_HUMAN                            ADNAVLSSGLTAAR 350
                                       *:*:**********
```

Figure 3.1 *Sequence alignment of the mouse CK2α'long (CK2α'_long) form in comparison with the wild type mouse CK2α'(CK2α'_MOUSE) and with the human CK2α'(CK2α'_HUMAN).*

Due to the difficulty on obtaining good diffracting crystals with all of the three CK2α' variants, we tried to obtain a chimeric holoenzyme (found also in testis and brain physiologically) composed of the regulatory β_2-dimer and of both the two catalytic subunits CK2α and CK2α'^{del}. The crystallization of the homogenous CK2α'$_2\beta_2$

holoenzyme had a limit on the dimension reached by the crystal probably due to the unfavourable crystal packing within the crystal. In order to favor the crystallographic contacts we added a subunit more prone to the crystallization like the CK2α^{pm} into the holoenzyme, purifying the chimeric holoenzyme CK2α^{pm}α'^{del}β$_2$. In order to purify the chimeric tetramer we firstly isolated the trimeric form CK2α^{pm}β$_2$ during the purification of the holoenzyme CK2α$^{pm}{}_2$β$_2$, and then we added free CK2α'^{del} previously purified (or expressed).

3.1.2 Cloning

1) CK2α'$_2{}^{wt}$β$_2$

To eliminate the 14 amino acids at the N-terminal tail, we decided to re-clone the entire fragment of CK2α' in a new vector, without the GST tag for the purification. The nucleotide sequence of CK2α' was amplified by PCR starting from the plasmid using two primers (in the box below) in order to insert a NdeI restriction site at the N-terminus and a HindIII restriction site at the C-terminus.

Table 3.1 Primers for the PCR amplification of the mouse CK2α'wt

Primers	base	Tm (°C)
5' TACATATGCCCGGCCCGGCC 3'	20	66.5
5' TTAAGCTTTCATCGTCGTGCTGCGGTGA 3'	28	61.6

MIX: 2.5 µl reaction buffer, 2 µl of plasmid containing the sequence of CK2α'^{long}, 4.5 µl of each primers (4.5 pmol), 0.5 µl of dNTPs, 11.0 µl of H_2O, 0.5 µl of DNA polimerase *Genespin* (2.5 U/µl). The amplified sequence was separated from the plasmid by extraction from agarose gel using PureLink Quick Gel Extraction Kit (Invitrogen).

The PCR product was firstly phosphorylated using T4 Polynucleotide Kinase (New England BioLabs) and inserted into the pBluescript II SK (+/−) storage phagemid (Agilent Technologies) previously digested to create blunt ends by EcoRV restriction enzyme; this intermediate passage was fundamental for a successful digestion with NdeI and HindIII. After the digestion with restriction enzymes, the fragment with sticky ends was inserted in a linearized pET-20b vector (Novagen) digested with the same enzymes.

2) GST-CK2α'$_2^{del}$β$_2$

Due to the difficulty on expressing the protein without the GST tag in *E. coli*, we decided to insert a new restriction site for *Prescission* protease after the 14 amino acids and exactly before the sequence for CK2α'. To insert the new restriction site we used QuickChange® Site-Directed Mutagenesis kit (Stratagene) and PfuTurbo® DNA polymerase with the two primers in the box below:

Table 3.2 Primers for the insertion of a new cleavage site for Prescission protease

Primers	base	Tm (°C)
5' CTGGAAGTTCTGTTCCAGGGCCCGGCCGCGGGCAGTCG	38	86.4
3' GCCTAGGCTTAAGGGCCCCTAGGGGGACCTTCAAGACAAGGT	42	84.1

MIX: 2.5 µl reaction buffer, 2 µl of plasmid containing the sequence of CK2α'^{long}, 4.5 µl of each primers (4.5 pmol), 0.5 µl of dNTPs, 11.0 µl of H_2O, 0.5 µl of PfuTurbo DNA polimerase (2.5 U/µl). After 16 PCR cycles we add 1 µl of Dpn I restriction enzyme (10 U/µl) for the digestion of non-mutated DNA.

3.1.3 Protein expression

E. coli BL21(DE3) cells, harbouring the plasmid pT7-CK2β, pET-20b-CK2α' (wt) and pGEX-CK2α' (long and del) were grown overnight (ON) at 37 °C in LB medium (10 g/l tryptone, 5 g/l yeast extract, and 10 g/l NaCl) supplemented with 50 µg/ml ampicillin. LB medium was inoculated with this ON culture (ratio 1:10) and grown at 37 °C, in a suitable shaker. Protein expression was induced at an OD_{600} of 0.6 by adding 1 mM IPTG and prolonged for 4-5 h at 30 °C under vigorous shaking. Bacteria were harvested by centrifugation at 5000 g for 30'.

3.1.4 Protein purification

Bacteria were suspended in buffer A [25 mM Tris-HCl (pH 8), 500 mM NaCl, 0.4 mM (tris(2-carboxyethyl)phosphine) (TCEP)] supplemented with protease inhibitors EDTA free (Roche) mixed together to allow the formation of the tetrameric complex and lysed with a French press (Thermo Spectronic) at high pressure.

The lysate was centrifuged to remove cell debris at 27000 g for 30' and filtered with 0.22 μm syringe filter. The sample is loaded onto an affinity resin Glutathione Sepharose Fast Flow (GE Healthcare) in batch and equilibrated with buffer A. After extensive washing with buffer A we added to the resin the protease (*Trombine* or *PreScission*), which recognises the cleavage site at the beginning of the CK2α' sequence, and incubated with the resin over night at 4 °C. After the cleavage the CK2α' is eluted from the resin simply by washing with buffer A, while the GST is still bounded to the glutathione present on the resin. Fractions containing the CK2α'$_2$β$_2$ were pooled and further purified by size exclusion chromatography using a Superdex 200 prep-grade 26/60 column or a Superdex 200 10/300 (GE Healthcare) equilibrated with buffer B [25 mM Tris-HCl (pH 8.5), 500 mM NaCl, and 0.2 mM TCEP].

For the chimeric holoenzyme we mixed the purified GST-CK2α$^{'del}$ (or its lysate) to the trimer CK2α^{pm}β$_2$ and the first purification step was composed of an affinity chromatography using resin Glutathione Sepharose Fast Flow (GE Healthcare) in batch with buffer A; this purification step was fundamental to separate the CK2 tetramer which had incorporate a GST-CK2α$^{'del}$ with respect to the small portion of homogenous CK2α$^{pm}{}_2$β$_2$. The second purification step was composed of a gel filtration chromatography with a Superdex 200 10/300 GL column with buffer B. The fastest method to obtain pure GST-CK2α$^{'del}$ is to purify the protein via an affinity column performed on a Äkta FPLC chromatographic system (GE Healthcare) using a HiTrap Heparin HP 5ml (GE Healthcare) equilibrated with buffer C [25 mM Tris-HCl (pH 8), 300 mM NaCl, and 0.4 mM TCEP].

3.1.5 Protein crystallization

Crystallization trials using commercial kits (Qiagen, Molecular Dimensions and Hampton Research) based on sparse matrix, grid screen, and/or ionic sampling, were performed by vapour diffusion (with the sitting drop method) techniques, using the Oryx8 automatic system (Douglas Instrument). CK2α'$_2$β$_2$ was concentrated to 8 mg/ml for crystallization purposes. Crystals for the CK2α'$_2^{long}$β$_2$ were grown at 20 °C with the vapor diffusion technique, using the following precipitant solution: 10% w/v PEG 4000, 20% v/v glycerol, 0.03 M of a mix composed of halogens, etilenglycol or monosaccharides and 0.1 M buffer (Bicine, HEPES, MES), pH 8.5, 7.5, 6.5. Crystals for the CK2α'$_2^{del}$β$_2$ grown

at 4 °C, using the following precipitant solution: PEG 400 25%, 0.1 M Tris pH 8.5, 150 mM sodium citrate.

CK2$\alpha^{pm}\alpha'^{del}\beta_2$ was concentrated to 8 mg/ml for crystallization purposes We obtained nice hexagonal crystal with the CK2$\alpha^{pm}\alpha'^{del}\beta_2$ grown at 20 °C, using the following precipitant solution: 0.24 M sodium malonate pH 7 and PEG 3350, 22%.

3.1.6 Data collection

We collected some images at the European *Synchrotron* Radiation Facility beamline ID23-2 *gemini* (ESRF Grenoble, France) and at the ELETTRA-Synchrotron beamline XDR1, (Trieste, Italy).

3.2 Results

3.2.1 GST-CK2α'$_2^{long}$β$_2$

3.2.1.1 Protein Expression and Purification

We expressed both the GST-CK2α'^{long} and the CK2β in *E. coli* BL21(DE3) in a ratio 1:2.5 of volume culture; even if the volume of the culture for the GST-CK2α'^{long} is less than a half of the volume for the CK2β, we would have an excess of the first subunit due to a high expression level of the protein with the GST tag. To permit the formation of a stable GST-CK2α'$_2^{long}$β$_2$ complex we lysated together the two bacterial pellets containing the two subunits and after the centrifugation and filtration we loaded the sample in an Glutathione Sepharose Fast Flow resin (GE Healthcare) in batch for the first affinity purification step. This step of purification uses the affinity between the fusion tag GST protein and the glutathione which the resin is functionalized with: only the protein with the GST tag would be able to bind to the resin while the bacterial lysate would elute from the column with the *flow-through* fraction. We worked with an excess of GST-CK2α'^{long} to avoid the formation of a double population of tetramers and trimers, like in the purification of the CK2α$_2$β$_2$ holoenzyme, which are difficult to separate and require more purification steps.

We performed several washing cycles with buffer A [25 mM Tris-HCl (pH 8), 500 mM NaCl, 0.4 mM TCEP] for eliminate the aspecific bindings. We didn't use the standard protocol of purification which required the elution of the protein of interest from the column with a 5 mM glutathione solution and a subsequent cleavage the specific protease of the GST tag in solution. We rather preferred to add the *Trombin* protease directly in the column and left it incubate with the GST-CK2α'$_2^{long}$β$_2$ over night at 4 °C; we decided to do this modification of the protocol to reduce the purification steps which may prompt to a degradation and loss of protein material due to the fact that the CK2α' is reported to be very instable after the expression.

After overnight incubation we eluted the protein form the column and the fraction was loaded in a coomassie-stained SDS–PAGE (Figure 3.2). After the incubation with the protease a huge amount of protein precipitated within the resin (Lane 6) and only a small part of the CK2α'$_2^{long}$β$_2$ remained soluble and could be eluted from the column (Lanes 7 and 8). By the way the SDS-PAGE confirmed that the complex between CK2α'^{long} and CK2β$_2$ was formed. The purity of the sample could be good enough but we performed a

size exclusion chromatography to recruit information about the aggregation state of the protein and compare the elution volume with the other purified holoenzymes. The size exclusion chromatography was performed also to put the protein of interest in the buffer solution B [25 mM Tris-HCl (pH 8.5), 500 mM NaCl, 0.2 mM TCEP].

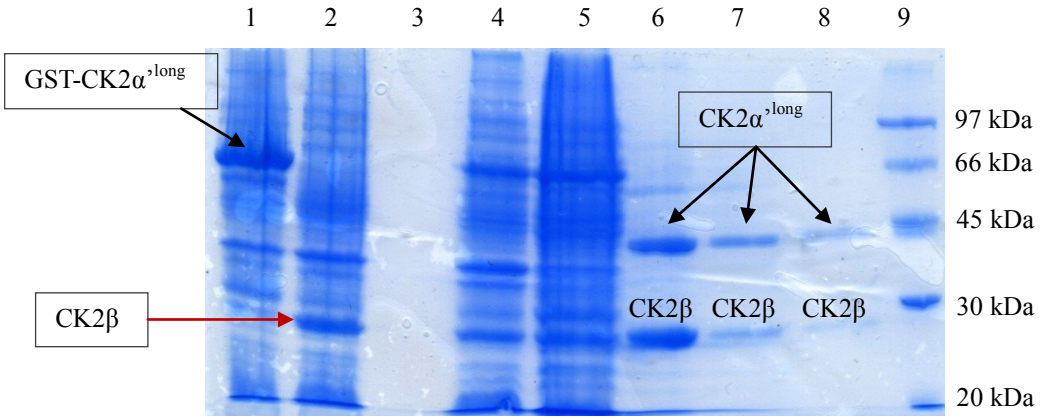

Figure 3.2 *Coomassie-stained SDS–PAGE of CK2α'$_2^{long}$β$_2$ purification. Lanes 1 corresponds to the IPTG induced cells of CK2α'$_2^{long}$. Lane 2 corresponds to the IPTG induced cells of CK2β. Lane 3 empty. Lane 4 soluble portion of bacterial lysate. Lane 5 insoluble fraction of bacterial lysate. Lane 6 resin after the cleavage. Lane 7 and 8 elution of the protein after the cleavage. Lane 9 low molecular weight protein markers.*

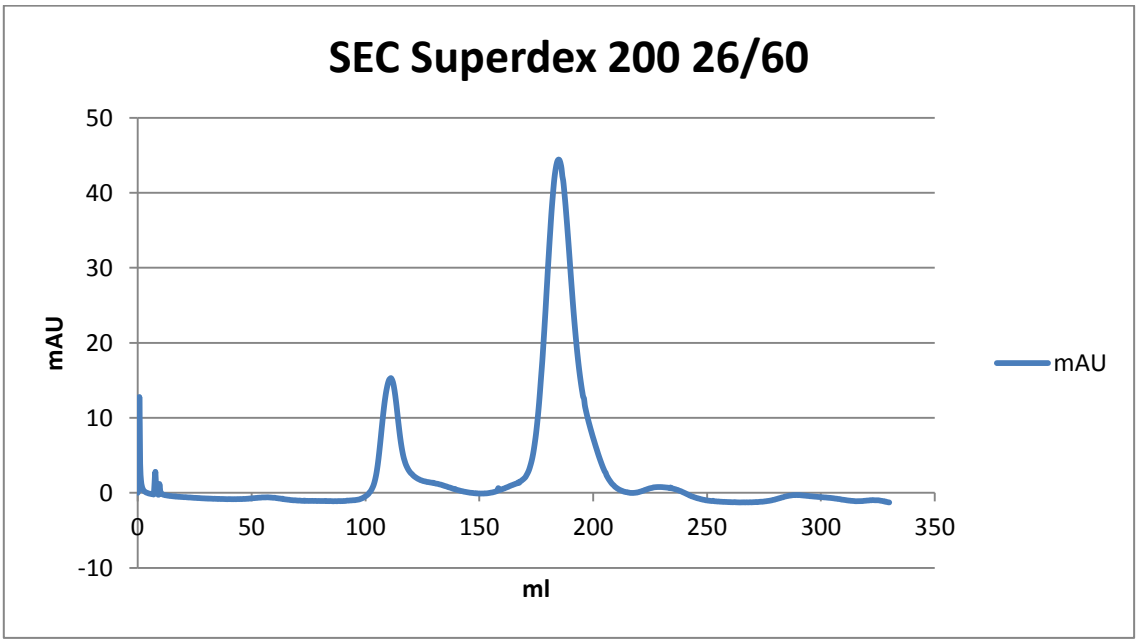

Figure 3.3 *Elution profile of CK2α'$_2^{long}$β$_2$ from size exclusion chromatography with a Superdex 200 prep-grade 26/60 column (GE Healthcare) equilibrated with buffer B [25 mM Tris-HCl (pH 8.5), 500 mM NaCl, and 0.2 mM TCEP].*

The elution volume of the CK2α'$_2^{long}$β$_2$ is comparable to the tetrameric form of the full-length CK2 holoenzyme. In this case we didn't have a double population of

holoenzymes because we worked with an excess of CK2α'^{long}. The sample was concentrated by ultrafiltration to a concentration of 8 mg/ml in a final volume of 160 µl with a final yield of 1.2 mg for 3.5 L of culture (0.3 mg per liter).

3.2.1.2 Protein Crystallization

Even with a low final yield of protein we were able to perform some crystallographic trials; we started from crystallization trials using commercial kits based on sparse matrix with the Oryx8 automatic system (Douglas Instrument). From the crystallization screenings that we tried, only the last kit, Morpheus (Molecular Dimension), gave several hits in the 96-wells plate, all containing very small and very thin microcrystals. All of the precipitant conditions which gave crystals had a similar precipitant composition made by 10% w/v PEG 4000, 20% v/v glycerol, 0.03 M of a mix composed by halogens, etilenglycol or monosaccharides and 0.1 M buffer (Bicine, HEPES, MES), pH 8.5, 7.5, 6.5. With the last aliquot of protein we tried to optimize the precipitant conditions, making some drops by hand; unfortunately the crystals grew only with the robot. However we were able to collect a data set at 8 Å for the CK2α'$_2^{long}$β$_2$ merging diffraction images coming from three different microcrystals; the radiation damage was very high for these crystals and after a small period of exposure the diffraction became null.

Figure 3.4 *Detail of the diffraction image collected at the European Synchrotron Radiation Facility beamline ID23-2 gemini (ESRF Grenoble, France); the external spots correspond to a maximum resolution of 8 Å.*

The quality of the diffraction was good (Figure 3.4) but the intensity of the few spots was very low and it was not possible to elaborate the data.

We obtained other crystals with the microseeding technique, but the limit was always the small dimension and the difficulty to manipulate the crystals. The difficulty on obtaining big diffracting crystals could be due to the high flexibility of some elements of the protein: we than decided to eliminate the 14 amino acids at the N-terminal tail of the CK2α'^{long}.

3.2.2 CK2α'$_2^{wt}$β$_2$

3.2.2.1 Cloning

The first approach to eliminate the 14 amino acids at the N-terminal tail of the protein was to re-clone the entire sequence of mouse CK2α' (CK2α'$_2^{wt}$) in a new expression vector. To do this we amplified the sequence of the CK2α'$_2^{wt}$β from the vector pGEX-CK2α'^{long} with the primers listed in Table 3.1, which also insert a new restriction sites for the following insertion in the new expression vector. After the PCR we loaded the PCR product in a agarose gel with *SYBR Green* Safe dye; the PCR product have a dimension of 1053 bp and it was visible as a strong band at the level of the 1 kb marker (Figure 3.5).

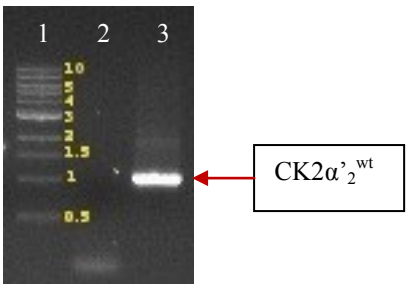

Figure 3.5 *Agarose gel electrophoresis of the PCR product stained with SYBR Green Safe dye. Lane 1 marker of molecular weight markers in kb. Lane 2 control, PCR without primers. Lane 3 PCR product.*

We performed an extraction from the gel using a PureLink Quick Gel Extraction Kit (Invitrogen) to obtain a pure PCR product. To insert the PCR product of CK2α'$_2^{wt}$ in a new expression vector we had to digest it with the restriction enzymes NdeI at the N-terminus and HindIII at the C-terminus. After the gel extraction we noticed that the efficiency of the digestion by the restriction enzymes was very low on this linearized fragment; to avoid this problem we added an intermediate step in the protocol, cloning the fragment CK2α'^{wt} into the pBluescript II SK (+/−) storage phagemid (Agilent Technologies). We firstly phosphorylated the PCR product with T4 Polynucleotide Kinase (New England BioLabs) and then inserted in the linearized pBSK vector previously digested to create blunt ends by EcoRV restriction enzyme. The efficiency of digestion by the restriction enzymes on a long DNA fragment, instead of the linearized PCR product, highly increased and this was confirmed by the agarose gel of the digested pBSK vector: the digestion was performed with the NdeI and HindIII restriction enzymes which were

able to recognize the restriction sites and digest the vector realising a sticky ends CK2α'$_2^{wt}$ fragment ready for the further insertion in the final expression vector.

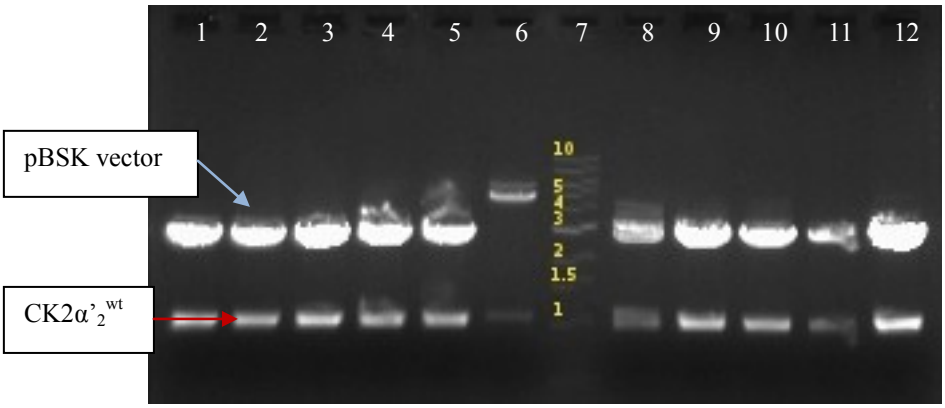

Figure 3.6 *Agarose gel electrophoresis of the digestion of pBSK vector containing the CK2α'$_2^{wt}$ fragment stained with SYBR Green Safe dye. Lanes 1-6 and 8-12 digestion products (pBSK vector = 3.4 kb and CK2α'$_2^{wt}$ = 1053 pb). Lane 7 marker of molecular weight markers in kb.*

The CK2α'$_2^{wt}$ fragment was than extracted from the gel with the same procedure described before and inserted in the final expression vector: the pET-20b was previously linearized with the restriction enzymes NdeI and HindIII, purified and dephosphorylated as from protocol. The final product of the ligation was than amplified in competent *E. coli* cells and digested with the same restriction enzymes: the digested sample was then loaded into an agarose gel for select the clones which had incorporated the correct vector. All the selected clones contained the CK2α'$_2^{wt}$ fragment correctly inserted in the pET-20b vector and the sequence was confirmed by DNA sequencing.

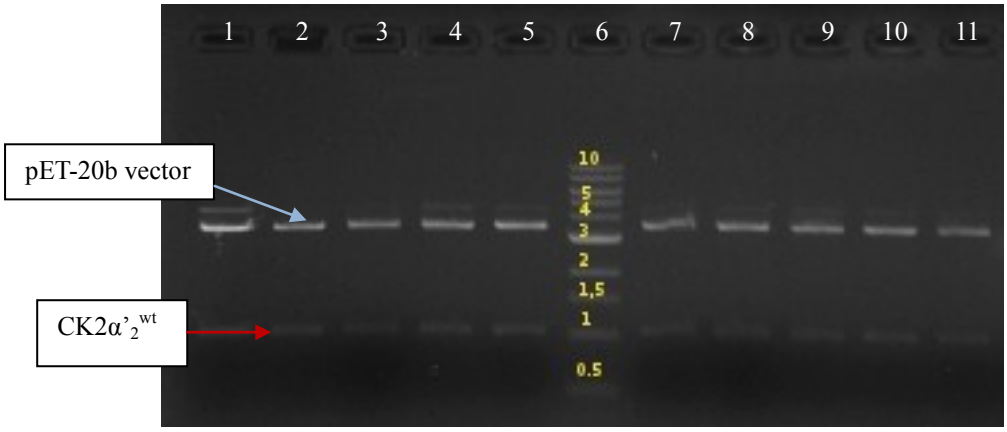

Figure 3.7 *Agarose gel electrophoresis of the digestion of pET-20b vector containing the CK2α'$_2^{wt}$ fragment stained with SYBR Green Safe dye. Lanes 1-5 and 7-11 digestion products (pET-20b vector = 3.7 kb and CK2α'$_2^{wt}$ = 1053 pb). Lane 6 molecular weight markers in kb.*

3.2.2.2 Protein Expression

Once obtained the final clone with the sequence codifying for CK2α'$_2^{wt}$ we verified the expression level in a small culture volume of *E. coli* BL21(DE3). We set up two different culture of 100 ml volume each with different induction temperature, 30 °C for 5 hours (flask 1) and 20 °C for 16 hours (flask 2), after the reaching the OD_{600} of 0.7. The culture was than lysed and centrifuged and the soluble and insoluble fractions were loaded in a Coomassie-stained SDS–PAGE.

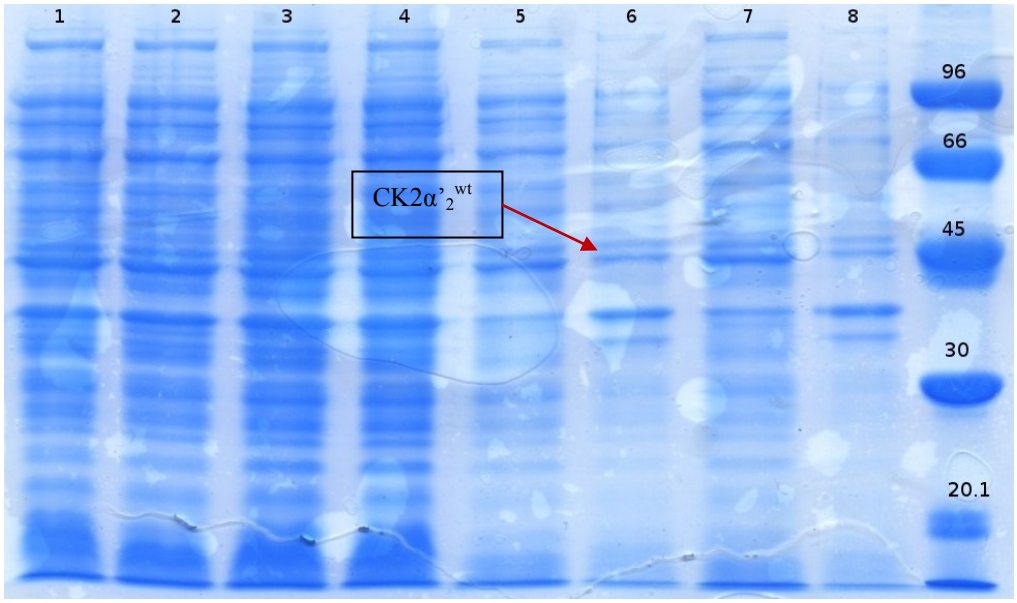

Figure 3.8 *Coomassie-stained SDS–PAGE of CK2α'$_2^{wt}$ expression. Lanes 1 corresponds to non-inducted flask 1. Lane 2 corresponds to the non-inducted flask 2. Lane 3 and 4 IPTG induced cell after 2 hours in flask 1 and 2 respectively. Lane 5 Soluble fraction of flask 1 expression. Lane 6 Insoluble fraction of flask 1 expression. Lane 7 Soluble fraction of flask 2 expression. Lane 8 Insoluble fraction of flask 2 expression. Lane 9 low molecular weight protein markers.*

The expression level of the protein was very low or pretty much null. The GST is fundamental for the correct expression of the protein as crucial is its localization at the N-terminus: in this way the expression of the fusion protein starts from the GST which permits the solubilisation of the CK2α'. Without the GST the protein seems to be insoluble and the bacterial cells are not able to express it; this in accordance with the fact that after the cleavage of the GST tag with the protease *Trombin*, more than a half of CK2α'$_2^{long}$β$_2$ precipitates in column and only a small amount of holoenzyme remains in solution. We than decided to leave the GST tag but to insert a new cleavage site precisely after the 14 amino acids fragment.

3.2.3 CK2α'$_2^{del}$β$_2$

3.2.3.1 Cloning

To eliminate the 14 amino acids at the N-terminus we inserted a sequence of recognition for the *PreScission Protease* exactly before the sequence of the mouse CK2α'. *PreScission Protease* is a genetically engineered fusion protein consisting of human rhinovirus 3C protease and GST. It can be used following affinity purification or while fusion proteins are bound to Glutathione Sepharose 4 Fast Flow. It specifically cleaves between the Gln and Gly residues of the recognition sequence of `Leu Glu Val Leu Phe Gln | Gly Pro`. We used the residues 3 and 4 of the wild type CK2α' as residues recognized by the *PreScission Protease* and we inserted the previous 6 residues by PCR mutagenesis. After the PCR the situation inside the plasmid is as it follows:

```
                                    Leu Glu Val Leu Phe Gln   Gly Pro Ala Ala Gly Ser
  <---------- 14 aa ----------  5' CTG GAA GTT CTG TTC CAG | GGC CCG GCC GCG GGC AGT CG 3'
5' G CCT AGG CTT AAG GGC CCC TAG GGG GAC CTT CAA GAC AAG GTC 3'    CK2α' sequence ---------->
```

Figure 3.9 *In red the nucleotide sequence of the primer complementary to the sequence of the 14 amino acids of the MCS; in black the sequence inserted by the primer recognized by the Prescission protease which cut at the level of the marker (|) between Gln and Gly and in green the sequence of the CK2α'.*

Note that after the digestion with the protease the first amino acids are Gly Pro while in the wild type form are Met Pro Gly Pro: we deleted 2 amino acids in the mutagenesis and the protein starts with residue Gly3 (GST-CK2α'^{del}).

The sequence has been confirmed by DNA sequencing.

3.2.3.2 Protein Expression and Purification

We expressed both the GST-CK2α'^{del} and the CK2β in *E. coli* BL21(DE3) in a ratio 1:2.5 of volume culture. We lysated together the two bacterial pellets within buffer A [25 mM Tris-HCl (pH 8), 500 mM NaCl, 0.4 mM TCEP], centrifuged and filtrated with 0.22 µm filter. The purification protocol is the same used for the purification of the CK2α'$_2^{long}$β$_2$ apart from the adding of the *PreScission Protease* instead of the *Trombine Protease* after the first affinity chromatography. We loaded the lysate in the glutathione sepharose resin and we washed the column with ten column volumes. We added the *PreScission Protease* and left it acts in the column overnight at 4 °C. We eluted the purified protein from the column and we loaded the fractions collected in a

Coomassie-stained SDS–PAGE. The *PreScission Protease* is fused with a GST tag and it remained bounded in the column.

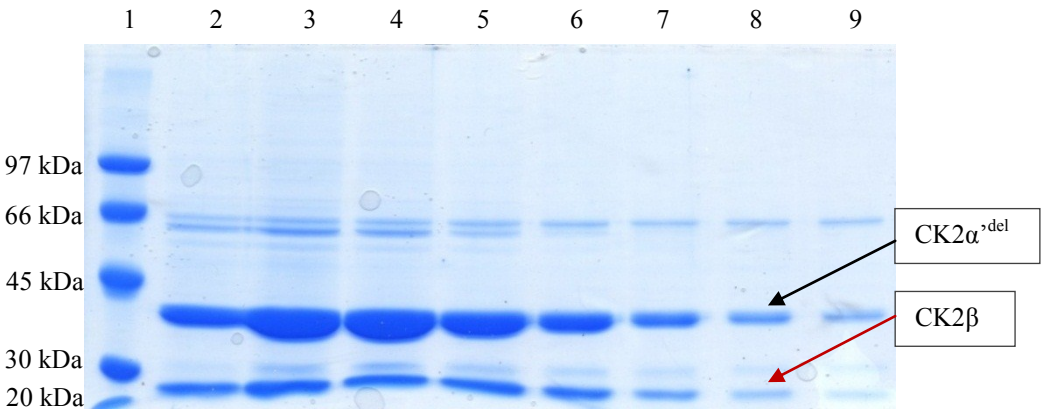

Figure 3.10 *Coomassie-stained SDS–PAGE of after the affinity chromatography. Lane 1 low molecular weight protein markers. Lanes 2-9 fractions of the elution of the protein after the cleavage.*

The *PreScission Protease* recognized the cleavage site and the result is a 40 kDa protein CK2α'^{del} confirmed by the presence of the bands below the of 45 kDa band of the molecular weight protein marker. Also the band corresponding to the CK2β was present; the intensity of the band is lower in comparison with the CK2α'^{del} because we worked in an excess of CK2α'^{del} in the expression volumes. We had an excess of free CK2α'^{del} in the elution sample and the next step of purification by size exclusion chromatography was fundamental to separate the holoenzyme from the free unbound catalytic subunit.

We pooled together the fractions containing the protein and, after a concentration by ultracentrifugation, we loaded the sample in a Superdex 200 10/300 (GE Healthcare) equilibrated with buffer B [25 mM Tris-HCl (pH 8.5), 500 mM NaCl, and 0.2 mM TCEP].

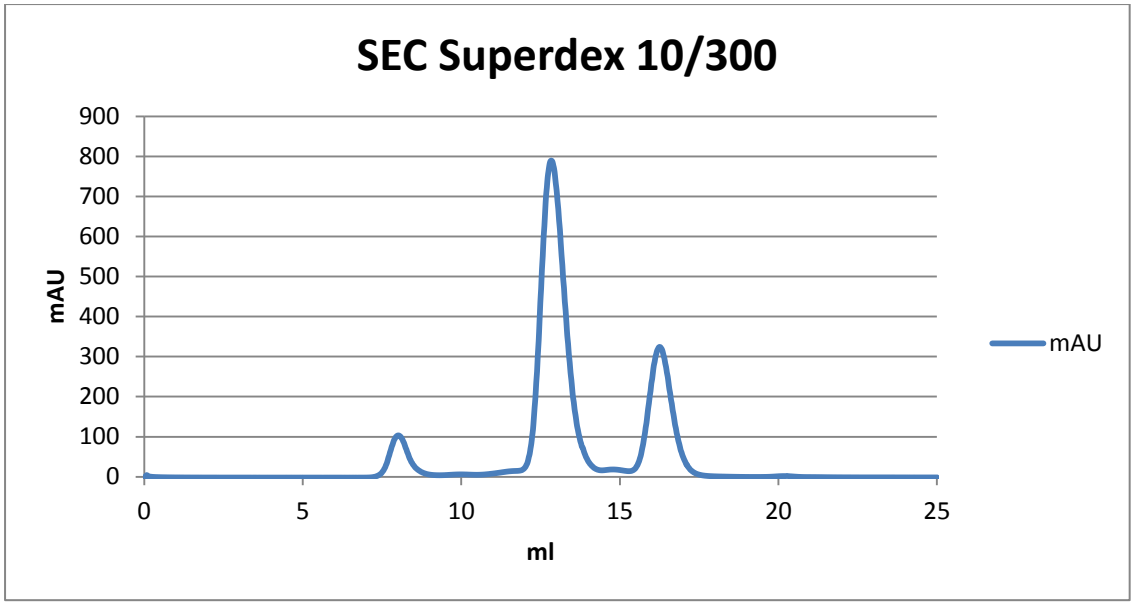

Figure 3.11 *Elution profile of CK2α'$_2^{del}$β$_2$ from size exclusion chromatography with a Superdex 200 10/300 column (GE Healthcare) equilibrated with buffer B [25 mM Tris-HCl (pH 8.5), 500 mM NaCl, and 0.2 mM TCEP]*

The elution profile of the CK2α'$_2^{del}$β$_2$ is composed of a major peak which corresponds to the holoenzyme form and a small peak after the major one, which corresponds to the excess of free CK2α'$_2^{del}$ present in the sample eluted from the affinity. The purity of the sample was confirmed by a Coomassie-stained SDS–PAGE of the fractions of the main peak.

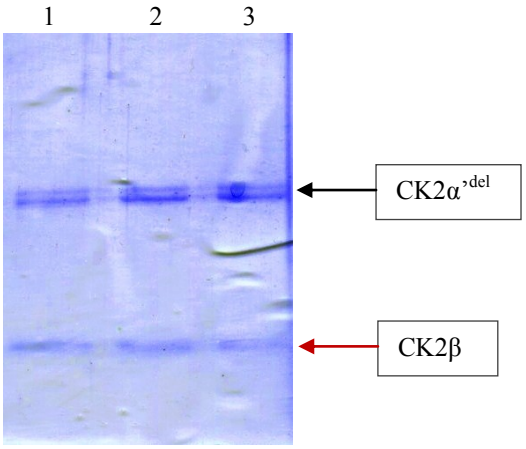

Figure 3.12 *Coomassie-stained SDS–PAGE of after the size exclusion chromatography. Lanes 1-3 fractions of main peak of the elution profile.*

The purity of the sample is very high and we proceeded with the concentration of the sample by ultracentrifugation; the holoenzyme has been concentrated to 12.8 mg/ml

and the fraction containing the CK2α'^{del} in excess were pulled together and concentrated to 7 mg/ml. The final yield had been optimized in respect to the first purification of the GST- CK2α'$_2^{long}$ and the final yield for the holoenzyme with this clone of CK2α'^{del} was 1 mg for 1 L of culture.

3.2.3.3 Protein Crystallization

We performed some crystallographic trials, starting from commercial kits based on sparse matrix with the Oryx8 automatic system (Douglas Instrument). From the crystallization trials we obtained different forms of microcrystals and some of them were tested at the the ELETTRA-Synchrotron beamline XDR1, (Trieste, Italy). We tried also different temperatures and the best condition reached the 7 Å resolution. The precipitant solution was composed of di PEG 400 25%, 0.1 M Tris-HCl pH 8.5, 150 mM sodium citrate; crystals were very difficult to reproduce and we took the photo (Figure 3.13) before the measurement at the synchrotron.

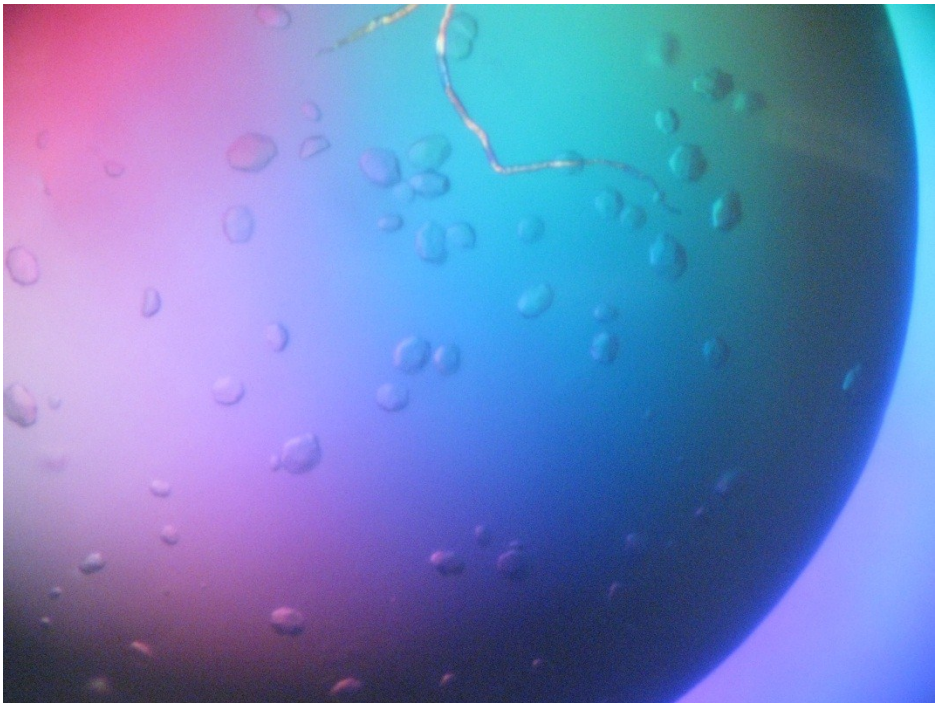

Figure 3.13 *Crystals of CK2α'$_2^{del}$β$_2$ in PEG 400 25%, 0.1 M Tris-HCl pH 8.5, 150 mM sodium citrate.*

One more time the main problem in the crystallization of an holoenzyme with CK2α'$_2^{del}$ was the dimension reached by the crystals. We were able to collect only a small

number of diffraction images before the radiation damage and the disruption of the crystal. The crystal packing is probably not very compact, the crystallographic contacts are not favorable and there is a high amount of water which all contribute to the low diffraction limit and to the difficulty on obtaining big crystals.

3.2.4 CK2α^{pm}α'^{del}β$_2$

3.2.4.1 Protein Expression and Purification

We expressed the GST-CK2α'^{del} in *E. coli* BL21(DE3). The best way to purify the chimeric holoenzyme is to purify separately the GST-CK2α'^{del} and the trimer CK2α^{pm}β$_2$ before the mixing. We lysated the bacterial pellet of GST-CK2α'^{del} within buffer C [25 mM Tris-HCl (pH 8), 300 mM NaCl, 0.2 mM TCEP], centrifuged and filtrated with 0.22 µm filter. We purified the GST-CK2α'^{del} with a single purification step with Äkta FPLC chromatographic system (GE Healthcare) using a HiTrap Heparin HP 5 ml column (GE Healthcare). The elution was performed with an increasing concentration of NaCl and the chromatogram obtained is very similar to the previously purified CK2α^{pm}.

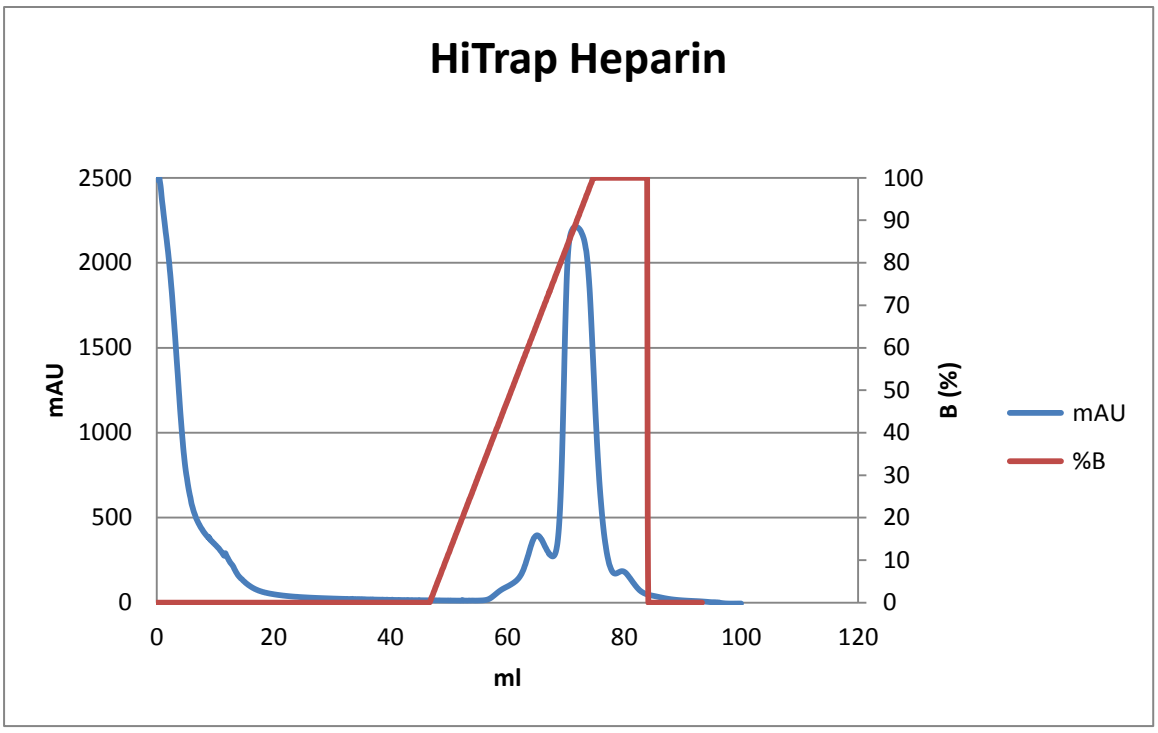

Figure 3.14 *Elution profile of affinity chromatography of GST-CK2α'^{del} on column: HiTrap Heparin (GE Healthcare) equilibrated with buffer C [25 mM Tris-HCl (pH 8), 300 mM NaCl, 0.4 mM TCEP]. Elution performed with increasing percentage of buffer D [25 mM Tris-HCl (pH 8), 1 M NaCl, 0.4 mM TCEP].*

We pooled the fraction of the main peak and we loaded the elute in a coomassie-stained SDS–PAGE (Figure 3.15); the GST-CK2α'^{del} has an overall molecular weight of 66 kDa (26 kDa of the GST and 40 kDa of the CK2α'^{del}).

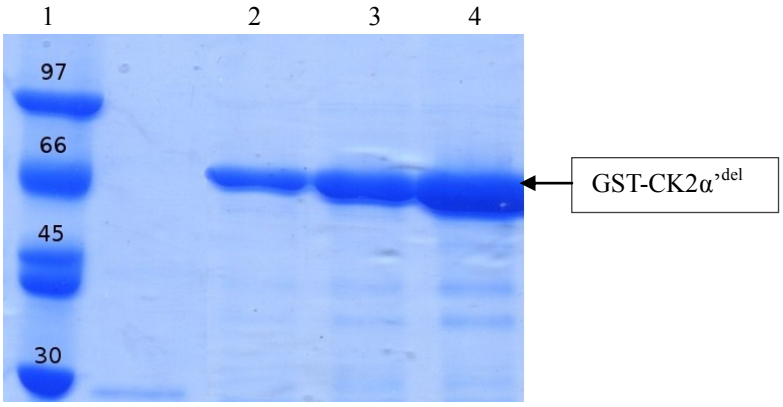

Figure 3.15 *Coomassie-stained SDS–PAGE after affinity chromatography. Lanes 2-5 correspond to fractions of the main peak of the chromatogram and lane 1 corresponds to low molecular weight protein markers in kDa.*

We mixed the purified the GST-CK2α'^{del} with the trimer of CK2αβ$_2$ isolated in the previous purification (Result 2.2.2.1). After a short incubation of 10 minutes in ice, we loaded the sample in a Glutathione Sepharose Fast Flow resin (GE Healthcare) in batch: only the tetramer which had incorporated the GST-CK2α'^{del} would be able to bind to the column unlike the contingent contamination of full tetramer CK2^{pm}. We added the *PreScission Protease* and left it acts in the column overnight at 4 °C. We eluted the purified protein from the column and we loaded the fractions collected in a Superdex 200 10/300 (GE Healthcare) equilibrated with buffer B [25 mM Tris-HCl (pH 8.5), 500 mM NaCl, and 0.2 mM TCEP]. With this purification step we isolated the chimeric CK2α^{pm}α'^{del}β$_2$ from the excess of CK2α'^{del} (Figure 3.14).

The shift of exclusion volume of the CK2α^{pm}α'^{del}β$_2$ in comparison with the isolated form of CK2α^{pm}β$_2$ used for the complex formation, confirms what was hypothesized during the first purification of the CK2 holoenzyme (Result 2.2.2.3): the trimeric form of CK2α^{pm}β$_2$ is stable in solution and is able to recruit the other catalytic subunit to form a complete tetrameric complex. The molecular weight of the CK2α^{pm}α'^{del}β$_2$ calculated is 214 kDa the elution volume is very similar to the CK2α$^{pm}{}_2$β$_2$ one which had a calculated molecular weight of 230 kDa. As anticipated before the overestimation of the molecular weight is due to the presence of a full-length α-subunit (CK2α^{pm}). The fact that the 55 amino acids C-terminal tail of the α-subunit is able to increase the hydrodynamic volume of the full-length protein is confirmed also by the comparison of the elution volume between CK2α^{pm}α'^{del}β$_2$ and CK2α'$^{del}{}_2$β$_2$ (figure 3.17): the calculated molecular weight of the CK2α$^{del}{}_2$β$_2$ is 170 kDa with respect to the 230 kDa of the last CK2α^{pm}α'^{del}β$_2$. The

difference of 60 kDa is due to the 41 amino acids more present in the CK2α^{pm} in the chimeric holoenzyme.

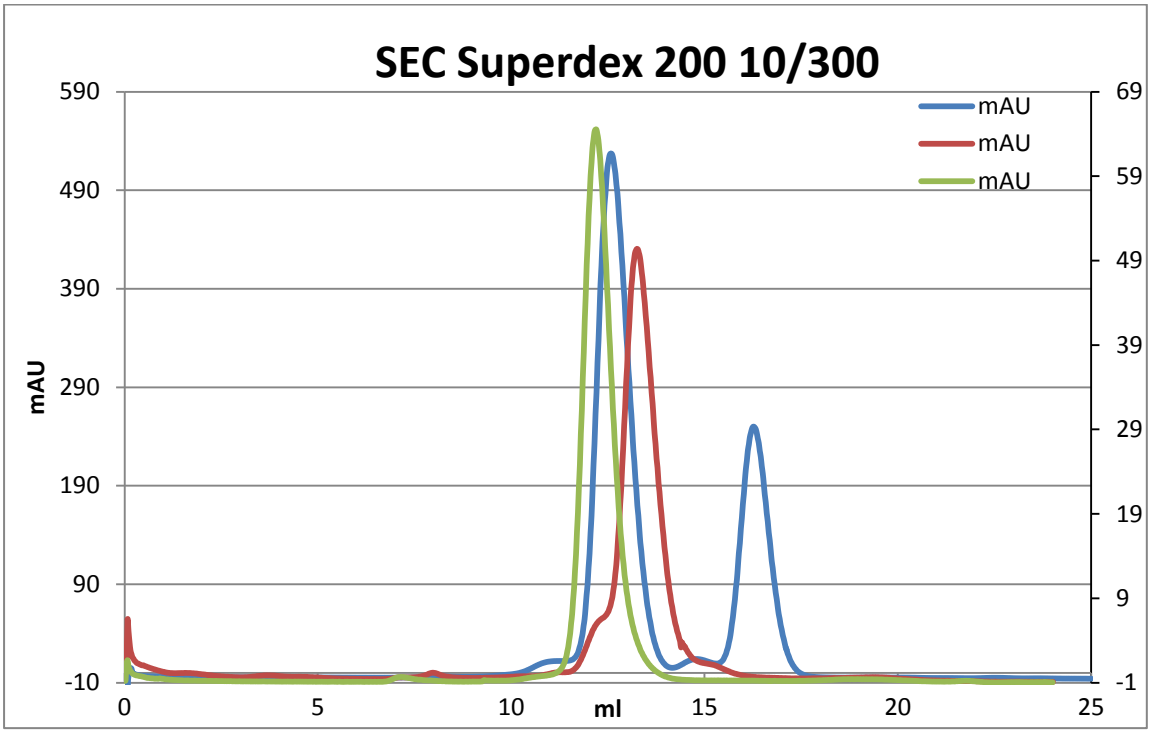

Figure 3.16 *Elution profile of size exclusion chromatography with a Superdex 200 10/300 column (GE Healthcare). In blue the elution profile of the CK2α^{pm}α'^{del}β$_2$: the main peak is the complete chimeric tetramer and the small peak is the excess of free CK2α'^{del}. In red the elution profile of the trimer CK2α^{pm}β$_2$ used for the formation of the chimeric holoenzyme. In green the elution profile of the complete CK2α$^{pm}{}_2$β$_2$ tetramer as confront.*

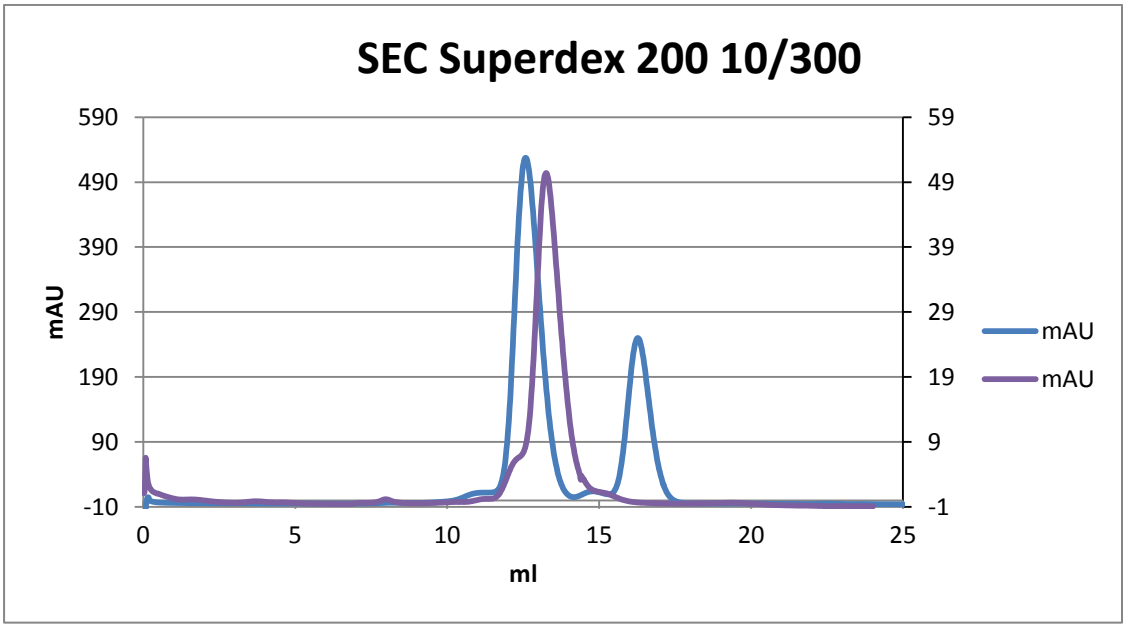

Figure 3.17 *Elution profile of size exclusion chromatography with a Superdex 200 10/300 column (GE Healthcare). In blue the elution profile of the CK2α^{pm}α'^{del}β$_2$. In violet the elution profile of CK2α'$^{del}{}_2$β$_2$.*

We loaded the fractions of the main peak in a Coomassie-stained SDS–PAGE to analyze the purity of the sample and the composition of the chimeric holoenzyme.

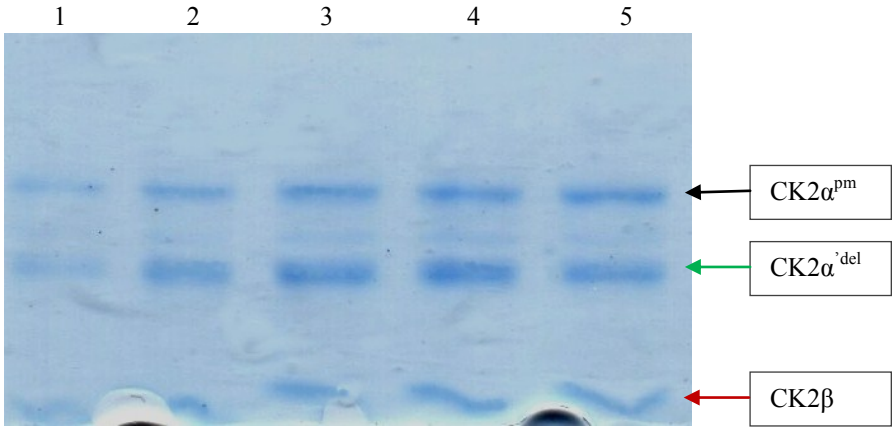

Figure 3.18 *Coomassie-stained SDS–PAGE after size exclusion chromatography. Lanes 1-5 correspond to fractions of the main peak of the chromatogram.*

From the SDS-PAGE we could confirm that the chimeric holoenzyme is composed of the α-subunits CK2α'^{del} and CK2α^{pm}, and by the regulatory β_2-dimer. The purity level was good enough and we proceed with the concentration of the sample by ultracentrifugation. The CK2α^{pm}α'$^{del}\beta_2$ was concentrated to 8 mg/ml and compared with the CK2α'$^{del}{}_2\beta_2$ in a coomassie-stained SDS-PAGE.

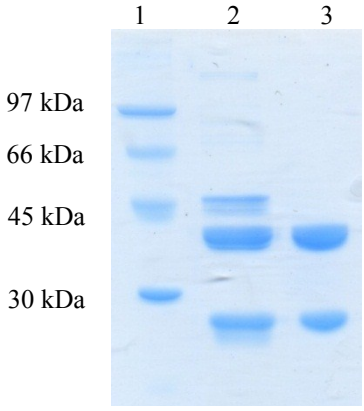

Figure 3.19 *Coomassie-stained SDS–PAGE after the concentration. Lane 1 corresponds to low molecular weight protein markers in kDa. Lane 2 and 3 correspond to CK2α^{pm}α'$^{del}\beta_2$ and CK2α'$^{del}{}_2\beta_2$ respectively.*

3.2.4.2 Protein Crystallization

We performed some crystallographic trials, starting from commercial kits based on sparse matrix with the Oryx8 automatic system (Douglas Instrument). We obtained nice small

hexagonal crystals but too small for being measured at the synchrotron (Figure 3.20). Again the dimension of the crystal is the limiting point of the experiment, but an enlargement of the photo shows that the crystal has a regular hexagonal symmetry. This hexagonal form could be a good starting point for the future optimization of the precipitant condition.

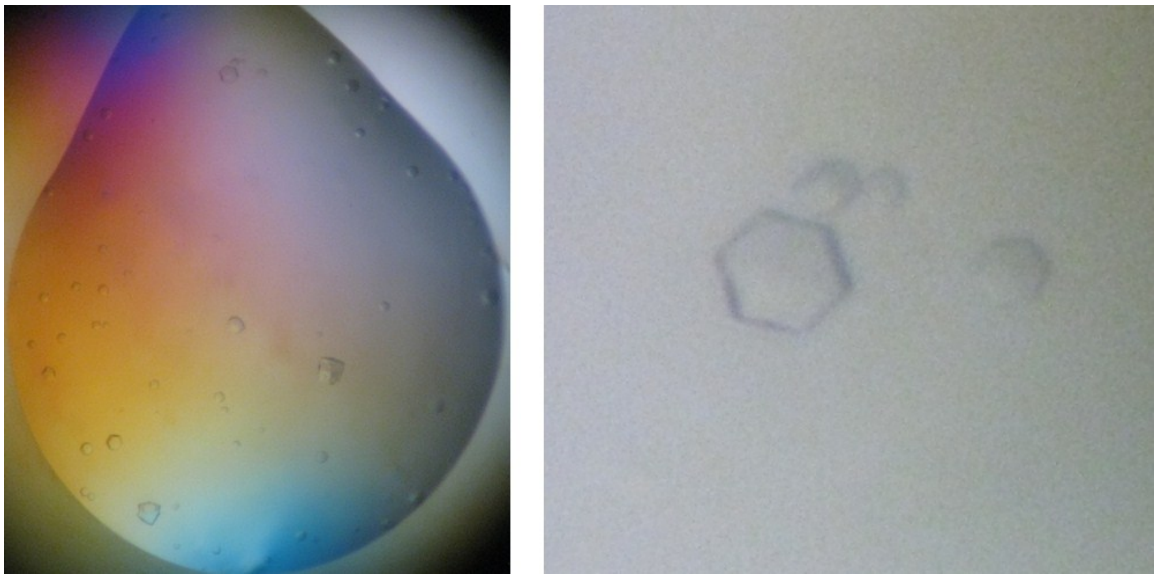

Figure 3.20 *Crystals of CK2α^{pm}α'^{del}β$_2$ grown in 0.24 M sodium malonate (pH 7) and PEG 3350 22%.*

3.3 Conclusions

With the final purpose to develop a protocol for the production of the holoenzyme with the mouse CK2α' subunit and the physiological chimeric holoenzyme composed of CK2α and CK2α', we started with the full-length CK2α' conjugated with the GST-tag which may increase the expression and solubility of the recombinant fusion protein. We were able to purify and crystallize the first form of CK2 holoenzyme with the α' subunit which had a tail of 14 amino acids coming from the MCS, the multiple cloning site, ($CK2\alpha'^{long}{}_2\beta_2$). Due to the low resolution reached with this isoform (8 Å), we considered eliminate the MCS because it could be flexible and unstructured in solution compromising the growth of big ordered crystals. Therefore we reclone the wt CK2α' (without the MCS, $CK2\alpha'^{wt}$) in a new expression vector without the fusion tag. In this case we were not able to purify the protein. We then proceeded with the cloning of a new form of CK2α' ($CK2\alpha'^{del}$) which was expressed with the GST fusion tag and which had a cleavage site precisely after the MCS. After the cleavage, the final product is a soluble form of CK2α' without the first two N-terminal amino acids. We were able to crystallize the latter form in a new crystallization condition, but the resolution achieved was only a little better than the first attempt (7 Å), but not enough to solve the structure.

Due to the difficulty on obtaining good diffracting crystals with all of the three CK2α' variants, we purified and crystallized a chimeric physiological holoenzyme composed of the regulatory β_2-dimer and by both the two catalytic subunits CK2α and $CK2\alpha'^{del}$ ($CK2\alpha^{pm}\alpha'^{del}\beta_2$). The crystallization of the homogenous $CK2\alpha'_2\beta_2$ holoenzyme had a limit on the dimension reached by the crystal probably due to the unfavourable crystal packing within the crystal. In order to favor the crystallographic contacts we added a subunit more prone to the crystallization like the $CK2\alpha^{pm}$ into the holoenzyme. We established a new protocol of purification starting from the isolation of the trimeric form $CK2\alpha^{pm}\beta_2$, followed by the adding of free $CK2\alpha'^{del}$ previously purified (or expressed). We obtained small hexagonal crystals, too small for the diffraction analysis, but very promising for future optimization.

4. CK2α^{336} inhibition

4.1 Methods

4.1.1 Overview

A part of my PhD project focused on the interaction between CK2 and small ligand which can compete with the ATP for the binding to the kinase. In collaboration with the laboratory of Professor Pinna, we studied the interaction between the CK2α^{336} (deleted at residue Ser336) and a potent and selective Type I ATP-competitive inhibitor, called K164. The inhibitor exhibits all the features which make a small ligand attractive for inhibition studies: all the structural characteristics like hydrophobicity and possibility to establish electrostatic interactions are satisfied like the high cell permeability which makes the molecule a useful biochemical tool also with pharmacological potentials, due to the fact also that is selective for two different kinases: CK2 and Pim1. Both of the kinases are involved in cancer development and have been considered as potential pharmacological target, and so having a potent inhibitor, cell permeable and selective for both of the kinases is surely of high interest.

4.1.2 Protein expression and purification

Recombinant human CK2α^{336} was purified, after expression in bacterial strain *E. coli* BL21(DE3), with three chromatographic step. The first step was an affinity cromatography performed on an Äkta FPLC chromatographic system (GE Healthcare) using a HiTrap Heparin HP 5ml (GE Healthcare) equilibrated with buffer A [25 mM Tris-HCl (pH 8), 0.4 M NaCl and 1 mM dithiothreitol (DTT) as a reducing agent]. The protein was eluted with a NaCl gradient (mM Tris-HCl (pH 8), 1 M NaCl, 1 mM DTT, buffer B) and the most pure fractions were pooled, dialysed into a buffer C [25 mM Tris (pH 8.5), 0.1 M NaCl, 1 mM DTT], and loaded onto an anionic exchange column (MonoQ, GE Healthcare) equilibrated with the same buffer. CK2α^{336} was eluted in a single peak after a NaCl gradient. The third purification step was a gel filtration chromatography using a Superdex 75 10/300 column (GE Healthcare) equilibrated with buffer D [25 mM Tris-

HCl (pH 8.5), 500 mM NaCl, and 1 mM DTT]. The purified protein was then concentrated to 10 mg/ml for crystallization purposes.

4.1.3 Protein crystallization

We solved the crystal structure of the complex obtained by soaking the inhibitor (5 mM) on a crystal growth by vapour diffusion (with the sitting drop method) techniques, made by hand with a CK2α^{336} concentrated to 10 mg/ml incubated for 10 minutes with an equal volume of milliq water with 1.5% DMSO. Crystals were grown at 20 °C, using the following precipitant solution: 0.2 M lithium sulfate, Tris-HCl pH 8.5, 32% w/v PEG 4000.

4.1.4 Data Collection, structure determination, and refinement

The data set was collected at the ELETTRA-Synchrotron beamline XDR1, (Trieste, Italy). Data set was measured at 100 K using the precipitant solution, including 10% glycerol as cryo-protectant, at the bromine absorption edge, 0.91 Å wavelength, to detect the anamalous signal and better define the position of the 4 bromines present in the inhibitor. CK2α^{336} crystals belonged to space group $P2_1$ with unit cell parameters reported in Table 3.1. Diffraction data were processed with XDS and reduced and merged with SCALA included in the CCP4 suite. The structure was solved by molecular replacement using the structure of the CK2αdel 3BQC. The model was then refined alternating several cycles of automatic refinement with REFMAC (CCP4) and manual model building with Coot.

4.2 Results

4.2.1 Protein Expression and Purification

The purification protocol of CK2α^{336} is the same used for the CK2α^{pm} with an additional intermediate chromatographic step between the affinity chromatography and the size exclusion chromatography: the anion exchange chromatography is fundamental to obtain a pure final protein.

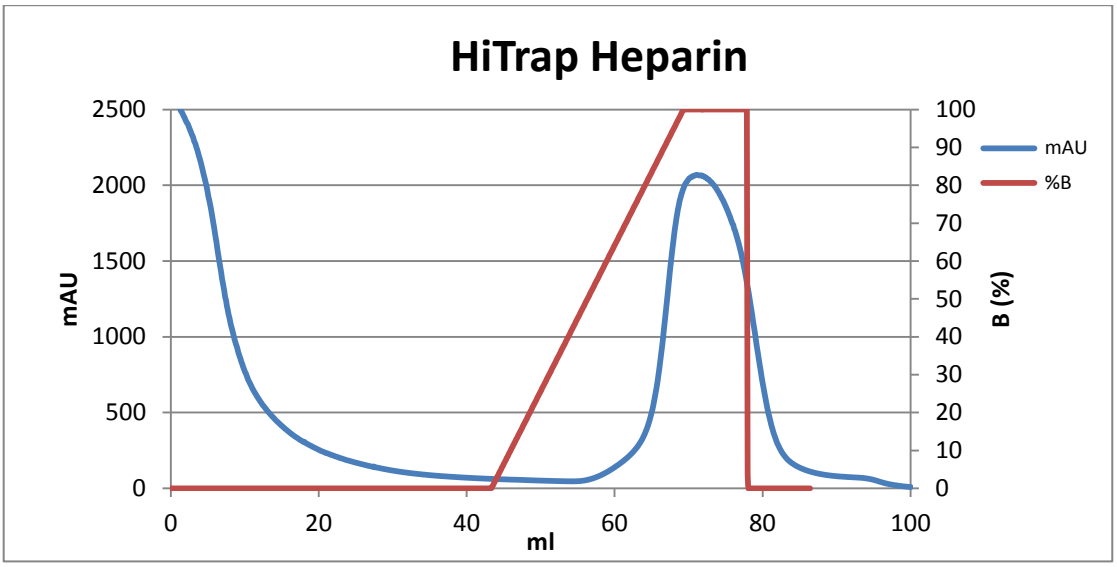

Figure 4.1 *Elution profile of affinity chromatography of CK2α^{336} on column: HiTrap Heparin (GE Healthcare) equilibrated with buffer A [25 mM Tris-HCl (pH 8), 350 mM NaCl, 1 mM DTT]. Elution performed with increasing percentage of buffer B [25 mM Tris-HCl (pH 8), 1 M NaCl, 1 mM DTT].*

After the affinity with the heparin column we dialyzed the protein into the buffer C [25 mM Tris (pH 8.5), 0.1 M NaCl, 1 mM DTT]: in this step a great amount of protein underwent to precipitation. We loaded the protein into the MonoQ column and we performed the elution with a NaCl gradient.

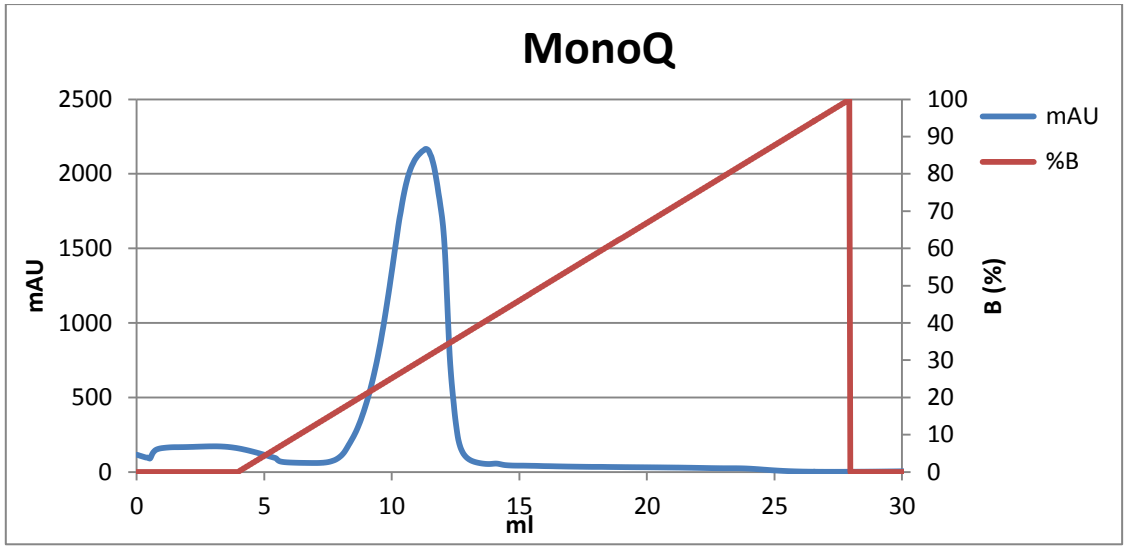

Figure 4.2 *Elution profile of affinity chromatography of CK2α^{336} on column: MonoQ (GE Healthcare) equilibrated with buffer C [25 mM Tris-HCl (pH 8.5), 0.1 mM NaCl, 1 mM DTT]. Elution performed with increasing percentage of buffer C^{a} [25 mM Tris-HCl (pH 8.5), 1 M NaCl, 1 mM DTT].*

After the anion exchange chromatography we pulled together the fractions and we performed the third purification step represented by a size exclusion chromatography using a Superdex 75 10/300 (GE Healthcare) equilibrated with buffer D, the final buffer of the purification.

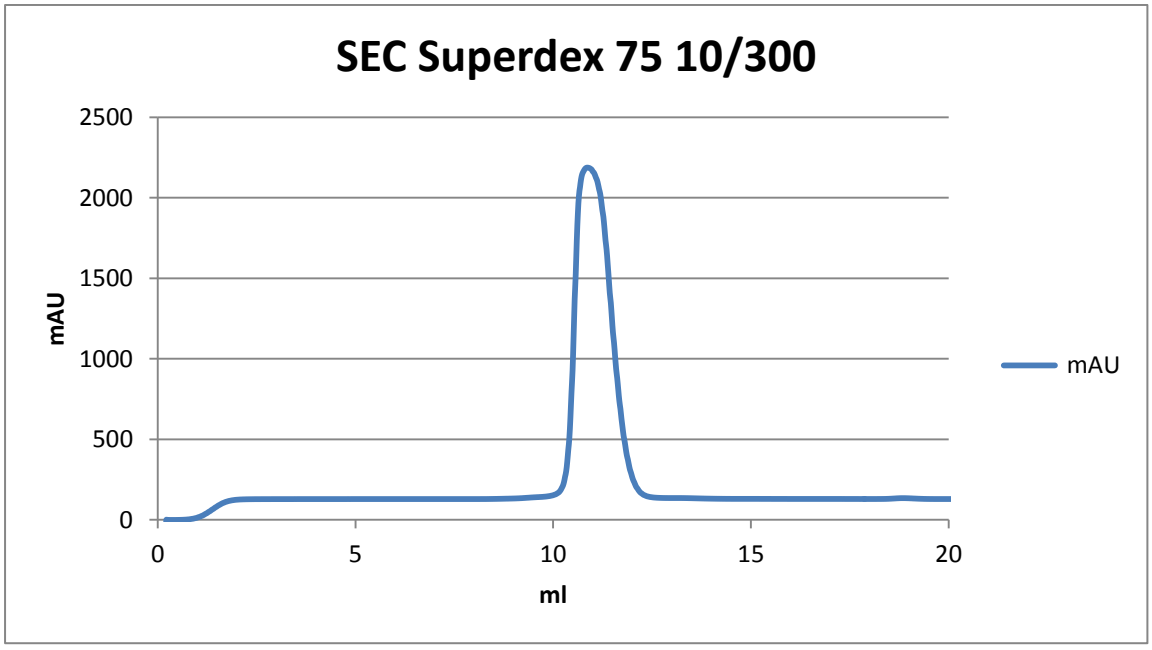

Figure 4.3 *Elution profile of size exclusion chromatography with a Superdex 75 10/300 column (GE Healthcare) equilibrated with buffer D [25 mM Tris-HCl (pH 8.5), 500 mM NaCl, and 1 mM DTT]*

The elution profile of the size exclusion chromatography showed a single slightly-tailed peak; we loaded the fractions of the main peak in a coomassie-stained SDS–PAGE for evaluate the purity level of the sample after the size exclusion chromatography.

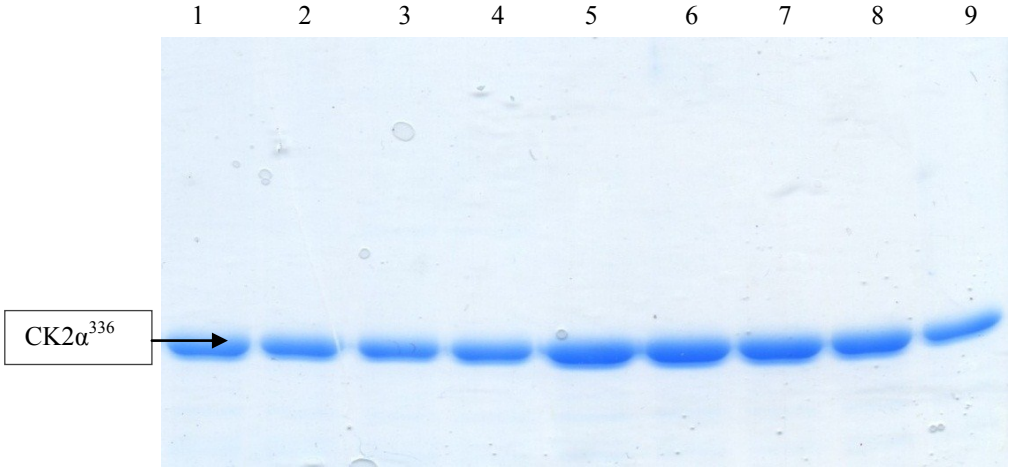

Figure 4.4 *Coomassie-stained SDS–PAGEs after size esclusion chromatography. Lanes 1-9 correspond to fractions of the main peak of the chromatogram.*

After the size exclusion chromatography the purity of the sample was high enough for the crystallization purpose. We collected all the fractions and the CK2α^{336} was concentrated to 10 mg/ml by ultrafiltration.

4.2.2 Protein crystallization

We knew that CK2α^{336} gives good diffracting crystal under an optimized precipitant solution with 0.1 M Tris-HCl (pH 8.5), 0.2 lithium sulphate and 32% w/v PEG 4000 in $P2_1$ space group. We optimized the condition to obtain crystal of the apo form of the protein and then we added the inhibitor by crystal soaking (co-precipitation did not work). To obtain big and good diffracting crystals we mixed the CK2α^{336} 10 mg/ml with an equal volume of distilled water with DMSO 1.5-2 %; the supplement of a small amount of DMSO is fundamental for the crystal formation of the apo form of the protein. After an incubation of 10 minutes the protein was centrifuged for 10 minutes at 5000 g at 4 °C. The crystallization drop for the apo form was composed by 1 µl of CK2α^{336} 5 mg/ml, 1 µl of the precipitant solution and equilibrated against 400 µl of reservoir. All crystals grew in about one week. The inhibitor solution used for the soaking was composed by the precipitant solution plus K164 10 mM. We added to the crystal 1 µl of the inhibitor solution to achieve a final concentration of 5 mM. The crystals were cryoprotected by

adding 2 µl of the inhibitor solution with *ethylene glycol* 10% to the drop before crystal freezing.

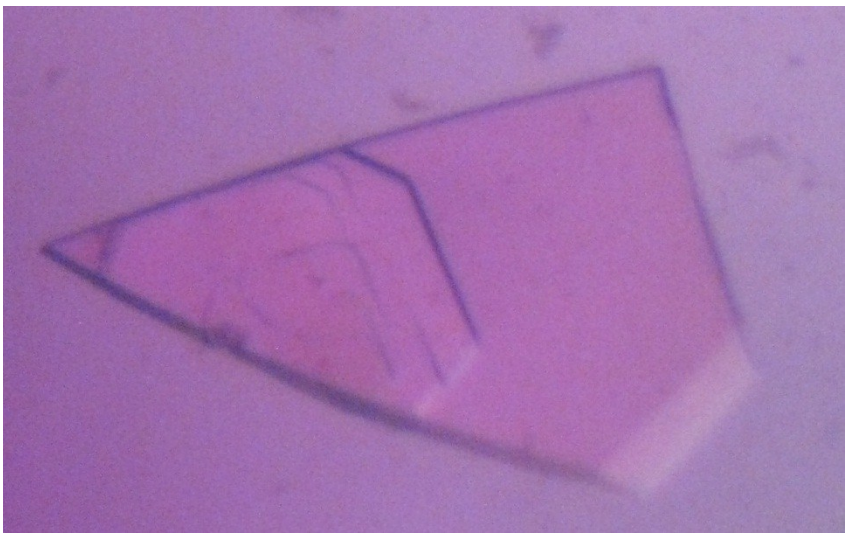

Figure 4.5 *Crystals of CK2α^{336} in 0.1 M Tris-HCl (pH 8.5), 0.2 lithium sulphate and 32% w/v PEG 4000.*

4.2.3 Structure determination

The structure was solved by molecular replacement using the structure of the CK2α^{del} 3BQC. Statistics on data collections and refinement are reported in table 4.1. CK2α^{336} crystallized in the space group $P2_1$. The overall structure of the enzyme within the crystal packing is identical to the published CK2α^{336}. The structure reached the 1.25 Å resolution which is the higher resolution ever published for CK2 α^{336} protein.

Table 4.1 Data collection and refinement statistics

Data collection statistics	**ELETTRA beamline XDR1, λ=0.91 Å**
Cell dimensions a, b, c (Å) α, β, γ (°)	 58.45 45.82 63.49 90 111.1 90
Total number of observations	471404 (22651)
Total number of unique	86589 (4286)
Resolution (Å)	45.82 (1.25)
R_{merge} (%)	0.061 (0.773)
R_{meas} (%)	0.075 (0.949)
I/σ(I)	12.5 (1.9)
Completeness (%)	99.8 (100.0)
Multeplicity	5.4 (5.3)
Refinement statistics	
R_{work} (%)	0.13437
R_{free} (%)	0.17543

The values in brackets are referred to the highest resolution shell.

4.2.4 CK2α^{336} structure in complex with the inhibitor K164

The first inhibitor for CK2 described in 1984 was the inhibitor DRB (IC_{50} is >10 μM) (Figure 4.6); later it was described that removing the sugar ring and replacing the two chlorines with up to 4 bromines prompt to an increasing of the potency of the inhibitors: 4,5,6,7-tetrabromo-benzimidazole (TBI) and 4,5,6,7-tetrabromo-benzotriazole (TBB) both display IC_{50} /K_i values lower than 1 μM. Further TBI was modified on its imidazole ring giving a variety of derivatives listed in Figure 4.6, with an improved potency.

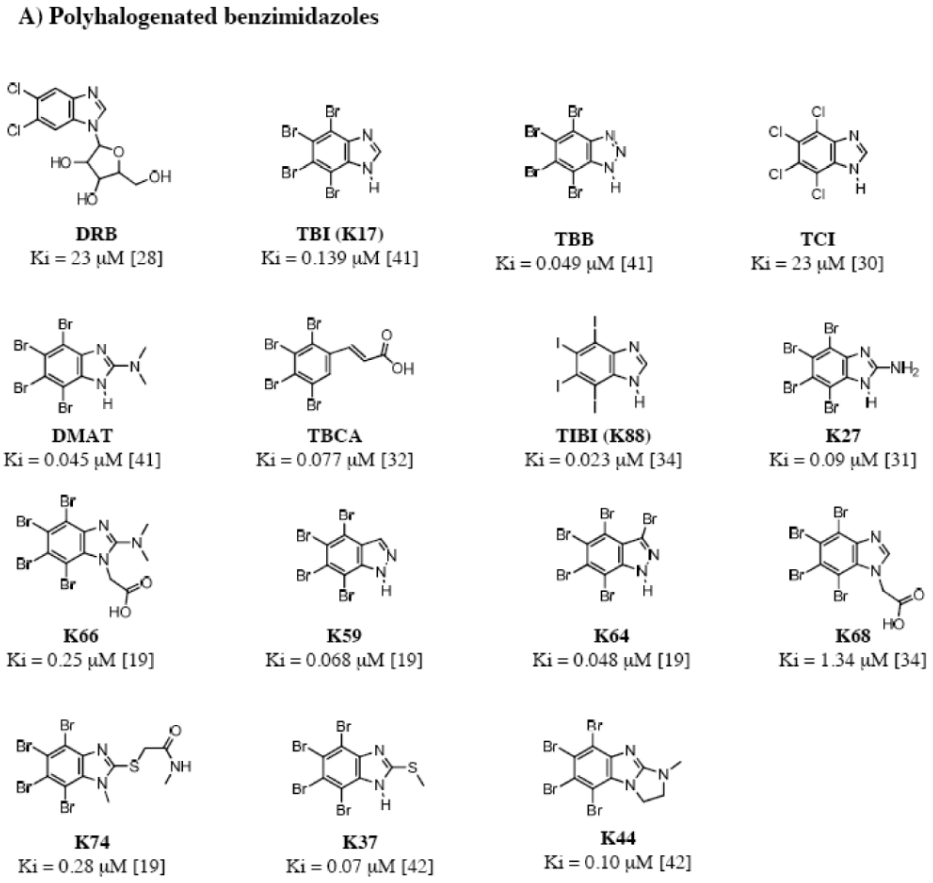

Figure 4.6 *Structure of selected ATP site-directed CK2 inhibitors polyhalogenated benzimidazoles.*

The most crucial binding interactions for TBB and TBI compounds are due to hydrophobic and van der Waals contributions, produced by the presence of the four apolar bulky bromine atoms which lead the inhibitor away from the aqueous phase towards the more apolar area of the CK2 active site. For the other derivatives, the preferred interaction is with the backbone of the hinge region: in particular, they establish two halogen bonds between bromine atoms and the carbonyls of Glu114 and Val116. It has

been shown that these compounds have two different orientations, one rotated about 60° around the axis perpendicular to the plane of the molecule with respect to the other (Figure 4.6).

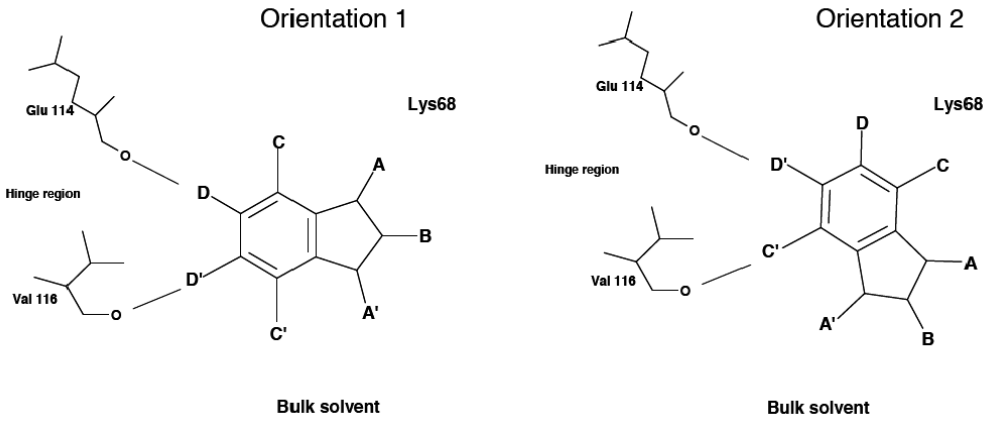

Figure 4.7 *The two different orientations of the tetrabromobenzo derivatives in the active site of protein kinase CK2α. In orientation 1 inhibitors (DMAT, K32, K22, K66 and K68) interact with the hinge region via two bromines in position D and D', while in orientation 2 (K44, K64 and K74) via bromines in position C' and D'. Orientation 1 is preferred when there are no functional groups in positions A and A', or if in position A there is a functional group capable of interacting with the positive area of the ATP binding site. Orientation 2 is preferred when position A' carries a hydrophobic substituent.*

From the analysis of all the published structures it can be conclude that if there are no functional groups in positions A and A', or if in position A there is a functional group capable of interacting with the positive area of the ATP binding site, the preferred conformation adopted by the inhibitors is the "conformation 1" (as in the case of DMAT, K32, K22, and K66 and K68 presented here), with Br5 and Br6 interacting with the hinge region. Instead, if position A' carries a hydrophobic moiety (as in the case of K44, K64 and K74), this group tends to orient itself towards the external part of the cleft and the whole orientation of the inhibitor is that indicated as "conformation 2", with Br4 and Br5 interacting with the hinge region (Sarno et al., 2011).

The inhibitor K164 is a potent dual inhibitor, specific for Pin1 and CK2, designed from the structure of the DRB. The sugar ring is kept in the formula but instead of the two chloride atoms, we have four bromines atoms with a final tetrabromobenzo derivative (Figure 4.8). The inhibitor was found in an orientation similar to the orientation 2 (Figure 4.7) showed above. The two bromines Br4 and Br5 point in the direction of the hinge region, towards the backbone of Val116 and Glu114 respectively. Like in K64 structure

the Br6 interacts with a conserved water molecule W2 and the Br7 makes an halogen bond with the side chain of Asp175. The Asp175 is shifted away from the canonical conformation towards the ligand but is still present the salt bridge with the Lys68 which is itself shifted towards the K164 molecule. This confirms that the presence of a bromine atom near the Asp175 leads a movement of the side chain. If compared with the other tetrabromobenzo derivatives, the K164 is shifted towards the N-terminal lobe of the protein and it goes less inside the cavity of CK2. This is probably due to the presence of the deoxyribose ring which is bulky and flexible and it doesn't allow the inhibitor to fill deeply the active site. In fact, a certain degree of flexibility of the deoxyribose ring is confirmed by the poor quality of its electron density; the deoxyribose ring doesn't contribute directly to the binding with CK2 but it can be important for the binding to the other kinase, Pim1.

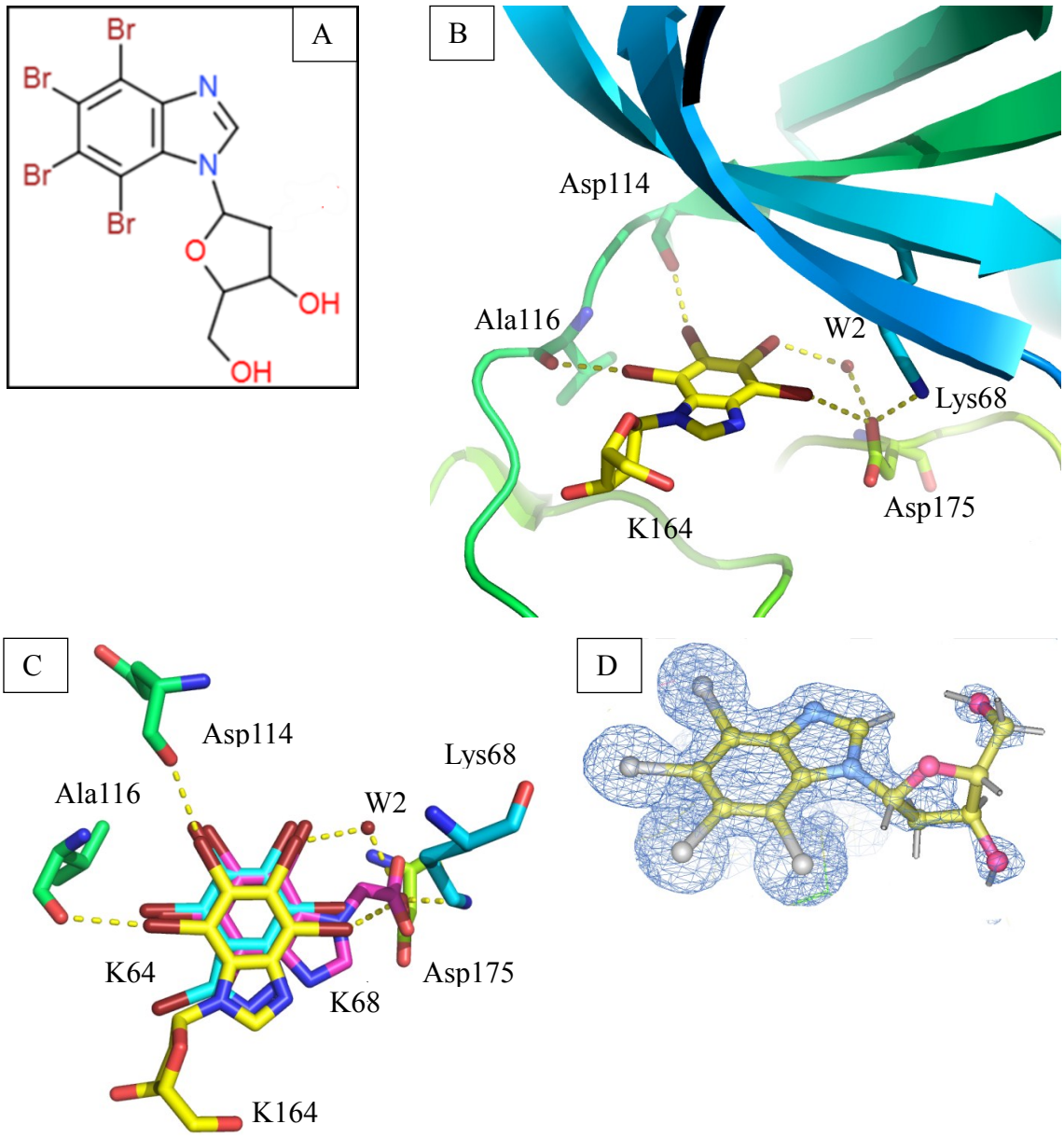

Figure 4.8 (A) *Structure of the inhibitor K164.* ***(B)*** *K164 bound to the ATP-binding site of CK2α*^{336}*. Main polar interactions are indicated with black yellow dashed lines and water molecule is indicated by a small red sphere.* ***(C)*** *Comparison between different inhibitors: note how the binding conformation of K164 (in yellow) is similar to the K64 (in cyan) with respect to the K68 (in purple) and how the inhibitor K164 is shifted towards the external part of the cavity.* ***(D)*** *Electron density of the K164 in complex with the CK2α*^{336}*: note the poor quality of the electron density of the deoxyribose ring with respect to the rest of the molecule.*

4.3 Conclusions

In order to study the interaction between the CK2α^{336} (deleted at residue Ser336) and a potent and selective Type I ATP-competitive inhibitor, called K164, we purified and crystallized CK2α^{336} in the apo form. To obtain a reproducible condition for the crystallization, we optimized the precipitant solution with the adding of a small percentage of DMSO. After the growth of these big crystals, we soaked the crystal with a solution containing the inhibitor. Then we collected the data and we solved the structure with the final resolution of 1.25 Å.

Concluding we solved the first structure of the human CK2α^{336} in complex with a tetrabromobenzo derivative and we were able to reach the highest resolution for the CK2 protein. The K164 interacts with the CK2α^{336} like it was described for the other tetrabromobenzo derivatives (Sarno et al., 2011) and the structure confirms the model proposed for the binding of this kind of ligands: if the molecule carries an hydrophobic moiety (like the deoxyribose ring), this part of the ligand is oriented towards the external part of the cavity and the inhibitor adopts conformation described as orientation 2 (Figure 4.7).

Being a dual inhibitor, this strucure is only the first half a more complex work: the structure in complex with the opther kinase would be crucial to understad the nature of the dual potency of the molecule and to put the basis for the design of more potent dual inhibitors for CK2 and Pim1 kinase.

5. Bibliography

Ahn, N. G. and Resing, K. A. (2001). Toward the phospho- proteome. *Nat. Biotechnol.* **19**: 317-318

Battistutta, R., Sarno, S., De Moliner, E., Marin, O., Issinger, O. G., Zanotti, G., Pinna, L. A. (2000). The crystal structure of the complex of Zea mays alpha subunit with a fragment of human beta subunit provides the clue to the architecture of protein kinase CK2 holoenzyme. *Eur J Biochem* **267**: 5184-5190

Battistutta, R. (2009). Protein kinase CK2 in health and disease: Structural bases of protein kinase CK2 inhibition. *Cell Mol Life Sci.* **66**: 1868-1889

Battistutta, R., Lolli, G. (2011). Structural and functional determinants of protein kinase CK2α: facts and open questions. *Mol Cell Biochem*. **356**: 67-73

Bischoff, N., Olsen, B., Raaf, J., Bretner, M., Issinger, O-G., Niefind, K. (2011). Structure of the Human Protein Kinase CK2 Catalytic Subunit CK2α' and Interaction Thermodynamics with the Regulatory Subunit CK2β. *J. Mol. Biol.* **407**: 1-12

Boldyreff, B., Meggio, F., Pinna, L. A., Issinger, O. G. (1993). Reconstitution of normal and hyperactivated forms of casein kinase-2 by variably mutated β-subunits. *Biochemistry.* **32**: 12672-12677

Bosc, D. G., Slominski, E., Sichler, C. and Litchfield, D. W. (1995). Phosphorylation of casein kinase II by p34cdc2. Identification of phosphorylation sites using phosphorylation site mutants in vitro. *J. Biol. Chem.* **270**: 25872-25878

Buchou, T., Vernet, M., Blond, O., Jensen, H. H., Pointu, H., Olsen, B. B., Cochet, C., Issinger, O. G., and Boldyreff, B. (2003). Disruption of the regulatory beta subunit of protein kinase CK2 in mice leads to a cell-autonomous defect and early embryonic lethality. *Mol. Cell. Biol.* **23**: 908-915

Burnett, G. and Kennedy, E. P. (1954). The enzymatic phosphorylation of proteins. *J. Biol. Chem.* **211**: 969-980

Canton, D.A., Zhang, C., Litchfield, D. W. (2001). Assembly of protein kinase CK2: investigation of complex formation between catalytic and regulatory subunits using a zinc-finger deficient mutant of CK2β. *Biochem J.* **358**: 87-94

Chantalat, L., Leroy, D., Filhol, O., Nueda, A., Benitez, M. J., Chambaz, E. M., Cochet, C., Dideberg, O. (1999). Crystal structure of the human protein kinase CK2 regulatory subunit reveals its zinc finger-mediated dimerization. *EMBO J.* **18**: 2930-2940

Cohen, P. (2000). The regulation of protein function by multisite phosphorylation – a 25 year update. *Trends Bio-chem. Sci.* **25**: 596-601

Di Maira, G., Brustolon, F., Tosoni, K., Belli, S., Kramer, S. D., Pinna, L. A. and Ruzzene, M. (2008). Comparative analysis of CK2 expression and function in tumor cell lines displaying sensitivity vs. resistance to chemical induced apoptosis. *Mol. Cell. Biochem.* **316**: 155-161

Emsley, P., Cowtan K. (2004). Coot: model-building tools for molecular graphics. *Acta Crystallogr D Biol Crystallogr* **60**(12 1): 2126-2132

Evans, P. (2005). Scaling and assessment of data quality. *Acta Crystallogr D Biol Crystallogr* **62**(1): 72-82

Fabbro, D., Cowan-Jacob, S. W., Mobitz, H., Martiny-Baron, G. (2012). Targeting cancer with small-molecular-weight kinase inhibitors. Methods Mol Biol 795: 1-34

Glover, C. V. (1986). A filamentous form of *Drosophila* casein kinase II. *J Biol Chem.* **261**: 14349-14354

Hanahan, D. and Weinberg, R. A. (2000). The hallmarks of cancer. *Cell* **100**: 57-70

Hanks, S. K. and Hunter, T. (1995). Protein kinases 6. The eukaryotic protein kinase superfamily:
kinase (catalytic) domain structure and classification. *FASEB J.* **9**: 576-596

Hemmings, B. A., Restuccia, D., Tonks, N. (2009). Targeting the Kinome II. *Curr Opin Cell Biol* **21**: 135-139

Hjerrild, M., Milne, D., Dumaz, N., Hay, T., Issinger, O. G. and Meek, D. (2001). Phosphorylation of murine double minute clone 2 (MDM2) protein at serine-267 by protein kinase CK2 in vitro and in cultured cells. *Biochem. J.* **355**: 347-356

Imming, P., Sinning, C., Meyer, A. (2006). Drugs, their targets and the nature and number of drug targets. *Nat Rev Drug Discov* **5**: 821-834

Kabsch, W. (2010) XDS. *Acta Cryst.* D**66:** 125-132

Kapoor, M. and Lozano, G. (1998). Functional activation of p53 via phosphorylation following DNA damage by UV but not gamma radiation. *Proc. Natl. Acad. Sci. USA* **95**: 2834-2837

Kornev, A. P., Haste, N. M., Taylor, S. S. and Ten Eyck, L. F. (2006). Surface comparison of active and inactive protein kinases identifies a conserved activation mechanism. *Proc. Natl Acad. Sci. USA* **103**(47): 17783 –17788

Kornev, A. P., Taylor, S. S., Ten Eyck, L. F. (2008). A helix scaffold for the assembly of active protein kinases. *Proc Natl Acad Sci USA.* **105**:14377-14382

Krebs, E. G. (1998). An accidental biochemist. *Annu. Rev. Biochem.* **67**: xii-xxxii

Krissinel, E. and Henrick K. (2007). Inference of macromolecular assemblies from crystalline state. *J Mol Biol* **372**(3): 774-97

Laudet, B., Barette, C., Dulery, V., Renaudet, O., Dumy, P., Metz, A., Prudent, R.,

Deshiere, A., Dideberg, O., Filhol, O., Cochet, C. (2007). Structure-based design of small peptide inhibitors of protein kinase CK2 subunit interaction. *Biochem J.* **408**: 363-373

Leroy, D., Schmid, N., Behr, J. P., Filhol, O., Pares, S., Garin, J., Bourgarit, J. J., Chambaz, E. M., Cochet, C. (1995). Direct identification of a polyamine binding domain on the regulatory subunit of the protein kinase casein kinase 2 by photoaffinity labeling. *J Biol Chem.* **270**: 17400-17406

Litchfield, D. W., Lozeman, F. J., Cicirelli, M. F., Harrylock, M., Ericsson, L. H., Piening, C. J. and Krebs, E. G. (1991). Phosphorylation of the beta subunit of casein kinase II in human A431 cells. Identification of the autophosphorylation site and a site phosphorylated by p34cdc2. *J. Biol. Chem.* **266**(30): 20380-20389

Litchfield, D. W. (2003). Protein kinase CK2: structure, regulation and role in cellular decisions of life and death. *Biochem. J.* **369**: 1-15

Lolli, G., Pinna, L. A., Battistutta, R. (2012). Structural determinants of protein kinase CK2 regulation by autoinhibitory polymerization. *ACS Chem Biol* **7**(7): 1158-1163

Lopez-Ramos, M., Prudent, R., Moucadel, V., Sautel, C. F., Barette, C., Lafanechere, L., Mouawad, L., Grierson, D., Schmidt, F., Florent, J. C., Filippakopoulos, P., Bullock, A. N., Knapp, S., Reiser, J. B., Cochet, C. (2010). New potent dual inhibitors of CK2 and Pim kinases: discovery and structural insights. *Faseb J* **24**: 3171-3185

Lorenz, P., Pepperkok, R., Ansorge, W. and Pyerin, W. (1993). Cell biological studies with monoclonal and polyclonal antibodies against human casein kinase II subunit beta demonstrate participation of the kinase in mitogenic signaling. *J. Biol. Chem.* **268**: 2733-2739

Lorenz, P., Pepperkok, R. and Pyerin, W. (1994). Requirement of casein kinase 2 for entry into and progression through early phases of the cell cycle. *Cell. Mol. Biol. Res.* **40**: 519-527

Lou, D. Y., Dominguez, I., Toselli, P., Landesman-Bollag, E., O'Brien, C. and Seldin, D. C. (2008). The alpha catalytic subunit of protein kinase CK2 is required for mouse embryonic development. *Mol. Cell. Biol.* **28**: 131-139

Manning, G., Whyte, D.B., Martinez, R., Hunter, T., Sudarsanam, S. (2002). The Protein Kinase Complement of the Human Genome. *Science* **298**(5600): 1912-1934

Manning, G., Plowman, G. D., Hunter, T., Sudarsanam, S. (2002 b). Evolution of protein kinase signaling from yeast to man. *Trends Biochem. Sci.* **27**: 514-520

Marchiori, F., Meggio, F., Marin, O., Borin, G., Calderan, A., Ruzza, P., Pinna, L.A. (1988). Synthetic peptide substrates for casein kinase 2. Assessment of minimum structural requirements for phosphorylation. *Biochim Biophys Acta* **971**: 332-338

McCoy, A. J., Grosse-Kunstleve, R. W., Adams, P. D., Winn, M. D., Storoni, L. C., Read R. J. (2007). Phaser crystallographic software. *J Appl Crystallogr* **40**(4): 658-674

McDonnell, M. A., Abedin, M.J., Melendez, M., Platikanova, T. N., Ecklund, J. R., Ahmed, K. and Kelekar, A. (2008). Phosphorylation of murine caspase-9 by the protein kinase casein kinase 2 regulates its cleavage by caspase-8. *J. Biol. Chem.* **283**: 20149-20158

Meggio, F., Pinna, L. A. (2003). One-thousand-and-one substrates of protein kinase CK2? *FASEB J.* **17**: 349-368

Messenger, M. M., Saulnier, R. B., Gilchrist, A. D., Diamond, P., Gorbsky, G. J. and Litchfield, D. W. (2002). Interactions between protein kinase CK2 and Pin1. Evidence for phosphorylation-dependent interactions. *J. Biol. Chem.* **277**: 23054-23064

Murshudov, G. N., Vagin, A. A., Dodson E. J. (1997). Refinement of macromolecular structures by the maximum-likelihood method. *Acta Crystallogr D Biol Crystallogr* **53**(3): 240-255

Nakaniwa, T., Kinoshita, T., Sekiguchi, Y., Tada, T., Nakanishi, K., Kitaura, Y., Suzuki, Y., Ohno, H., Hirasawa, A., Tsujimoto, G. (2009). Structure of human protein kinase CK2a2 with a potent indazolederivative inhibitor. *Acta Crystallogr. Sect. F* **65**: 75-79

Nasmyth, K. (1996). Viewpoint: putting the cell cycle in order. *Science* **274**: 1643-1645

Niefind, K., Battistutta, R.(2012) Structural bases of protein kinase CK2 function and inhibition.

Niefind, K., Guerra, B., Pinna, L. A., Issinger, O. G., Schomburg, D. (1998). Crystal structure of the catalytic subunit of protein kinase CK2 from *Zea mays* at 2.1 Å resolution. *EMBO J.* **17**: 2451-2462

Niefind, K., Guerra, B., Ermakowa, I., Issinger, O. G. (2001). Crystal structure of human protein kinase CK2: insights into basic properties of the CK2 holoenzyme. *EMBO J.* **20**: 5320-5331

Niefind, K., Raaf, J., Issinger, O.G. (2009). Protein kinase CK2 in health and disease: Protein kinase CK2: from structures to insights. *Cell Mol Life Sci.* **66**: 1800-1816

Olsen, B. B., Boldyreff, B., Niefind, K. and Issinger, O. G. (2006). Purification and characterization of the CK2a'-based holoenzyme, and isozyme of CK2a: a comparative analysis. *Protein Expression Purif.* **47**: 651–661

Pagano, M. A., Sarno, S., Poletto, G., Cozza, G., Pinna, L. A., and Meggio, F. (2005). Autophosphorylation at the regulatory beta subunit reflects the supramolecular organization of protein kinase CK2. *Mol. Cell. Biochem.* **274**: 23−29

Papinutto, E., Ranchio, A., Lolli, G., Pinna, L. A., Battistutta, R. (2012). Structural and functional analysis of the flexible regions of the catalytic alpha-subunit of protein kinase CK2. *J Struct Biol.* **177**: 382-391

Pepperkok, R., Lorenz, P., Ansorge, W. and Pyerin, W. (1994). Casein kinase II is required for transition of G_0/G_1, early G_1, and G_1/S phases of the cell cycle. *J. Biol. Chem.* **269**: 6986-6991

Pierre, F., Chua, P. C., O'Brien, S. E., Siddiqui-Jain, A., Bourbon, P., Haddach, M., Michaux, J., Nagasawa, J., Schwaebe, M. K., Stefan, E., Vialettes, A., Whitten, J. P, Chen, T. K., Darjania, L., Stansfield, R., Anderes, K., Bliesath, J., Drygin, D., Ho, C., Omori, M., Proffitt, C., Streiner, N., Trent, K., Rice, W. G., Ryckman, D. M. (2011). Discovery and SAR of 5-(3-chlorophenylamino)benzo[c][2,6]naphthyridine-8-carboxylic acid (CX-4945), the first clinical stage inhibitor of protein kinase CK2 for the treatment of cancer. *J Med Chem* **54**: 635-654

Pinna, L. A., Meggio, F., Marchiori, F., Borin, G. (1984). Opposite and mutually incompatible structural requirements of type-2 casein kinase and cAMP-dependent protein kinase as visualized with synthetic peptide substrates. *FEBS Lett.* **171**: 211-214

Pinna, L. A. (1994). A historical view of protein kinase CK2. *Cell. Mol. Biol. Res.* **40**: 383-390

Pinna, L. A. (2002). Protein kinase CK2: a challenge to canons. *J Cell Sci.* **115**: 3873-3878

Poole, A., Poore, T., Bandhakavi, S., McCann, R. O., Hanna, D. E., Glover, C. V. (2005). A global view of CK2 function and regulation. *Mol Cell Biochem.* **274**: 163-170

Raaf, J., Brunstein, E., Issinger, O. G., Niefind, K. (2008). The interaction of CK2α and CK2β, the subunits of protein kinase CK2, requires CK2β in a preformed conformation and is enthalpically driven. *Protein Sci.* **17**: 2180-2186

Raaf, J., Brunstein, E., Issinger, O. G., Niefind, K. (2008b). The CK2α/CK2β interface of human protein kinase CK2 harbors a binding pocket for small molecules. *Chem Biol.* **15**: 111-117

Rodnight, R., Lavin, B. E. (1964). Phosvitin kinase from brain: activation by ions

and subcellular distribution. *Biochem. J.* **93**: 84-91

Ruzzene, M., Pinna, L. A. (2010). Addiction to protein kinase CK2: a common denominator of diverse cancer cells? *Biochimica et Biophysica Acta* **1804**(3): 499-504

Salvi, M., Sarno, S., Cesaro, L., Nakamura, H. and Pinna, L. A. (2009). Extraordinary pleiotropy of protein kinase CK2 revealed by weblogo phosphoproteome analysis. *Biochim. Biophys. Acta* **1793**(5): 847-859

Sarno, S., Papinutto, E., Franchin, C., Bain, J., Elliott, M., Meggio, F., Kazimierczuk, Z., Orzeszko, A., Zanotti, G., Battistutta, R. and Pinna, L. A.(2001). ATP Site-Directed Inhibitors of Protein Kinase CK2: An Update. *Current Topics in Medicinal Chemistry* **11**(11): 1340-51

Scheer, M., Grote, A., Chang, A., Schomburg, I., Munaretto, C., Rother, M., Söhngen, C., Stelzer, M., Thiele, J., Schomburg, D. (2011). BRENDA, the enzyme information system in 2011. *Nucleic Acids Res.* **39**: D670-676

Sherr, C. J. and McCormick, F. (2002). The RB and p53 pathways in cancer. *Cancer Cell* **2**: 103-112

Shin, S., Lee, Y., Kim, W., Ko, H., Choi, H. and Kim, K. (2005). Caspase-2 primes cancer cells for TRAIL-mediated apoptosis by processing procaspase-8. *EMBO J.* **24**: 3532-3542

St-Denis, N. A., Derksen, D. R. and Litchfield, D. W. (2009). Evidence for regulation of mitotic progression through temporal phosphorylation and dephosphorylation of CK2a. *Mol. Cell. Biol.* **29**: 2068-2081

St-Denis, N.A. and Litchfield, D. W. (2009). From birth to death: The role of protein kinase CK2 in the regulation of cell proliferation and survival. *Cell. Mol. Life Sci.* **66**: 1817-1829

Tarrant, M. K., Rho, H. S., Xie, Z., Jiang, Y. L., Gross, C., Culhane, J. C., Yan, G.,

Qian, J., Ichikawa, Y., Matsuoka, T., Zachara, N., Etzkorn, F. A., Hart, G. W., Jeong, J. S., Blackshaw, S., Zhu, H., Cole, P. A. (2012). Regulation of CK2 by phosphorylation and O-GlcNAcylation revealed by semisynthesis. *Nat Chem Biol*. **8**: 262-269

Taylor, S. S. and Kornev, A. P. (2011). Protein kinases: evolution of dynamic regulatory proteins. *Trends Biochem. Sci.* **36**: 65-77

Taylor, S. S., Keshwani, M. M., Steichen, J. M. and Kornev A. P. (2012). Evolution of the eukaryotic protein kinases as dynamic molecular switches. *Phil. Trans. R. Soc. B* **367**: 2517-2528

Theis-Febvre, N., Martel, V., Laudet, B., Souchier, C., Grunwald, D., Cochet, C., Filhol, O. (2005). Highlighting protein kinase CK2 movement in living cells. *Mol Cell Biochem* **274**: 15-22

Tozser, J., Bagossi, P., Zahuczky, G., Specht, S. I., Majerova, E. and Copeland, T. D. (2003). Effect of caspase cleavage-site phosphorylation on proteolysis. *Biochem. J.* **372**: 137-143

Valero, E., De Bonis, S., Filhol, O., Wade, R. H., Langowski, J., Chambaz, E. M., Cochet C. (1995). Quaternary structure of casein kinase 2. Characterization of multiple oligomeric states and relation with its catalytic activity. *J Biol Chem.* **270**: 8345-8352

Walsh, D. A., Perkins, J. P., Krebs E. G. (1968). An adenosine 3',5' - monophosphate-dependant protein kinase from rabbit skeletal muscle. *J. Biol. Chem.* **243**: 3763-3765

Xu, X., Toselli, P.A., Russell, L. D. and Seldin, D. C. (1999). Globozoospermia in mice lacking the casein kinase II alpha' catalytic subunit. *Nat. Genet.* **23**: 118-121

Ringraziamenti

Prima di tutto, ringrazio la mia happy family: mamma, papà, fede e cate… ricorderò per sempre il mio dottorato per tutto quello che ci è successo durante questi 3 anni! se penso a quante ne abbiamo passate! ma quello che è veramente importante è che sono qui a ricordare quei momenti con un sorriso e a godermi questi giorni tanto attesi. Abbiamo affrontato prove che nessuno meriterebbe di passare, ma sono tanto felice per noi, perché le abbiamo superate uniti.

Un ringraziamento particolare alla mia sorellina Caterina. Sei stata, soprattutto nei momenti più cupi, fonte di sorriso e di forza quando rientravo da lavoro. Non lo dimenticherò mai.

Ringrazio la mia Gre. Non ho parole per descrivere quanto tu sia stata importante per me durante questi 3 anni. Abbiamo affrontato tante avventure insieme, tantissimi ricordi, tante emozioni. Non avrei voluto avere vicino nessun altro. Grazie.

Ringrazio particolarmente Roberto, per avermi accolto nel suo laboratorio per questi 3 anni e per le stimolanti discussioni scientifiche (e non) che mi hanno accompagnato durante il dottorato.

Un ringraziamento particolare a Graziano, per tutto il "sapere" che hai cercato di trasmettermi…ne avessi appreso anche solo la metà, sarebbe già un gran risultato! Ricorderò sicuramente con piacere tutti i momenti che abbiamo passato insieme e le nostre chiacchierate…sempre in compagnia delle nostre amiche "bionde".

Ringrazio gli altri ragazzi del gruppo del Prof. Battistutta, Elisa, Denise, Michele per tutto il tempo che abbiamo condiviso.

Ancora, mi trovo a ringraziare i miei amici Niec, Max, Panis, L.L.R., Alberto, Pier, Manu per aver avuto l'incredibile capacità di alleggerire qualsiasi momento pesante passato in questi 3 anni.

Ringrazio i ragazzi del calcio amatori fossa lunga: vi siete presi la mia anima, ma

senza di voi non avrei un fisico (e che fisico!!!).

Ringrazio il Big Fede, ogni venerdì era come un film di Spike Lee.

In generale, mi piace pensare che ricorderò tutte le persone con cui ho condiviso momenti più o meno simpatici duranti questi 3 anni. E' mia volontà non dimenticarvi, perché il ricordo è l'unica via per l'immortalità!